This is to certify that the

dissertation entitled

Characterization of the Interior of an Inhomogeneous Body Using Surface Measurements

presented by

Mahmud Khodadadi-Saryazdi

has been accepted towards fulfillment
of the requirements for

Ph.D. degree in Mechanics

Nicholas J Altiero
Major professor

Date August 2, 1990

CHARACTERIZATION OF THE INTERIOR OF AN INHOMOGENEOUS BODY USING SURFACE MEASUREMENTS

By

Mahmud Khodadadi-Saryazdi

A DISSERTATION

Submitted to
Michigan State University
in partial fulfillment of the requirements
for the degree of

DOCTOR OF PHILOSOPHY

Department of Metallurgy, Mechanics and Materials Science

1990

646-5766

ABSTRACT

CHARACTERIZATION OF THE INTERIOR OF AN INHOMOGENEOUS BODY USING SURFACE MEASUREMENTS

By

Mahmud Khodadadi-Saryazdi

In this study, the feasibility of characterizing the internal structure of an inhomogeneous body using a discrete number of surface measurements is explored. The inverse problem is formulated for steady state heat transfer and linear elasticity. In the heat transfer portion of this study, the problem of determining the location, size and thermal conductivity of an inclusion in a body of arbitrary shape using a discrete number of surface temperature and/or heat flux measurements is examined. In the elasticity portion, the estimation of the location, size, Poisson's ratio and shear modulus of the same inclusion using a discrete number of surface displacement and/or traction measurements is investigated. The boundary element method is adapted for application to this parameter estimation problem.

Several questions arise in this inverse application of the boundary element method which have not been adequately addressed in previous investigations. Among these are (1) does the "initial guess" for the unknown parameters have an effect on the convergence to the correct parameters and, if so, what is this effect, (2) how many surface measurements and what combination of measurements are required to simultaneously estimate the unknown parameters, (3) how should the locations of these surface measurement points be selected, (4) what effect will the inevitable errors in experimental measurements have on the ability to estimate the sought parameters, and (5) what effect does the size of the inclusion have on the estimation of the unknown parameters? These questions will be systematically addressed using the boundary element method coupled with the method of parameter estimation.

To my father and mother, and my wife.

Acknowledgments

I would like to express my appreciation to my advisor, Dr. Nicholas J. Altiero, for his support and valuable assistance throughout this work. I also would like to thank Dr. James V. Beck and the members of my guidance committee, Dr. Gary Cloud, Dr. Dahsin Liu, and Dr. David Yen, for their support and assistance. A final note of appreciation must go to my wife, Mahdokht, for her patience and encouragement.

Funding of this research by the State of Michigan Research Excellence Fund through Michigan State University's Center for Composite Materials and Structures is most gratefully acknowledged.

Table of Contents

List of Tables

List of Figures

Chapter 1

Introduction and Background

Material characterization is one of the fundamental tasks of engineering and science. It involves the study of inverse problems which usually imply identification of inputs from outputs. In this study, the feasibility of characterizing the internal structure of an inhomogeneous body using a discrete number of surface measurements is explored. In particular, we examine the problem of determining the location, size and material properties of an inclusion in a body of arbitrary shape using a discrete number of surface temperature and/or heat flux measurements and a discrete number of surface displacement and/or traction measurements. The boundary element method [1] is adapted for application to this parameter estimation [2] problem.

Other numerical techniques, most notably finite differences and finite elements , have been used to investigate various types of inverse problems. However , for the nonlinear inverse problem investigated here, an iterative scheme is required . Thus the boundary element method, which requires only the discretization of the boundary, must be employed in order to avoid the costly and unnecessary task of grid generation

for the entire multiply connected domain at each iteration.

Application of the boundary element method to the inverse problem of material characterization is not entirely new. Murai and Kagawa [3] investigated the estimation of the shape of an inclusion in a two-dimensional region using impedance measurements on the domain surface. They considered the problem simply as the interface boundary determination between two domains of different (but known) conductivities, governed by Laplace's equation. The boundary element method was used in conjunction with a simple linearized estimation scheme. The authors did not address any of the questions regarding convergence, measurement errors, or inclusion size.

Ohnaka and Uosaki [4] utilized surface temperature measurements to simultaneously estimate the diffusion constant of a homogeneous body as well as discrete unknown internal heat sources. The mathematical formulation of the identification problem was presented using the weighted residual expression and the boundary element partition. The unknowns were identified using noisy or noise-free state observations taken at points on the boundary by minimizing a certain criterion function which is the sum of the squares of the relative errors. The maximum number of temperature measurements used was 16. Two cases were considered : (1) the internal source location is close to the boundary and (2) the source location is close to the middle of the body. One set of noisy observation data with a standard deviation of 0.1 was considered. It was revealed that the accuracy of the identification results is lower when the actual heat source is located close to the boundary. The influence of the "initial guess" of the unknown parameters was not investigated, nor was the question of measurement point selection.

Dulikravich [5] investigated the optimal sizes and locations of coolant flow passages for a user-specified steady distribution of surface temperatures and heat fluxes. The Laplace equation for steady conduction was treated using the boundary element method. If the temperatures on the boundary were given as the boundary condition, then an error function based on a normalized least squares formulation for the difference between the desired and computed surface heat fluxes was formed and if the heat fluxes on the boundary were given as the boundary condition, an error function based on a normalized least squares formulation for the difference between the desired and computed surface temperatures was formed. This function was then used in a constrained optimization routine to determine the new updated sizes and locations of the coolant flow passages so that the difference between the desired and the computed surface heat fluxes and/or temperatures was minimized. As in the other investigations, questions regarding the convergence process were not addressed.

Kishimoto, et. al. [6] investigated inverse problems in galvanic corrosion. A boundary element procedure was developed to estimate the densities across the anods using potential values which were assumed to be known at several points in the electrolyte. An approach associated with the single value decomposition of the coefficient matrix and a criterion for determining its effective rank was presented. It was concluded that the effective rank should be determined so that both the coefficient matrix's condition number and the square sum of the residuals

$$Q = \sum (\phi_{inappl} - \phi_{incomp})^2$$

took small values where ϕ_{inappl} represent applied potential values and ϕ_{incomp} the values computed using the boundary element method. The authors assumed that the potential values used as extra information were given in advance. Therefore they did not address the errors involved if the potentials were to be measured experimentally. The effect of the initial guesses of the densities on the estimation process and also the question of how many potential values are needed and the potential corresponding to what location points in the electrolyte are better to use, were not addressed.

Tanaka and Yamagiwa [7] estimated the shape of an internal flaw using elastodynamics with given eigenfrequencies. First the eigenfrequencies corresponding to the assumed defect shape were computed using a boundary-domain element method, i.e. discretization of the domain was also necessary. Then the boundary integral equations were solved using the boundary element method to find the displacements and tractions corresponding to the assumed defect shape. This procedure was repeated until

$$\delta\omega = (\omega^{E} - \omega^{A}) \ \rightarrow 0$$

where ω^E and ω^A were the eigenfrequencies corresponding to the exact and assumed defect shape, respectively. It was revealed that the greater the number of additional data (eigenfrequencies), the closer and faster the exact defect shape would be obtained. The authors did not address the effect of the initial shape and size of the assumed flaw on the ability to estimate it. Although the boundary element was used in this investigation, the additional information, i.e. the eigenfrequencies, were not measured on the surface boundary, but were computed using a boundary-domain element method, at the interface. Therefore, the authors did not address the measurement errors if the eigenfrequencies were measured experimentally. Also the question of how many eigenfrequencies are needed, and what are the optimum locations at which to compute them was not addressed.

Gao and Mura [8] utilized surface displacement data to evaluate the residual stress field in the vicinity of a damaged region caused by a series of unknown loadings. A relation between the residual surface displacements and plastic strains was found. The residual surface displacements were relative and were defined as the difference between before and after loading. Plastic strains were determined using the measured residual surface displacement data and then the stress field on the boundary and outside the damaged area were computed. It was shown that the equivalent plastic strains, though different from the actual ones, induced the actual stresses outside of the equivalent damage domain.

Das and Mitra [9] found the location and size of a flaw using measured surface temperatures. An algorithm for the detection of the flaw was employed in solving several exmple problems. In all the calculations, the boundary element solution for the real flaw was used as the experimental data. It was observed that for a satisfactory detection of the flaw, the error in the measured temperatures should be less than 0.25% .

In the heat transfer portion of this study, a body of some arbitrary but given shape is subjected to a steady thermal state, i.e. a specified temperature is applied to one portion of the surface and a specified heat flux is applied to the remainder of the surface. The body is assumed to contain an inclusion of circular shape but unknown location, size and thermal conductivity. The simultaneous estimation of these parameters is to be accomplished by measuring temperatures at surface locations where the flux has been specified and/or measuring fluxes at selected surface locations where temperature has been specified.

In the elasticity portion, a body of some arbitrary but given shape is subjected to uniaxial tension. The body is assumed to contain an inclusion of circular shape but unknown location, size, Poisson's ratio and shear modulus. The simultaneous estimation of these parameters is to be accomplished by measuring displacements at surface locations where the traction has been specified and/or measuring tractions at selected surface locations where displacement has been specified.

Several questions arise in this inverse application of the boundary element method which have not been adequately addressed in previous investigations. Among these are (1) does the "initial guess" for the unknown parameters have an effect on the convergence to the correct parameters and, if so, what is this effect, (2) how many surface measurements and what combination of measurements are required to simultaneously estimate the unknown parameters, (3) how should the locations of these surface measurement points be selected, (4) what effect will the inevitable errors in experimental measurements have on the ability to estimate the sought parameters, and (5) what effect does the size of the inclusion have on the estimation process?

The present investigation assumes a two-dimensional body containing a single inclusion, but the method of analysis is not limited in principle. Extension to three-dimensional problems and more complex internal structure is straightforward but the additional question of how many parameters one can hope to determine simultaneously requires further study. Nonetheless, the success of the technique demonstrated here shows great promise for application in the area of non-destructive evaluation.

Chapter 2

Boundary Element Method

2.1) Heat Transfer

The differential equation representing steady state heat transfer through an isotropic, homogeneous, two-dimensional region, Ω , is

$$k \nabla^2 T = 0 \qquad \text{in } \Omega \qquad (2.1.1)$$

where $T(x_1 , x_2)$ is the temperature, k is the thermal conductivity of the material, and

$$\nabla^2 = \frac{\partial^2}{\partial x_1^2} + \frac{\partial^2}{\partial x_2^2} .$$

The boundary conditions can be written as

$$T = T_0 (s) \qquad \text{on } \Gamma_a \qquad (2.1.2)$$

$$q = k \frac{\partial T}{\partial n} = q_0 (s) \qquad \text{on } \Gamma_b \qquad (2.1.3)$$

where $T_0(s)$ and $q_0(s)$ are specified functions and the boundary of region Ω is given as $\Gamma = \Gamma_a + \Gamma_b$, n is the outward normal direction to Γ, q is the heat flux in the n direction and s is a coordinate along the boundary as shown in **Figure (2.1)**. Consider now a weighting function $W(x_1, x_2)$ which is assumed to be sufficiently differentiable. Multiplying equation (2.1.1) by $W(x_1, x_2)$ and integrating by parts twice, yields

$$\int_{\Omega} T\, k\, \nabla^2 W\, dx_1\, dx_2 + \int_{\Gamma} W\, k \frac{\partial T}{\partial n}\, ds - \int_{\Gamma} k \frac{\partial W}{\partial n}\, T\, ds = 0. \qquad (2.1.4)$$

In order to convert equation (2.1.4) into a boundary integral equation, a weighting function which satisfies the Laplace equation and represents the field generated by a unit point source acting at point (x_1^i, x_2^i) is used. The governing equation representing this field is written as

$$k\, \nabla^2 T^* = -\,\delta\,(x_1 - x_1^i,\, x_2 - x_2^i) \qquad (2.1.5)$$

where $\delta\,(x_1 - x_1^i,\, x_2 - x_2^i)$ is the Dirac delta function. The solution to equation (2.1.5) is called the fundamental solution and is given by

$$T^* = \frac{1}{2\pi k}\left(\ln \frac{1}{r}\right) \qquad (2.1.6)$$

where

$$r = \left[(x_1 - x_1^i)^2 + (x_2 - x_2^i)^2 \right]^{1/2} .$$

Let us choose $W = T^*(x_1, x_2, x_1^i, x_2^i)$ and define,

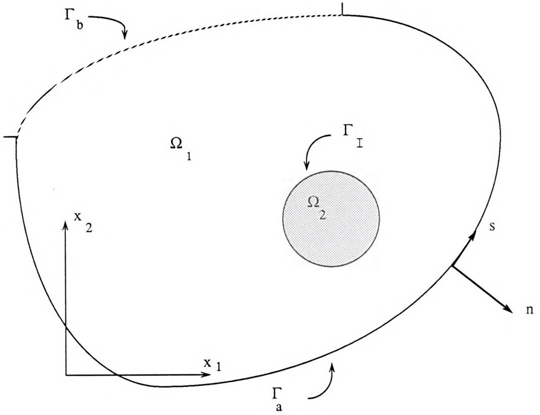

Figure (2.1) - Plane Inhomogeneous Body .

$$q^* = k\frac{\partial T^*}{\partial n} \quad . \tag{2.1.7}$$

Then eq (2.1.4) at a point (x_1^i , x_2^i) in Ω becomes

$$T(x_1^i , x_2^i) = \int_\Gamma q\, T^*\, ds - \int_\Gamma T\, q^*\, ds \tag{2.1.8}$$

where

$$q^* = -\frac{1}{2\pi k}\,(\, \rho_1 n_1 + \rho_2 n_2 \,)\,, \tag{2.1.9}$$

n_1 and n_2 are the components of the outward directed unit normal to Γ, and

$$\rho_1 = \frac{x_1 - x_1^i}{r}$$

$$\rho_2 = \frac{x_2 - x_2^i}{r} \quad .$$

Inserting equations (2.1.6) and (2.1.9) into equation (2.1.8), for (x_1^i , x_2^i) in Ω yields

$$T(x_1^i , x_2^i) = \frac{1}{2\pi}\left[\, \int_\Gamma T\, \frac{\rho_1 n_1 + \rho_2 n_2}{r}\, ds + \frac{1}{k} \int_\Gamma q\, \ln(\frac{1}{r})\, ds \right] \quad . \tag{2.1.10}$$

Equation (2.1.10) is also applicable as (x_1^i , x_2^i) goes to the boundary Γ , but as the integration variables (x_1, x_2) go to (x_1^i, x_2^i), i.e. r goes to zero, the integrands of equation (2.1.10) are singular. This is not a problem for the integral containing $\ln(\frac{1}{r})$ since this function is integrable but it is a problem for the integral containing $\frac{1}{r}$. To avoid this singularity, we integrate around singular point (x_1^i, x_2^i) as shown in **Figure (2.2)**. Thus

$$\int_\Gamma T\frac{\rho_1 n_1+\rho_2 n_2}{r}\, ds = \lim_{\varepsilon\to 0}\int_{\Gamma_\varepsilon} T\frac{\rho_1 n_1+\rho_2 n_2}{r}\, ds + \lim_{\varepsilon\to 0}\int_{\Gamma-\Gamma_\varepsilon} T\frac{\rho_1 n_1+\rho_2 n_2}{r}\, ds \quad (2.1.11)$$

where

$$\lim_{\varepsilon\to 0}\int_{\Gamma_\varepsilon} T\,\frac{\rho_1 n_1+\rho_2 n_2}{r}\, ds = (2\pi - \omega^i)\, T(x_1^i, x_2^i) \quad (2.1.12)$$

and equation (2.1.11) at (x_1^i, x_2^i) on Γ becomes

$$\int_\Gamma T\frac{\rho_1 n_1+\rho_2 n_2}{r}\, ds = (2\pi - \omega^i)\, T^i + \int_\Gamma T\,\frac{\rho_1 n_1+\rho_2 n_2}{r}\, ds \quad (2.1.13)$$

where the integral on the right hand side is interpreted in the Cauchy principle value sense and $\omega^i = \omega(x_1^i, x_2^i)$ is equal to π if the boundary is smooth at (x_1^i, x_2^i). Inserting equation (2.1.13) into (2.1.10), yields

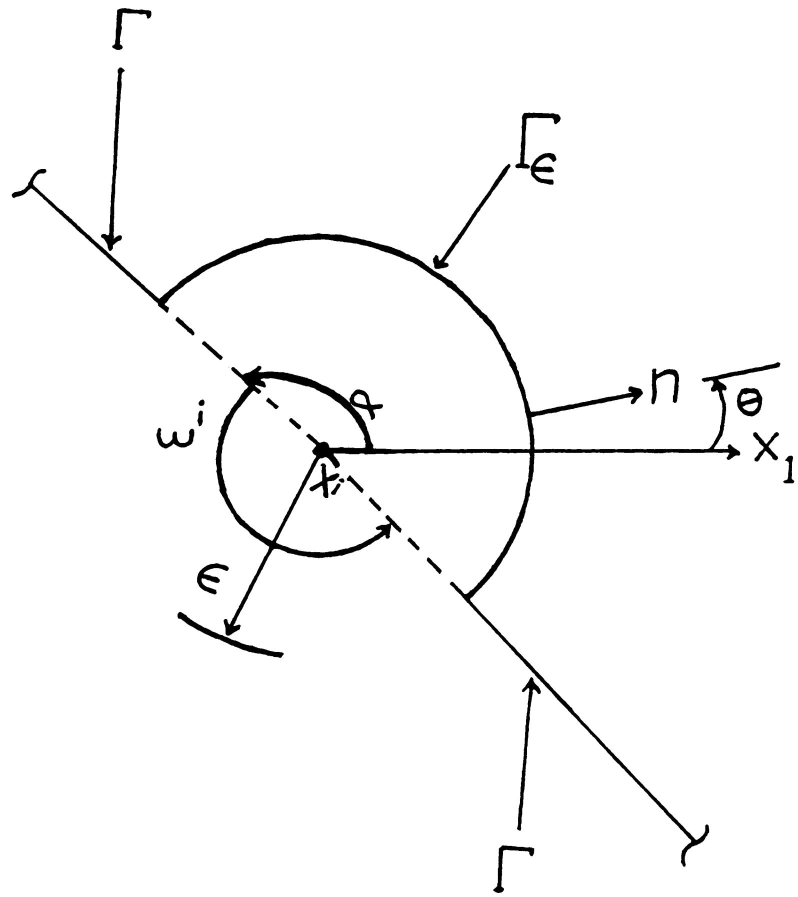

Figure (2.2) Integration path around singular point.

$$\omega^i\, T^i - \int_\Gamma T\, \frac{\rho_1 n_1 + \rho_2 n_2}{r}\, ds = \frac{1}{k} \int_\Gamma q\, \ln\left(\frac{1}{r}\right) ds \qquad (2.1.14)$$

for $(x_1^{\,i}, x_2^{\,i})$ on Γ and $T^i = T(x_1^{\,i}, x_2^{\,i})$. Equations (2.1.14) are the "boundary-integral equations" [1]. Since either T or q is specified at each point on Γ, i.e. T is specified on portion Γ_a and q is specified on portion Γ_b, equations (2.1.14) are employed to determine T on Γ_b and q on Γ_a .

Subdividing the boundary Γ into N segments, equations (2.1.14) become

$$\omega^i\, T^i - \sum_{j=1}^{N} \int_{\Gamma_j} T\, \frac{\rho_1 n_1 + \rho_2 n_2}{r}\, ds = \frac{1}{k} \sum_{j=1}^{N} \int_{\Gamma_j} q\, \ln\left(\frac{1}{r}\right) ds \ . \qquad (2.1.15)$$

To employ linear isoparametric elements, let :

$$\begin{aligned}
s &= \phi_1\, s^{(j-1)} + \phi_2\, s^{(j)} \\
x_1 &= \phi_1\, x_1^{(j-1)} + \phi_2\, x_1^{(j)} \\
x_2 &= \phi_1\, x_2^{(j-1)} + \phi_2\, x_2^{(j)} \qquad (2.1.16) \\
T &= \phi_1\, T^{(j-1)} + \phi_2\, T^{(j)} \\
q &= \phi_1\, q^{(2j-1)} + \phi_2\, q^{(2j)}
\end{aligned}$$

on element j, where

$$\phi_1 = (1 - \xi) / 2 \tag{2.1.17}$$

$$\phi_2 = (1 + \xi) / 2$$

are linear shape functions and $-1 \leq \xi \leq 1$.

Then

$$ds = \left[-\frac{1}{2} s^{(j-1)} + \frac{1}{2} s^{(j)} \right] d\xi = \frac{l_j}{2} d\xi \tag{2.1.18}$$

where l_j is the length of the element j. Note that the temperature is assumed to be piecewise linear and continuous whereas heat flux is assumed to be piecewise linear and discontinuous. Equations (2.1.15) can now be written in the form

$$\omega^i T^i - \sum_{j=1}^{N} \sum_{k=1}^{2} T^{(j-2+k)} \int_{-1}^{1} h_k^{ij} \, d\xi = \frac{1}{k} \sum_{j=1}^{N} \sum_{k=1}^{2} q^{(2j-2+k)} \int_{-1}^{1} g_k^{ij} d\xi \tag{2.1.19}$$

where $T^{(0)}$ is taken to be $T^{(N)}$ and h_k^{ij} and g_k^{ij} are known functions. Equations (2.1.19) are written in matrix form as :

$$[H] \{T\} = [G] \{q\} \tag{2.1.20}$$

where [H] has dimension NxN, and [G] has dimension Nx2N. The column matrix {T} contains the values of temperature at the N boundary nodes and column matrix

$\{q\}$ contains two values of flux at each boundary node, i.e. the value of flux "before" the node and the value of flux "after" the node.

For an inhomogeneous body, the domain Ω is divided into two subdomains Ω_1 and Ω_2 , each having its own thermal conductivity and equations (2.1.20) are applied to each subdomain. For two subdomains :

$$\left[H\right]_1 \left\{T\right\}_1 = \left[G\right]_1 \left\{q\right\}_1$$

$$\left[H\right]_2 \left\{T\right\}_2 = \left[G\right]_2 \left\{q\right\}_2$$

or

$$\begin{bmatrix} [\,H\,]_1 & [\,0\,] \\ [\,0\,] & [\,H\,]_2 \end{bmatrix} \begin{Bmatrix} \left\{T\right\}_1 \\ \left\{T\right\}_2 \end{Bmatrix} = \begin{bmatrix} [\,G\,]_1 & [\,0\,] \\ [\,0\,] & [\,G\,]_2 \end{bmatrix} \begin{Bmatrix} \left\{q\right\}_1 \\ \left\{q\right\}_2 \end{Bmatrix} \tag{2.1.21}$$

Equations (2.1.21) are then reduced by imposition of interface conditions on Γ_I , the interface of the two subdomains. At a point i on Γ_I :

$$T_1^{\,i} = T_2^{\,i} \tag{2.1.22}$$

$$q_1^{(2i-1)} = q_1^{(2i)} = -\,q_2^{(2i-1)} = -\,q_2^{(2i)}$$

where continuity of heat flux at the interface nodes is assumed. Imposition of (2.1.22) gives us:

$$\left[H^* \right] \left\{ \begin{matrix} \left\{ T \right\}_{1-I} \\ \left\{ T \right\}_{I} \end{matrix} \right\} = \left[G^* \right] \left\{ \begin{matrix} \left\{ q \right\}_{1-I} \\ \left\{ q \right\}_{I} \end{matrix} \right\} \tag{2.1.23}$$

where the subscript " I " denotes the interface boundary and the subscript " 1-I " denotes the outer boundary. The matrix $[H^*]$ is $(N_1 + 2N_2) \times (N_1 + N_2)$ and $[G^*]$ is $(2N_1 + 4N_2) \times (2N_1 + N_2)$, where N_1 is the number of outer boundary nodes and N_2 is the number of interface boundary nodes. Equations (2.1.23) can be written as :

$$\left[H^{**} \right] \left\{ \begin{matrix} \left\{ T \right\}_{1-I} \\ \left\{ T \right\}_{I} \\ \left\{ q \right\}_{I} \end{matrix} \right\} = \left[G^{**} \right] \left\{ q \right\}_{1-I} \tag{2.1.24}$$

where the matrix $[H^{**}]$ is $(N_1 + 2N_2) \times (N_1 + 2N_2)$ and $[G^{**}]$ is $(2N_1 + 4N_2) \times (2N_1)$. Equations (2.1.24) are reordered based on known outer boundary conditions i.e. all the known outer boundary temperatures in $\{T\}_{1\text{-}I}$ are taken to the right hand side and all unknown outer boundary heat fluxes in $\{q\}_{1\text{-}I}$ to the left hand side. Then

$$\left[A \right] \left\{ X \right\} = \left[B \right] \tag{2.1.25}$$

which is solved for { X }, which contains the values of unknown temperatures and heat fluxes at the outer boundary nodes as well as all temperatures and heat fluxes at the interface boundary nodes .

Let us consider the example shown in **Figure (2.3)**. A rectangular body with a circular inclusion of radius 2 located at (3,3) is subjected to the boundary conditions shown. The coefficient of thermal conductivity of the matrix material is 164 and that of the inclusion is 73. The outer boundary and the interface boundary are each divided into 24 linear elements of equal length as shown in **Figure (2.4)**.The unknown nodal temperatures and heat fluxes are computed and are presented in **Table (2.1)**.

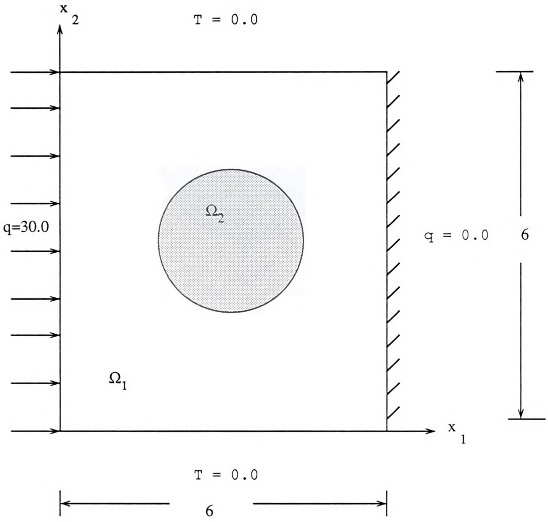

Figure (2.3) - Heat Transfer Example Problem.

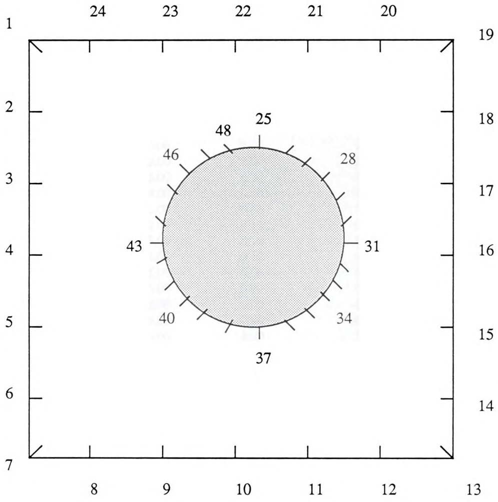

Figure (2.4) - Boundary Element Model .

Table (2.1) Nodal Temperature and Heat Flux Values for Heat Transfer Example Problem.

node #	x-coord.	y-coord.	Temperature	Flux "before"	Flux "after"
1	0.00	6.00	0.00	-88.64	30.00
2	0.00	5.00	0.33	30.00	30.00
3	0.00	4.00	0.52	30.00	30.00
4	0.00	3.00	0.60	30.00	30.00
5	0.00	2.00	0.52	30.00	30.00
6	0.00	1.00	0.33	30.00	30.00
7	0.00	0.00	0.00	30.00	-88.64
8	1.00	0.00	0.00	-25.51	-25.51
9	2.00	0.00	0.00	-11.56	-11.56
10	3.00	0.00	0.00	2.41	2.41
11	4.00	0.00	0.00	-0.14	-0.14
12	0.00	5.00	0.00	-6.76	-6.76
13	0.00	6.00	0.00	-9.06	0.00
14	6.00	1.00	0.06	0.00	0.00
15	6.00	2.00	0.12	0.00	0.00
16	6.00	3.00	0.16	0.00	0.00
17	6.00	4.00	0.12	0.00	0.00
18	6.00	5.00	0.06	0.00	0.00
19	6.00	6.00	0.00	0.00	-9.06
20	5.00	6.00	0.00	-6.76	-6.76
21	4.00	6.00	0.00	-0.14	-0.14
22	3.00	6.00	0.00	2.41	2.41
23	2.00	6.00	0.00	-11.56	-11.56
24	1.00	6.00	0.00	-25.51	-25.51
25	3.00	5.00	-0.03	-10.81	-10.81
26	3.52	4.93	-0.03	-10.31	-10.31
27	4.00	4.73	0.00	-9.02	-9.02
28	4.41	4.41	0.05	-4.96	-4.96
29	4.73	4.00	0.13	1.67	1.67
30	4.93	3.52	0.19	8.17	8.17
31	5.00	3.00	0.22	1 0.99	10.99
32	4.93	2.48	0.19	8.17	8.17
33	4.73	2.00	0.13	1.67	1.67
34	4.41	1.59	0.05	-4.96	-4.96
35	4.00	1.27	0.00	-9.02	-9.02
36	3.52	1.07	-0.03	-10.31	-10.31
37	3.00	1.00	-0.03	-10.81	-10.81
38	2.48	1.07	0.00	-11.45	-11.45
39	2.00	1.27	0.08	-9.64	-9.64
40	1.59	1.59	0.02	-2.30	-2.30
41	1.27	2.00	0.34	9.64	9.64
42	1.07	2.48	0.47	20.80	20.80
43	1.00	3.00	0.52	25.42	25.42
44	1.07	3.52	0.47	20.80	20.80
45	1.27	4.00	0.34	9.64	9.64
46	1.59	4.41	0.20	-2.30	-2.30
47	2.00	4.73	0.08	-9.64	-9.64
48	2.48	4.93	0.00	-11.45	-11.45

2.2) Elasticity

A linear elastic solid of uniform thickness h, and loaded in some manner, is considered. The equations of equilibrium are :

$$\frac{\partial \sigma_{11}}{\partial x_1} + \frac{\partial \sigma_{12}}{\partial x_2} = 0 \qquad (2.2.1)$$

$$\frac{\partial \sigma_{12}}{\partial x_1} + \frac{\partial \sigma_{22}}{\partial x_2} = 0$$

where σ_{11}, σ_{22}, σ_{12} are the in-plane components of stress and it is assumed there are no body forces. The boundary conditions are :

$$u_i = f_i\ (s) \qquad \text{on } \Gamma_a \qquad (2.2.2)$$

$$t_i = \sigma_{ij}\ n_j\ h = g_i\ (s) \qquad \text{on } \Gamma_b \qquad (2.2.3)$$

for i=1,2 and j=1,2, where u_i is the component of displacement in the i direction, t_i is the component of traction in the i direction, n_1 and n_2 are the components of the outward-directed unit normal to the boundary Γ, s is a coordinate along the boundary as shown in **Figure (2.1)**, and f_i (s) and g_i (s) are prescribed functions. To express equation (2.2.1) and equation (2.2.3) in terms of displacements, Hooke's law is used, i.e.

$$\sigma_{11} = C_{11}\frac{\partial u_1}{\partial x_1} + C_{12}\frac{\partial u_2}{\partial x_2} \qquad (2.2.4)$$

$$\sigma_{22} = C_{12}\frac{\partial u_1}{\partial x_1} + C_{22}\frac{\partial u_2}{\partial x_2}$$

$$\sigma_{12} = C_{33} \left(\frac{\partial u_1}{\partial x_2} + \frac{\partial u_2}{\partial x_1} \right)$$

where C_{11}, C_{22}, C_{12}, and C_{33} are material constants. Substituting equations (2.2.4) into equations (2.2.1) , the equations of equilibrium are obtained in terms of displacements,

$$\frac{\partial}{\partial x_1}(c_{11}\frac{\partial u_1}{\partial x_1} + c_{12}\frac{\partial u_2}{\partial x_2}) + \frac{\partial}{\partial x_2}(c_{33}\frac{\partial u_2}{\partial x_1} + c_{33}\frac{\partial u_1}{\partial x_2}) = 0 \qquad (2.2.5)$$

$$\frac{\partial}{\partial x_1}(c_{33}\frac{\partial u_2}{\partial x_1} + c_{33}\frac{\partial u_1}{\partial x_2}) + \frac{\partial}{\partial x_2}(c_{12}\frac{\partial u_1}{\partial x_1} + c_{22}\frac{\partial u_2}{\partial x_2}) = 0$$

and substituting equations (2.2.4) into equations (2.2.3), the tractions in terms of displacements are obtained,

$$t_1 = (c_{11}\frac{\partial u_1}{\partial x_1} + c_{12}\frac{\partial u_2}{\partial x_1})n_1 + (c_{33}\frac{\partial u_2}{\partial x_1} + c_{33}\frac{\partial u_1}{\partial x_2})n_2 \qquad (2.2.6)$$

$$t_2 = (c_{33}\frac{\partial u_2}{\partial x_1} + c_{33}\frac{\partial u_1}{\partial x_2})n_1 + (c_{12}\frac{\partial u_1}{\partial x_1} + c_{22}\frac{\partial u_2}{\partial x_2})n_2$$

where c_{ij} is equal to $C_{ij}h$. Consider now the weighting functions $W_1(x_1 , x_2)$ and $W_2(x_1 , x_2)$ which are assumed to be sufficiently differentiable. Multiplying the first of equations (2.2.5) by $W_1(x_1 , x_2)$ and the second by $W_2(x_1 , x_2)$, and integrating by parts twice yields

$$\int_\Omega u_1 \left[\frac{\partial}{\partial x_1}(c_{11}\frac{\partial W_1}{\partial x_1} + c_{12}\frac{\partial W_2}{\partial x_2}) + \frac{\partial}{\partial x_2}(c_{33}\frac{\partial W_2}{\partial x_1} + c_{33}\frac{\partial W_1}{\partial x_2}) \right] dx_1\, dx_2 \quad (2.2.7)$$

$$+ \int_\Omega u_2 \left[\frac{\partial}{\partial x_1}(c_{33}\frac{\partial W_2}{\partial x_1} + c_{33}\frac{\partial W_1}{\partial x_2}) + \frac{\partial}{\partial x_2}(c_{12}\frac{\partial W_1}{\partial x_1} + c_{22}\frac{\partial W_2}{\partial x_2}) \right] dx_1\, dx_2$$

$$- \int_\Gamma u_1 \left[(c_{11}\frac{\partial W_1}{\partial x_1} + c_{12}\frac{\partial W_2}{\partial x_2})n_1 + (c_{33}\frac{\partial W_2}{\partial x_1} + c_{33}\frac{\partial W_1}{\partial x_2})n_2 \right] ds$$

$$- \int_\Gamma u_2 \left[(c_{33}\frac{\partial W_2}{\partial x_1} + c_{33}\frac{\partial W_1}{\partial x_2})n_1 + (c_{12}\frac{\partial W_1}{\partial x_1} + c_{22}\frac{\partial W_2}{\partial x_2})n_2 \right] ds$$

$$+ \int_\Gamma W_1\, t_1\, ds + \int_\Gamma W_2\, t_2\, ds = 0$$

where the two expressions have been added. For an isotropic material:

$$c_{11} = c_{22} = \frac{2Gh}{(1 - \nu')} \quad (2.2.8)$$

$$c_{12} = \frac{2\nu' Gh}{(1 - \nu')}$$

$$c_{33} = Gh$$

where G is the shear modulus and

$$\nu' = \begin{cases} \nu & \text{plane stress} \\ \dfrac{\nu}{(1 - \nu)} & \text{plane strain} \end{cases}$$

where ν is Poisson's ratio. For simplicity let us denote $x^i = (x_1^{\,i} , x_2^{\,i})$ as the coordinates of the field point "i" and $x = (x_1 , x_2)$ as the coordinates of the source point.

In order to convert equation (2.2.7) into a boundary integral equation, $W_1(x)$ is set equal to $U_1(x , x^i)$ and $W_2(x)$ is set equal to $U_2(x , x^i)$ such that

$$\frac{1+\nu'}{1-\nu'}\left[\frac{\partial^2 U_1}{\partial {x_1}^2}+\frac{\partial^2 U_2}{\partial x_1 \partial x_2}\right]+\nabla^2 U_1=-\frac{1}{Gh}\delta\,(x_1-x_1^{\,i} , x_2-x_2^{\,i})\, e_1(x^i) \qquad (2.2.9)$$

$$\frac{1+\nu'}{1-\nu'}\left[\frac{\partial^2 U_1}{\partial x_1 \partial x_2}+\frac{\partial^2 U_2}{\partial {x_2}^2}\right]+\nabla^2 U_2=-\frac{1}{Gh}\delta\,(x_1-x_1^{\,i} , x_2-x_2^{\,i})\, e_2(x^i)$$

where $e_1(x^i)$ and $e_2(x^i)$ are unit vectors in the x_1 and x_2 directions, $\delta\,(x_1 - x_1^{\,i} , x_2 - x_2^{\,i})$ is the Dirac delta function, and

$$\nabla^2=\frac{\partial^2}{\partial {x_1}^2}+\frac{\partial^2}{\partial {x_2}^2} \quad .$$

In addition

$$T_1 = Gh\left[\frac{2}{1-\nu}\frac{\partial U_1}{\partial x_1}n_1+\frac{2\nu'}{1-\nu}\frac{\partial U_2}{\partial x_2}n_1+\frac{\partial U_2}{\partial x_1}n_2+\frac{\partial U_1}{\partial x_2}n_2\right] \qquad (2.2.10)$$

$$T_2 = Gh\left[\frac{\partial U_2}{\partial x_1}n_1+\frac{\partial U_1}{\partial x_2}n_1+\frac{2\nu'}{1-\nu}\frac{\partial U_1}{\partial x_1}n_2+\frac{2}{1-\nu}\frac{\partial U_2}{\partial x_2}n_2\right]$$

are defined. Inserting equations (2.2.9) and (2.2.10) into equations (2.2.7), yields

$$u_1(x^i)e_1(x^i) + u_2(x^i)e_2(x^i) = - \int_\Gamma T_1 (x , x^i)u_1(x) ds \tag{2.2.11}$$

$$- \int_\Gamma T_2 (x , x^i)u_2(x) ds + \int_\Gamma U_1 (x , x^i)t_1(x) ds + \int_\Gamma U_2 (x , x^i)t_2(x) ds$$

for (x^i) in Ω . Now we can write

$$U_1(x , x^i) = U_{11}(x , x^i)e_1(x^i) + U_{12}(x , x^i)e_2(x^i) \tag{2.2.12}$$

$$U_2(x , x^i) = U_{21}(x , x^i)e_1(x^i) + U_{22}(x , x^i)e_2(x^i)$$

$$T_1(x , x^i) = T_{11}(x , x^i)e_1(x^i) + T_{12}(x , x^i)e_2(x^i)$$

$$T_2(x , x^i) = T_{21}(x , x^i)e_1(x^i) + T_{22}(x , x^i)e_2(x^i)$$

where U_{11} and U_{21} are the displacements and T_{11} and T_{21} are the tractions at a point x in the infinite plane caused by a unit force in the x_1 direction applied at x^i . Similarly U_{12} and U_{22} and T_{12} and T_{22} are the displacements and tractions at a point x due to a unit force in the x_2 direction applied at x^i . Inserting equations (2.2.12) into equations (2.2.11) and equating coefficients of $e_1(x^i)$ and $e_2(x^i)$, respectively, yields

$$u_j (x^i) = - \int_\Gamma T_{kj} (x , x^i) u_k(x) ds(x) + \int_\Gamma U_{kj} (x , x^i) t_k(x) ds(x) \tag{2.2.13}$$

where j=1,2 , k=1,2 and summation on k is implied. The Galerkin function, $\Phi(x , x^i)$, is introduced such that

$$U_1 = \nabla^2 \Phi_1 - \frac{1+\nu'}{2}\left[\frac{\partial^2\Phi_1}{\partial {x_1}^2} + \frac{\partial^2\Phi_2}{\partial x_1 \partial x_2}\right] \tag{2.2.14}$$

$$U_2 = \nabla^2 \Phi_2 - \frac{1+\nu'}{2}\left[\frac{\partial^2\Phi_1}{\partial x_1 \partial x_2} + \frac{\partial^2\Phi_2}{\partial {x_2}^2}\right]$$

which is inserted into equations (2.2.9) to obtain

$$Gh\ \nabla^2 (\nabla^2 \Phi_j) = -\ \delta(x_1 - {x_1}^i,\ x_2 - {x_2}^i)\ e_j(x^i) \qquad j = 1,2\ . \tag{2.2.15}$$

The solution to equations (2.2.15) is

$$\Phi_j = \frac{1}{8\pi Gh}\ r^2 \ln\left[\frac{1}{r}\right] e_j \tag{2.2.16}$$

where

$$r = \left[\ (x_1 - {x_1}^i)^2 + (x_2 - {x_2}^i)^2\right]^{1/2}\ .$$

Substitution of equations (2.2.16) into equations (2.2.14) yields

$$U_1 = \frac{1}{8\pi Gh}\left\{\left[(3-\nu')\ln\frac{1}{r} + (1+\nu')\rho_1^{\ 2}\right]e_1 + (1+\nu')\rho_1\ \rho_2\ e_2\right\} \tag{2.2.17}$$

$$U_2 = \frac{1}{8\pi Gh}\left\{\left[(3 - v')\ln\frac{1}{r} + (1 + v')\rho_2^{\,2}\right]e_2 + (1 + v')\rho_1\,\rho_2\,e_1\right\}$$

where

$$\rho_1 = \frac{x_1 - x_1^{\,i}}{r}$$

$$\rho_2 = \frac{x_2 - x_2^{\,i}}{r}$$

and substitution of equations (2.2.17) into equations (2.2.10) yields

$$T_1 = \frac{1}{4\pi r}\left\{\left[2(1+v')(n_2\,\rho_2^{\,3} - n_1\,\rho_1^{\,3}) - (1-v')n_1\,\rho_1 - (3+v')n_2\,\rho_2\right]e_1\right.$$

$$\left. + \left[2(1 + v')(n_2\,\rho_1^{\,3} + n_1\,\rho_2^{\,3}) - (3 + v')n_2\,\rho_1 - (1 + 3v')n_1\,\rho_2\right]e_2\right\}$$

(2.2.18)

$$T_2 = \frac{1}{4\pi r}\left\{\left[2(1 + v')(n_2\,\rho_1^{\,3} + n_1\,\rho_2^{\,3}) - (1 + 3v')n_2\,\rho_1 - (3 + v')n_1\,\rho_2\right]e_1\right.$$

$$\left. + \left[2(1 + v')(n_1\,\rho_1^{\,3} - n_2\,\rho_2^{\,3}) - (3 + v')n_1\,\rho_1 - (1 - v')n_2\,\rho_2\right]e_2\right\}.$$

The influence functions are determined by comparing equations (2.2.17) and equations (2.2.18) to equations (2.2.12), i.e.

$$U_{11} = \frac{1}{8\pi Gh}\left[(3 - v')\ln\frac{1}{r} + (1 + v')\rho_1^2\right]$$

$$U_{12} = \frac{1}{8\pi Gh}(1 + v')\rho_1\,\rho_2$$

$$U_{21} = \frac{1}{8\pi Gh}(1 + v')\rho_1\,\rho_2$$

$$U_{22} = \frac{1}{8\pi Gh}\left[(3 - v')\ln\frac{1}{r} + (1 + v')\rho_2^2\right]$$

and

$$T_{11} = \frac{1}{4\pi r}\left[2(1 + v')(n_2\,\rho_2^3 - n_1\,\rho_1^3) - (1 - v')n_1\,\rho_1 - (3 + v')n_2\,\rho_2\right]$$

$$T_{12} = \frac{1}{4\pi r}\left[2(1 + v')(n_2\,\rho_1^3 + n_1\,\rho_2^3) - (3 + v')n_2\,\rho_1 - (1 + 3v')n_1\,\rho_2\right]$$

$$T_{21} = \frac{1}{4\pi r}\left[2(1 + v')(n_2\,\rho_1^3 + n_1\,\rho_2^3) - (3 + v')n_2\,\rho_1 - (1 + 3v')n_1\,\rho_2\right]$$

$$T_{22} = \frac{1}{4\pi r}\left[2(1 + v')(n_1\,\rho_1^3 - n_2\,\rho_2^3) - (3 + v')n_1\,\rho_1 - (1 - v')n_2\,\rho_2\right].$$

Recall that equations (2.2.13) are valid at any point x^i in Ω. They are also applicable as x^i goes to the boundary Γ but, as x goes to x^i, i.e. r goes to zero, the integrands are singular. Here T_{kj} varies as $\frac{1}{r}$ and U_{kj} varies as $\ln(\frac{1}{r})$. The first of these requires special treatment. As before, we integrate around x^i and write

$$u_j^i = -\Psi_{kj}^i \, u_k^i - \int_\Gamma T_{kj} \, u_k \, ds + \int_\Gamma U_{kj} \, t_k \, ds \qquad (2.2.19)$$

where $u_j^i = u_j (x^i)$ and

$$\Psi_{kj}^i = \lim_{\varepsilon \to 0} \int_{\Gamma_\varepsilon} T_{kj} \, ds$$

where ε and Γ_ε are shown in **Figure (2.2).** The first integral on the right hand side of equations (2.2.19) is interpreted in the Cauchy principle value sense. Equations (2.2.19) can be rewritten as

$$\alpha_{kj}^i \, u_k^i + \int_\Gamma T_{kj} \, u_k \, ds = \int_\Gamma U_{kj} \, t_k \, ds \qquad x^i \text{ on } \Gamma \qquad (2.2.20)$$

where $\alpha_{kj}^i = \delta_{kj} + \Psi_{kj}^i$ and δ_{kj} is the Kronecker delta. Equations (2.2.20) are the "boundary integral equations" .

Subdividing the boundary Γ into N segments, equations (2.2.20) become

$$\alpha_{kj}^i \, u_k^i + \sum_{r=1}^{N} \int_{\Gamma_r} u_k(x) \, T_{kj}(x , x^i) \, ds = \sum_{r=1}^{N} \int_{\Gamma_r} t_k(x) \, U_{kj}(x , x^i) \, ds \, . \qquad (2.2.21)$$

To employ linear elements, we introduce

$$s = \phi_1 \, s^{(r-1)} + \phi_2 \, s^{(r)}$$

$$x_1 = \phi_1 \, x_1^{(r-1)} + \phi_2 \, x_1^{(r)}$$

$$x_2 = \phi_1 \, x_2^{(r-1)} + \phi_2 \, x_2^{(r)} \qquad (2.2.22)$$

$$u_1 = \phi_1 \, u_1^{(r-1)} + \phi_2 \, u_1^{(r)}$$

$$u_2 = \phi_1 \, u_2^{(r-1)} + \phi_2 \, u_2^{(r)}$$

$$t_1 = \phi_1 \, t_1^{(2r-1)} + \phi_2 \, t_1^{(2r)}$$

$$t_2 = \phi_1 \, t_2^{(2r-1)} + \phi_2 \, t_2^{(2r)}$$

on element r, where

$$\phi_1 = (1 - \xi) / 2$$

$$\phi_2 = (1 + \xi) / 2$$

are linear shape functions and $-1 \leq \xi \leq 1$. Note that the displacements are assumed to be piecewise linear and continuous whereas tractions are assumed to be piecewise linear and discontinuous. Equation (2.2.21) can now be written in the form

$$\alpha_{kj}^{\,i} \, u_k^{\,i} + \sum_{r=1}^{N} \sum_{p=1}^{2} u_k^{(r-2+p)} \int_{-1}^{1} h_p^{\,ir} \, d\xi = \sum_{r=1}^{N} \sum_{p=1}^{2} t_k^{(2r-2+p)} \int_{-1}^{1} g_p^{\,ir} d\xi \qquad (2.2.23)$$

where $u_k^{(0)}$ is taken to be $u_k^{(N)}$ and $h_p^{\,ir}$ and $g_p^{\,ir}$ are known functions. Equations (2.2.23) are written in matrix form as :

$$\left[H\right]\left\{u\right\}=\left[G\right]\left\{t\right\} \tag{2.2.24}$$

where [H] has dimension 2Nx2N, and [G] has dimension 2Nx4N. The column matrix {u} contains the values of displacements in the x_1 and x_2 directions at the N boundary nodes and column matrix {t} contains four values of tractions at each boundary node, i.e. the value of tractions in the x_1 and x_2 directions "before" the node and the values of tractions in the x_1 and x_2 directions "after" the node.

As before, for an inhomogeneous body, the domain Ω is divided into two subdomains Ω_1 and Ω_2 , each having its own Poisson's ratio and shear modulus and equations (2.2.24) are applied to each subdomain. For two subdomains :

$$\left[H\right]_1\left\{u\right\}_1=\left[G\right]_1\left\{t\right\}_1$$

$$\left[H\right]_2\left\{u\right\}_2=\left[G\right]_2\left\{t\right\}_2$$

or

$$\begin{bmatrix} [H]_1 & [0] \\ [0] & [H]_2 \end{bmatrix}\begin{Bmatrix} \{u\}_1 \\ \{u\}_2 \end{Bmatrix}=\begin{bmatrix} [G]_1 & [0] \\ [0] & [G]_2 \end{bmatrix}\begin{Bmatrix} \{t\}_1 \\ \{t\}_2 \end{Bmatrix}. \tag{2.2.25}$$

Equations (2.2.25) are then reduced by imposition of interface conditions on Γ_I , the interface of the two subdomains. At a point i on Γ_I :

$$u_1^{\,i}\,|_1 = u_1^{\,i}\,|_2 \tag{2.2.26}$$

$$u_2^{\,i}\,|_1 = u_2^{\,i}\,|_2$$

$$t_1^{(2i-1)}\,|_1 = t_1^{(2i)}\,|_1 = -\,t_1^{(2i-1)}\,|_2 = -\,t_1^{(2i)}\,|_2$$

$$t_2^{(2i-1)}\,|_1 = t_2^{(2i)}\,|_1 = -\,t_2^{(2i-1)}\,|_2 = -\,t_2^{(2i)}\,|_2$$

where continuity of tractions at the interface nodes is assumed. Imposition of (2.2.26) gives us:

$$\left[\, H^* \,\right] \left\{ \begin{array}{c} \{u\}_{1-I} \\ \{u\}_{I} \end{array} \right\} = \left[\, G^* \,\right] \left\{ \begin{array}{c} \{t\}_{1-I} \\ \{t\}_{I} \end{array} \right\} \tag{2.2.27}$$

where the subscript " I " denotes the interface boundary and the subscript " 1-I " denotes the outer boundary. The matrix [H^*] is ($2N_1 + 4N_2$) x ($2N_1 + 2N_2$) and [G^*] is ($4N_1 + 8N_2$) x ($4N_1 + 2N_2$), where N_1 is the number of outer boundary nodes and N_2 is the number of interface boundary nodes. Equations (2.2.27) can be written as :

$$\left[H^{**} \right] \left\{ \begin{array}{l} \left\{ u \right\}_{1-I} \\ \left\{ u \right\}_{I} \\ \left\{ t \right\}_{I} \end{array} \right\} = \left[G^{**} \right] \left\{ t \right\}_{1-I} \tag{2.2.28}$$

where the matrix $[H^{**}]$ is $(2N_1 + 4N_2) \times (2N_1 + 4N_2)$ and $[G^{**}]$ is $(4N_1 + 8N_2) \times (4N_1)$. Equations (2.2.28) are reordered based on known outer boundary conditions i.e. all the known outer boundary displacements in $\{u\}_{1\text{-}I}$ are taken to the right hand side and all unknown outer boundary tractions in $\{t\}_{1\text{-}I}$ to the left hand side so that

$$\left[A \right] \left\{ X \right\} = \left[B \right] \tag{2.2.29}$$

which is solved for {X}, which contains the values of unknown displacements and tractions at the outer boundary nodes as well as all displacements and tractions at the interface boundary nodes .

Let us consider the examples shown in **Figures (2.5)**, **(2.6)**, and **(2.7)**. A rectangular body with a circular inclusion of radius 2 located at (3,3) is subjected to the boundary conditions shown in each figure. The shear modulus and Poisson's ratio of the matrix material are 3.0×10^6 and 0.3 respectively, and those of the inclusion are 1.0×10^6 and 0.2 . The outer boundary and the interface boundary are each divided into 24 linear elements of equal length as shown in **Figure (2.4)**. The unknown nodal displacements and tractions are computed and are presented in **Tables (2.2)**, **(2.3)**, and **(2.4)**.

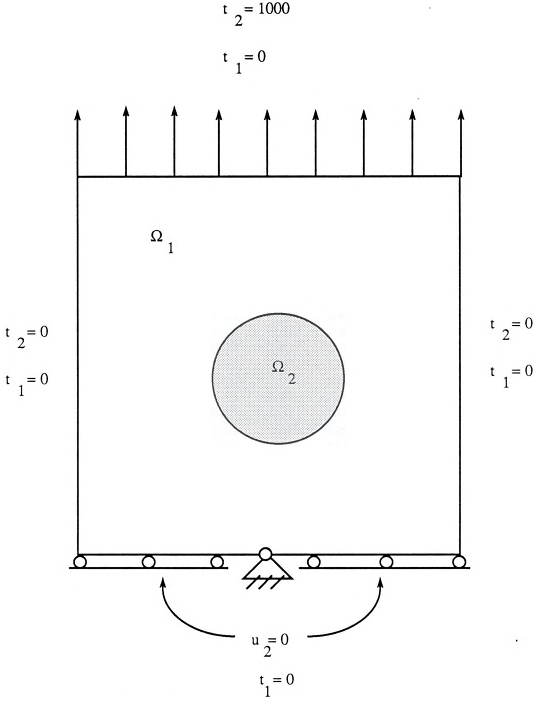

Figure (2.5) - Elasticity Example Problem #1.

Table (2.2) Nodal Displacement and Traction Values for Elasticity Example Problem #1.

node #	(x,y) coord.	u_1	u_2	t_1 "before"	t_2 "before"	t_1 "after"	t_2 "after"
1	(0.00,6.00)	0.11E-04	0.11E-02	0.00	1000.00	0.00	0.00
2	(0.00,5.00)	-0.22E-04	0.92E-03	0.00	0.00	0.00	0.00
3	(0.00,4.00)	-0.99E-04	0.75E-03	0.00	0.00	0.00	0.00
4	(0.00,3.00)	-0.16E-03	0.52E-03	0.00	0.00	0.00	0.00
5	(0.00,2.00)	-0.11E-03	0.29E-03	0.00	0.00	0.00	0.00
6	(0.00,1.00)	-0.33E-04	0.12E-03	0.00	0.00	0.00	0.00
7	(0.00,0.00)	-0.73E-06	0.00E+00	0.00	0.00	0.00	-876.69
8	(1.00,0.00)	-0.35E-04	0.00E+00	0.00	-1142.70	0.00	-1142.70
9	(2.00,0.00)	-0.37E-04	0.00E+00	0.00	-984.68	0.00	-984.68
10	(3.00,0.00)	0.00E+00	0.00E+00	0.00	-866.64	0.00	-866.64
11	(4.00,0.00)	0.37E-04	0.00E+00	0.00	-984.68	0.00	-984.68
12	(0.00,5.00)	0.35E-04	0.00E+00	0.00	-1142.70	0.00	-1142.70
13	(0.00,6.00)	0.73E-06	0.00E+00	0.00	-876.69	0.00	0.00
14	(6.00,1.00)	0.33E-04	0.12E-03	0.00	0.00	0.00	0.00
15	(6.00,2.00)	0.11E-03	0.29E-03	0.00	0.00	0.00	0.00
16	(6.00,3.00)	0.16E-03	0.52E-03	0.00	0.00	0.00	0.00
17	(6.00,4.00)	0.99E-04	0.75E-03	0.00	0.00	0.00	0.00
18	(6.00,5.00)	0.22E-04	0.92E-03	0.00	0.00	0.00	0.00
19	(6.00,6.00)	-0.11E-04	0.11E-02	0.00	0.00	0.00	1000.00
20	(5.00,6.00)	0.30E-04	0.10E-02	0.00	1000.00	0.00	1000.00
21	(4.00,6.00)	0.41E-04	0.11E-02	0.00	1000.00	0.00	1000.00
22	(3.00,6.00)	-0.30E-09	0.11E-02	0.00	1000.00	0.00	1000.00
23	(2.00,6.00)	-0.41E-04	0.11E-02	0.00	1000.00	0.00	1000.00
24	(1.00,6.00)	-0.30E-04	0.10E-02	0.00	1000.00	0.00	1000.00
25	(3.00,5.00)	-0.83E-10	0.99E-03	0.00	675.65	0.00	675.65
26	(3.52,4.93)	0.35E-04	0.97E-03	56.35	637.87	56.35	637.87
27	(4.00,4.73)	0.72E-04	0.92E-03	118.08	542.15	118.08	542.15
28	(4.41,4.41)	0.12E-03	0.84E-03	194.65	414.03	194.65	414.03
29	(4.73,4.00)	0.17E-03	0.74E-03	294.19	269.61	294.19	269.61
30	(4.93,3.52)	0.22E-03	0.64E-03	406.34	124.97	406.34	124.97
31	(5.00,3.00)	0.25E-03	0.52E-03	469.11	-10.77	469.11	-10.77
32	(4.93,2.48)	0.23E-03	0.40E-03	422.61	-144.76	422.61	-144.76
33	(4.73,2.00)	0.19E-03	0.30E-03	317.40	-286.99	317.40	-286.99
34	(4.41,1.59)	0.14E-03	0.20E-03	227.22	-429.93	227.22	-429.93
35	(4.00,1.27)	0.95E-04	0.13E-03	165.04	-543.00	165.04	-543.00
36	(3.52,1.07)	0.50E-04	0.89E-04	96.04	-602.36	96.04	-602.36
37	(3.00,1.00)	0.12E-10	0.74E-04	0.00	-616.90	0.00	-616.90
38	(2.48,1.07)	-0.50E-04	0.89E-04	-96.04	-602.36	-96.04	-602.36
39	(2.00,1.27)	-0.95E-04	0.13E-03	-165.04	-543.00	-165.04	-543.00
40	(1.59,1.59)	-0.14E-03	0.20E-03	-227.22	-429.93	-227.22	-429.93
41	(1.27,2.00)	-0.19E-03	0.30E-03	-317.40	-286.99	-317.40	-286.99
42	(1.07,2.48)	-0.23E-03	0.40E-03	-422.61	-144.76	-422.61	-144.76
43	(1.00,3.00)	-0.25E-03	0.52E-03	-469.11	-10.77	-469.11	-10.77
44	(1.07,3.52)	-0.22E-03	0.64E-03	-406.34	124.97	-406.34	124.97
45	(1.27,4.00)	-0.17E-03	0.74E-03	-294.19	269.61	-294.19	269.61
46	(1.59,4.41)	-0.12E-03	0.84E-03	-194.65	414.03	-194.65	414.03
47	(2.00,4.73)	-0.72E-04	0.92E-03	-118.08	542.15	-118.08	542.15
48	(2.48,4.93)	-0.35E-04	0.97E-03	-56.35	637.87	-56.35	637.87

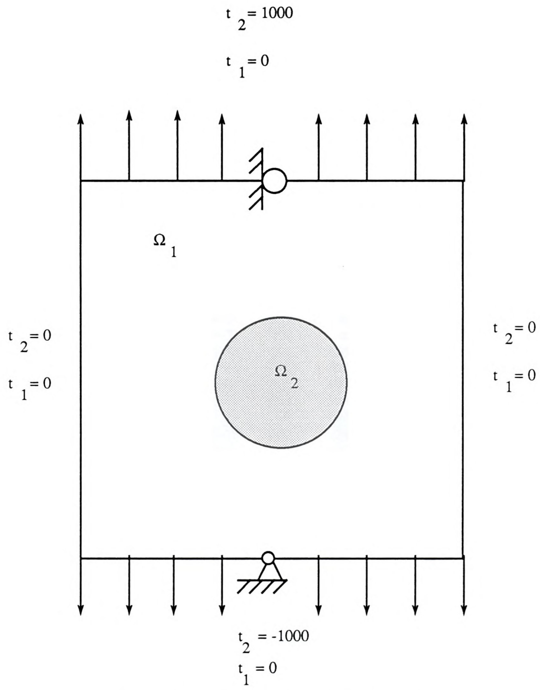

Figure (2.6) - Elasticity Example Problem #2.

Table (2.3) Nodal Displacement and Traction Values for Elasticity Example Problem #2.

node #	(x,y) coord.	u_1	u_2	t_1 "before"	t_2 "before"	t_1 "after"	t_2 "after"
1	(0.00,6.00)	0.94E-05	0.11E-02	0.00	1000.00	0.00	0.00
2	(0.00,5.00)	-0.29E-04	0.95E-03	0.00	0.00	0.00	0.00
3	(0.00,4.00)	-0.11E-03	0.79E-03	0.00	0.00	0.00	0.00
4	(0.00,3.00)	-0.17E-03	0.55E-03	0.00	0.00	0.00	0.00
5	(0.00,2.00)	-0.11E-03	0.32E-03	0.00	0.00	0.00	0.00
6	(0.00,1.00)	-0.29E-04	0.15E-03	0.00	0.00	0.00	0.00
7	(0.00,0.00)	0.94E-05	0.27E-04	0.00	0.00	0.00	-1000.00
8	(1.00,0.00)	-0.31E-04	0.46E-04	0.00	-1000.00	0.00	-1000.00
9	(2.00,0.00)	-0.41E-04	0.23E-04	0.00	-1000.00	0.00	-1000.00
10	(3.00,0.00)	0.00E+00	0.00E+00	0.00	-1000.00	0.00	-1000.00
11	(4.00,0.00)	0.41E-04	0.23E-04	0.00	-1000.00	0.00	-1000.00
12	(0.00,5.00)	0.31E-04	0.46E-04	0.00	-1000.00	0.00	-1000.00
13	(0.00,6.00)	-0.94E-05	0.27E-04	0.00	-1000.00	0.00	0.00
14	(6.00,1.00)	0.29E-04	0.16E-03	0.00	0.00	0.00	0.00
15	(6.00,2.00)	0.11E-03	0.32E-03	0.00	0.00	0.00	0.00
16	(6.00,3.00)	0.17E-03	0.55E-03	0.00	0.00	0.00	0.00
17	(6.00,4.00)	0.11E-03	0.79E-03	0.00	0.00	0.00	0.00
18	(6.00,5.00)	0.29E-04	0.95E-03	0.00	0.00	0.00	0.00
19	(6.00,6.00)	-0.94E-05	0.11E-02	0.00	0.00	0.00	1000.00
20	(5.00,6.00)	0.31E-04	0.11E-02	0.00	1000.00	0.00	1000.00
21	(4.00,6.00)	0.41E-04	0.11E-02	0.00	1000.00	0.00	1000.00
22	(3.00,6.00)	0.00E+00	0.11E-02	0.00	1000.00	0.00	1000.00
23	(2.00,6.00)	-0.41E-04	0.11E-02	0.00	1000.00	0.00	1000.00
24	(1.00,6.00)	-0.31E-04	0.11E-02	0.00	1000.00	0.00	1000.00
25	(3.00,5.00)	-0.30E-08	0.10E-02	0.00	669.62	0.00	669.62
26	(3.52,4.93)	0.38E-04	0.10E-02	60.68	632.64	60.68	632.64
27	(4.00,4.73)	0.79E-04	0.94E-03	126.79	538.56	126.79	538.56
28	(4.41,4.41)	0.13E-03	0.87E-03	208.39	412.49	208.39	412.49
29	(4.73,4.00)	0.18E-03	0.77E-03	313.39	271.23	313.39	271.23
30	(4.93,3.52)	0.23E-03	0.67E-03	427.85	131.19	427.85	131.19
31	(5.00,3.00)	0.26E-03	0.55E-03	485.14	0.00	485.14	0.00
32	(4.93,2.48)	0.23E-03	0.44E-03	427.85	-131.19	427.85	-131.19
33	(4.73,2.00)	0.18E-03	0.33E-03	313.39	-271.23	313.39	-271.23
34	(4.41,1.59)	0.13E-03	0.25E-03	208.39	-412.49	208.39	-412.49
35	(4.00,1.27)	0.79E-04	0.16E-03	126.79	-538.56	126.79	-538.56
36	(3.52,1.07)	0.38E-04	0.11E-03	60.68	-632.64	60.68	-632.64
37	(3.00,1.00)	0.30E-08	0.86E-04	0.00	-669.62	0.00	-669.62
38	(2.48,1.07)	-0.38E-04	0.11E-03	-60.68	-632.64	-60.68	-632.64
39	(2.00,1.27)	-0.79E-04	0.16E-03	-126.79	-538.56	-126.79	-538.56
40	(1.59,1.59)	-0.13E-03	0.24E-03	-208.39	-412.49	-208.39	-412.49
41	(1.27,2.00)	-0.18E-03	0.33E-03	-313.39	-271.23	-313.39	-271.23
42	(1.07,2.48)	-0.23E-03	0.44E-03	-427.85	-131.19	-427.85	-131.19
43	(1.00,3.00)	-0.26E-03	0.55E-03	-485.14	0.00	-485.14	0.00
44	(1.07,3.52)	-0.23E-03	0.67E-03	-427.85	131.19	-427.85	131.19
45	(1.27,4.00)	-0.18E-03	0.77E-03	-313.39	271.23	-313.39	271.23
46	(1.59,4.41)	-0.13E-03	0.87E-03	208.39	412.49	-208.39	412.49
47	(2.00,4.73)	-0.79E-04	0.94E-03	-126.79	538.56	-126.79	538.56
48	(2.48,4.93)	-0.38E-04	0.10E-02	-60.68	632.64	-60.68	632.64

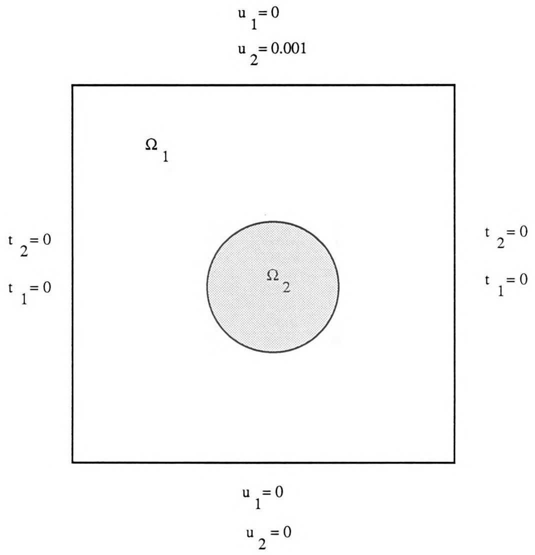

Figure (2.7) - Elasticity Example Problem #3.

Table (2.4) Nodal Displacement and Traction Values for Elasticity Example Problem #3.

node #	(x,y) coord.	u_1	u_2	t_1 "before"	t_2 "before"	t_1 "after"	t_2 "after"
1	(0.00,6.00)	0.00E+00	0.10E-02	-219.37	658.79	0.00	0.00
2	(0.00,5.00)	-0.36E-04	0.91E-03	0.00	0.00	0.00	0.00
3	(0.00,4.00)	-0.16E-03	0.75E-03	0.00	0.00	0.00	0.00
4	(0.00,3.00)	-0.24E-03	0.50E-03	0.00	0.00	0.00	0.00
5	(0.00,2.00)	-0.16E-03	0.25E-03	0.00	0.00	0.00	0.00
6	(0.00,1.00)	-0.36E-04	0.93E-04	0.00	0.00	0.00	0.00
7	(0.00,0.00)	0.00E+00	0.00E+00	0.00	0.00	-219.37	-658.79
8	(1.00,0.00)	0.00E+00	0.00E+00	172.16	-1081.03	172.16	-1081.03
9	(2.00,0.00)	0.00E+00	0.00E+00	191.67	-1059.01	191.67	-1059.01
10	(3.00,0.00)	0.00E+00	0.00E+00	0.00	-961.46	0.00	-961.46
11	(4.00,0.00)	0.00E+00	0.00E+00	-191.67	-1059.01	-191.67	-1059.01
12	(0.00,5.00)	0.00E+00	0.00E+00	-172.16	-1081.03	-172.16	-1081.03
13	(0.00,6.00)	0.00E+00	0.00E+00	219.37	-658.79	0.00	0.00
14	(6.00,1.00)	0.36E-04	0.93E-04	0.00	0.00	0.00	0.00
15	(6.00,2.00)	0.16E-03	0.25E-03	0.00	0.00	0.00	0.00
16	(6.00,3.00)	0.24E-03	0.50E-03	0.00	0.00	0.00	0.00
17	(6.00,4.00)	0.16E-03	0.75E-03	0.00	0.00	0.00	0.00
18	(6.00,5.00)	0.36E-04	0.91E-03	0.00	0.00	0.00	0.00
19	(6.00,6.00)	0.00E+00	0.10E-02	0.00	0.00	219.37	658.79
20	(5.00,6.00)	0.00E+00	0.10E-02	172.16	-1081.03	172.16	-1081.00
21	(4.00,6.00)	0.00E+00	0.10E-02	191.67	-1059.01	191.67	-1059.01
22	(3.00,6.00)	0.00E+00	0.10E-02	0.00	-961.46	0.00	-961.46
23	(2.00,6.00)	0.00E+00	0.10E-02	-191.67	-1059.01	-191.67	-1059.01
24	(1.00,6.00)	0.00E+00	0.10E-02	-172.16	-1081.03	-172.16	-1081.03
25	(3.00,5.00)	-0.69E-11	0.92E-03	0.00	620.83	0.00	620.83
26	(3.52,4.93)	0.45E-04	0.90E-03	69.23	598.37	69.23	598.37
27	(4.00,4.73)	0.96E-04	0.86E-03	137.63	523.43	137.63	523.43
28	(4.41,4.41)	0.16E-03	0.79E-03	221.16	393.49	221.16	393.49
29	(4.73,4.00)	0.23E-03	0.71E-03	355.67	240.15	355.67	240.15
30	(4.93,3.52)	0.31E-03	0.61E-03	523.44	106.42	523.44	106.42
31	(5.00,3.00)	0.34E-03	0.50E-03	609.45	0.00	609.45	0.00
32	(4.93,2.48)	0.31E-03	0.40E-03	523.44	-106.42	523.44	-106.42
33	(4.73,2.00)	0.23E-03	0.30E-03	355.67	-240.15	355.67	-240.15
34	(4.41,1.59)	0.16E-03	0.21E-03	221.16	-393.49	221.16	-393.49
35	(4.00,1.27)	0.96E-04	0.14E-03	137.63	-523.43	137.63	-523.43
36	(3.52,1.07)	0.45E-04	0.98E-04	69.23	-598.37	69.23	-598.37
37	(3.00,1.00)	0.37E-11	0.84E-04	0.00	-620.83	0.00	-620.83
38	(2.48,1.07)	-0.45E-04	0.98E-04	-69.23	-598.37	-69.23	-598.37
39	(2.00,1.27)	-0.96E-04	0.14E-03	-137.63	-523.43	-137.63	-523.43
40	(1.59,1.59)	-0.16E-03	0.21E-03	-221.16	-393.49	-221.16	-393.49
41	(1.27,2.00)	-0.23E-03	0.30E-03	-355.67	-240.15	-355.67	-240.15
42	(1.07,2.48)	-0.31E-03	0.40E-03	-523.44	-106.42	-523.44	-106.42
43	(1.00,3.00)	-0.34E-03	0.50E-03	-609.45	0.00	-609.45	0.00
44	(1.07,3.52)	-0.31E-03	0.61E-03	-523.44	106.42	-523.44	106.42
45	(1.27,4.00)	-0.23E-03	0.71E-03	-355.67	240.15	-355.67	240.15
46	(1.59,4.41)	-0.16E-03	0.79E-03	-221.16	393.49	-221.16	393.49
47	(2.00,4.73)	-0.96E-04	0.86E-03	-137.63	523.43	-137.63	523.43
48	(2.48,4.93)	-0.45E-04	0.90E-03	-69.23	598.37	-69.23	598.37

Chapter 3

Inverse Problem and Parameter Estimation

In the previous chapter the use of the boundary element method to solve the direct steady state heat transfer and linear elasticity problems for homogeneous and inhomogeneous bodies was demonstrated. In the direct problems, the governing equation, geometry, material properties and the boundary conditions are given and the unknnown boundary data is computed. In the inverse problem some of the geometric features and/or material properties are unknown, but some of the unknown boundary data can be measured and used as additional information necessary to estimate the unknown input parameters.

3.1) Heat Transfer

Let us investigate the simplest case of estimating one parameter, i.e. the thermal conductivity of the circular inclusion, Ω_2, using temperatures measured on the outer boundary Γ_b. Let Y_i denote the measured boundary temperatures, T_i denote the boundary temperatures corresponding to a guess of the unknown parameter, computed using the boundary element method, and k_2 the sought thermal conductivity of the inclusion. The sum of the squared differences between Y_i and T_i is

$$Z = \sum_{i=1}^{n} (Y_i - T_i)^2 \tag{3.1.1}$$

where n is the number of boundary temperature measurements used to estimate the unknown parameter. In order to find the best estimate of k_2, Z is minimized by setting its derivative with respect to k_2 equal to zero. Note that

$$\frac{dZ}{dk_2} = -2 \sum_{i=1}^{n} \left[\frac{dT_i(k_2)}{dk_2} \right] \left[Y_i - T_i(k_2) \right] . \tag{3.1.2}$$

Let us define

$$X_i(k_2) = \frac{dT_i(k_2)}{dk_2} \tag{3.1.3}$$

where X_i are called the sensitivity coefficients. Since temperature is a nonlinear function of k_2, X_i will be nonlinear functions of k_2. Inserting equations (3.1.3) into equations (3.1.2) and setting it equal to zero, yields

$$\sum_{i=1}^{n} X_i(k_2) \left[Y_i - T_i(k_2) \right] = 0 \tag{3.1.4}$$

which gives the value of k_2 at which Z is minimized. Note that equation (3.1.4) is nonlinear in k_2. Suppose T has a continuous first derivative in k_2. Then using the first two terms of a Taylor Series for T (k_2) about $\tilde{k}_2$ which is an estimate of k_2, i.e.

$$T(k_2) = T(\tilde{k}_2) + \frac{dT(\tilde{k}_2)}{d\tilde{k}_2}(k_2 - \tilde{k}_2) \tag{3.1.5}$$

and approximating X_i as function of $\tilde{k}_2$, i.e.

$$X_i(\tilde{k}_2) = \frac{dT_i(\tilde{k}_2)}{d\tilde{k}_2} \quad ,$$

equation (3.1.4) becomes

$$\sum_{i=1}^{n} X_i \left[Y_i - T_i - X_i (k_2 - \tilde{k}_2) \right] = 0 \qquad (3.1.6)$$

where X_i and T_i are functions of $\tilde{k}_2$. Note that now equations (3.1.6) are linear in k_2 . To indicate an iterative procedure let

$$\tilde{k}_2 = \tilde{k}_2^{(M)} \quad , \quad k_2 = \tilde{k}_2^{(M+1)} \quad , \quad T = T^{(M)} \quad , \quad X = X^{(M)}$$

so that equations (3.1.6) become

$$\tilde{k}_2^{(M+1)} = \tilde{k}_2^{(M)} + \frac{\sum_{i=1}^{n} X_i^{(M)} \left[Y_i - T_i^{(M)} \right]}{\sum_{i=1}^{n} \left[X_i^{(M)} \right]^2} \qquad (3.1.7)$$

where iteration on M is required. It is possible to estimate thermal conductivity by only one measurement of the temperature on the boundary. For this case, equation (3.1.7) simplifies to

$$\tilde{k}_2^{(M+1)} = \tilde{k}_2^{(M)} + \frac{\left[Y - T^{(M)} \right]}{X^{(M)}} \quad . \qquad (3.1.8)$$

To estimate k_2 using heat flux measurements, the same procedure is used to obtain :

$$\tilde{k}_2^{(M+1)} = \tilde{k}_2^{(M)} + \frac{\sum_{i=1}^{n} X_i^{(M)} \left[Q_i - q_i^{(M)} \right]}{\sum_{i=1}^{n} \left[X_i^{(M)} \right]^2} \tag{3.1.9}$$

where

$$X_i(\tilde{k}_2) = \frac{dq_i(\tilde{k}_2)}{d\tilde{k}_2}$$

and Q_i denote the measured boundary heat fluxes and q_i denote the boundary heat fluxes corresponding to a guess of the unknown parameter, computed using the boundary element method. For the case that only one boundary measured heat flux is used to estimate k_2, equation (3.1.9) simplifies to

$$\tilde{k}_2^{(M+1)} = \tilde{k}_2^{(M)} + \frac{\left[Q - q^{(M)} \right]}{X^{(M)}} \; . \tag{3.1.10}$$

Next let us discuss the estimation of thermal conductivity, location, and size of the inclusion shown in **Figure (2.1)** using temperatures measured on Γ_b and/or heat fluxes measured on Γ_a .

Let us introduce the following column matrices :

$\{T\}_e$ = a column matrix containing m measured boundary temperatures,

$\{T\}_c$ = a column matrix containing the same m boundary temperatures, computed using the boundary element method,

$\{q\}_e$ = a column matrix containing n measured boundary heat fluxes,

$\{q\}_c$ = a column matrix containing the same n boundary heat fluxes, computed using the boundary element method,

and

$$\{\beta\} = \begin{Bmatrix} k_2 \\ x_c \\ y_c \\ R_c \end{Bmatrix}$$

which contains the thermal conductivity of the inclusion, k_2, the coordinates of the center of the circular inclusion, (x_c , y_c) , and the radius of the inclusion, R_c .

The sum of the squared differences between measured and computed temperatures and heat fluxes is :

$$Z = \left\{\{T\}_e - \{T\}_c\right\}^T \left\{\{T\}_e - \{T\}_c\right\} + \left\{\{q\}_e - \{q\}_c\right\}^T \left\{\{q\}_e - \{q\}_c\right\} \quad (3.1.11)$$

where the superscript T indicates the transpose of the matrix, and $\{T\}_c$ and $\{q\}_c$ are functions of $\{\beta\}$. In order to find the best estimate of the unknown parameters, function Z is minimized by setting its derivative with respect to $\{\beta\}$ equal to zero. The matrix derivative of Z with respect to $\{\beta\}$ is :

$$\{\partial_\beta\}Z = -2\left[\{\partial_\beta\}\{T\}_c^{\ T}\right]\left\{\{T\}_e - \{T\}_c\right\} - 2\left[\{\partial_\beta\}\{q\}_c^{\ T}\right]\left\{\{q\}_e - \{q\}_c\right\} \quad (3.1.12)$$

where $\{\partial_\beta\}$ is the matrix derivative operator,

$$\{\partial_\beta\} = \begin{Bmatrix} \dfrac{\partial}{\partial k_2} \\ \dfrac{\partial}{\partial x_c} \\ \dfrac{\partial}{\partial y_c} \\ \dfrac{\partial}{\partial R_c} \end{Bmatrix} .$$

Let us define

$$[\, X_T \,] = \left[\{\partial_\beta\} \{T\}_c^{\ T} \right]^T \tag{3.1.13}$$

$$[\, X_q \,] = \left[\{\partial_\beta\} \{q\}_c^{\ T} \right]^T$$

where $[\, X_T \,]$, which is mx4, and $[\, X_q \,]$,which is nx4, are both functions of $\{\beta\}$, and are called sensitivity matrices. The "ij" components of the sensitivity matrices are called the sensitivity coefficients. $[\, X_T \,]$ contains the sensitivities of temperatures with respect to $\{\beta\}$ and $[\, X_q \,]$ contains the sensitivities of heat fluxes with respect to $\{\beta\}$. Since the temperatures and heat fluxes are nonlinear functions of $\{\beta\}$, the sensitivity coefficients are also nonlinear functions of $\{\beta\}$. Inserting equations (3.1.13) into equations (3.1.12) and setting $\{\partial_\beta\}$ Z = 0, yields

$$[\,X_T\,]^T\left\{\{T\}_e-\{T\}_c\right\}+[\,X_q\,]^T\left\{\{q\}_e-\{q\}_c\right\}=0 \tag{3.1.14}$$

which gives the value of $\{\beta\}$ at which Z is minimized. Note that equations (3.1.14) are nonlinear in $\{\beta\}$. Therefore the first two terms of a Taylor series in matrix form for $\{T\}_c$ and $\{q\}_c$ about $\{\tilde{\beta}\}$ are used, where $\{\tilde{\beta}\}$ is an estimate of $\{\beta\}$, and approximate $[\,X_T\,]$ and $[\,X_q\,]$ as functions of $\{\tilde{\beta}\}$, i.e.

$$\{T\}_c(\{\beta\})=\{T\}_c(\{\tilde{\beta}\})+[\,X_T\,](\{\beta\}-\{\tilde{\beta}\}) \tag{3.1.15}$$

$$\{q\}_c(\{\beta\})=\{q\}_c(\{\tilde{\beta}\})+[\,X_q\,](\{\beta\}-\{\tilde{\beta}\})\,. \tag{3.1.16}$$

Substituting equations (3.1.15) and (3.1.16) into equation (3.1.14), yields

$$[\,X_T\,]^T\left[\{T\}_e-\{T\}_c-[\,X_T\,]\left\{\{\beta\}-\{\tilde{\beta}\}\right\}\right]+ \tag{3.1.17}$$

$$[\,X_q\,]^T\left[\{q\}_e-\{q\}_c-[\,X_q\,]\left\{\{\beta\}-\{\tilde{\beta}\}\right\}\right]=0\ .$$

Note that now equations (3.1.17) are linear in $\{\beta\}$.

To indicate an iterative procedure we let :

$$\{\tilde{\beta}\}=\{\tilde{\beta}\}^{(M)} \qquad \{\beta\}=\{\tilde{\beta}\}^{(M+1)}$$

$$\{T\}_c=\{T\}_c^{(M)} \qquad [\,X_T\,]=[\,X_T\,]^{(M)}$$

$$\left\{q\right\}_c = \left\{q\right\}_c^{(M)} \qquad [\,X_q\,] = [\,X_q\,]^{(M)}$$

and obtain four equations for the four parameters, i.e.

$$\begin{Bmatrix} k_2 \\ x_c \\ y_c \\ R_c \end{Bmatrix}^{(M+1)} = \begin{Bmatrix} k_2 \\ x_c \\ y_c \\ R_c \end{Bmatrix}^{(M)} + \tag{3.1.18}$$

$$\left[\,P\,\right]^{-1} \left[\,[\,X_T\,]^{(M)} \left\{ \left\{T\right\}_e - \left\{T\right\}_c^{(M)} \right\} + [\,X_q\,]^{(M)} \left\{ \left\{q\right\}_e - \left\{q\right\}_c^{(M)} \right\} \right]$$

where

$$\left[\,P\,\right] = \left[\,[\,[\,X_T\,]^T\,[\,X_T\,]\,]^{(M)} + [\,[\,X_q\,]^T\,[\,X_q\,]\,]^{(M)}\,\right] \;.$$

Iterations stop when the following criteria are satisfied :

$$\frac{|\tilde{\beta}_j^{(M+1)} - \tilde{\beta}_j^{(M)}|}{|\tilde{\beta}_j^{(M)}| + \delta_1} < \delta \qquad \text{for } j = 1, \ldots, 4 \tag{3.1.19}$$

where δ and δ_1 are small numbers. Here, following [2], δ is set equal to 10^{-4}, and $\delta_1 = 10^{-10}$.

3.2) Elasticity

In this section, a body that is known to contain a circular inclusion but its location, size and mechanical properties are unknown is considered. We wish to determine these unknown parameters by using the measurements of displacements on the portion of the boundary where tractions are prescribed and/or tractions on the portion of the boundary where displacements are prescribed.

Let us introduce the following column matrices :

$\{u\}_e$ = a column matrix containing m measured boundary displacements,

$\{u\}_c$ = a column matrix containing the same m boundary displacements, computed using the boundary element method.

$\{t\}_e$ = a column matrix containing n measured boundary tractions,

$\{t\}_c$ = a column matrix containing the same n boundary tractions, computed using the boundary element method.

and

$$\{\beta\} = \begin{Bmatrix} G_2 \\ \nu_2 \\ x_c \\ y_c \\ R_c \end{Bmatrix}$$

where G_2 is the shear modulus of the inclusion, ν_2 is the Poisson's ratio of the inclusion, (x_c , y_c) are the coordinates of the center of the circular inclusion, and R_c is the radius of the inclusion.

Following the same procedure as in section 3.1, an equation is obtained to estimate the five unknown parameters in $\{\beta\}$ using the displacements measured on Γ_b and/or tractions measured on Γ_a, i.e.

$$\begin{Bmatrix} G_2 \\ \nu_2 \\ x_c \\ y_c \\ R_c \end{Bmatrix}^{(M+1)} = \begin{Bmatrix} G_2 \\ \nu_2 \\ x_c \\ y_c \\ R_c \end{Bmatrix}^{(M)} + \tag{3.2.1}$$

$$\left[P \right]^{-1} \left[[\, X_u \,]^{(M)} \left\{ \left\{ u \right\}_e - \left\{ u \right\}_c^{(M)} \right\} + [\, X_t \,]^{(M)} \left\{ \left\{ t \right\}_e - \left\{ t \right\}_c^{(M)} \right\} \right]$$

where

$$\left[P \right] = \left[[\, [\, X_u \,]^T [\, X_u \,] \,]^{(M)} + [\, [\, X_t \,]^T [\, X_t \,] \,]^{(M)} \right] .$$

Iterations stop when the criteria indicated in equations (3.1.19) are satisfied. Note that estimation of the parameters using equations (3.1.18) and (3.2.1) involves computing $[\ P\ ]^{-1}$ which requires $[\ P\ ]$ to be non-singular.

3.3) Sensitivity Coefficients

Sensitivity coefficients are very important in the parameter estimation method. They indicate the magnitude of change of the responses such as temperature, heat flux, displacement, or traction due to a small change in the values of the unknown parameters. There are some cases for which it is not possible to uniquely estimate all parameters from the measurements, but it is possible to estimate certain functions or ratios of the parameters. The sensitivity coefficients can provide insight into the cases for which parameters can or cannot be estimated. *Parameters can be estimated if the sensitivity coefficients over the range of the observations are not linearly dependent* [2]. Linear dependence occurs when

$$C_1 \frac{\partial T_i}{\partial k_2} + C_2 \frac{\partial T_i}{\partial x_c} + C_3 \frac{\partial T_i}{\partial y_c} + C_4 \frac{\partial T_i}{\partial R_c} = 0 \qquad (3.3.1)$$

is true for all i measurements, and not all C_i 's equal zero. One way to check linear dependence is to find the determinant of the matrix [P], and see how close it is to zero. In order to uniquely estimate all parameters in the parameter vector $\{\beta\}$, it is necessary that the determinant of the matrix [P] not be equal to zero.

Finite differences are used to approximate the sensitivity coefficients, i.e.

$$(X_T)_{ij} = \frac{\partial T_i}{\partial \tilde{\beta}_j} = \frac{T_i (\tilde{\beta}_1 ,...,\tilde{\beta}_j + \delta \tilde{\beta}_j,..,\tilde{\beta}_4) - T_i (\tilde{\beta}_1 ,...,\tilde{\beta}_j,..,\tilde{\beta}_4)}{\delta \tilde{\beta}_j}$$

$$(X_q)_{ij} = \frac{\partial q_i}{\partial \tilde{\beta}_j} = \frac{q_i (\tilde{\beta}_1 ,...,\tilde{\beta}_j + \delta \tilde{\beta}_j,..,\tilde{\beta}_4) - q_i (\tilde{\beta}_1 ,...,\tilde{\beta}_j,..,\tilde{\beta}_4)}{\delta \tilde{\beta}_j}$$

$$\qquad (3.3.2)$$

$$(X_u)_{ij} = \frac{\partial u_i}{\partial \tilde{\beta}_j} = \frac{u_i (\tilde{\beta}_1 ,...,\tilde{\beta}_j + \delta \tilde{\beta}_j,..,\tilde{\beta}_5) - u_i (\tilde{\beta}_1 ,...,\tilde{\beta}_j,..,\tilde{\beta}_5)}{\delta \tilde{\beta}_j}$$

$$(X_t)_{ij} = \frac{\partial t_i}{\partial \tilde{\beta}_j} = \frac{t_i (\tilde{\beta}_1 ,...,\tilde{\beta}_j + \delta \tilde{\beta}_j,..,\tilde{\beta}_5) - t_i (\tilde{\beta}_1 ,...,\tilde{\beta}_j,..,\tilde{\beta}_5)}{\delta \tilde{\beta}_j}$$

which are the sensitivities of the i^{th} temperature, i^{th} heat flux, i^{th} displacement, and i^{th} traction with respect to the j^{th} parameter, respectively. Note that equations (3.3.2) lead to difficulty if the initial value of $\tilde{\beta}_j$ is chosen to be zero or if it approaches zero. There are two kinds of errors which contribute to inaccuracies in computing the sensitivity coefficients. The first kind is the rounding error which is found when two close values of temperature or heat flux are subtracted and the second kind is the truncation error which is due to the inexact nature of the finite difference method. In order to reduce the truncation error the difference δ in equation (3.3.2) is made small. However, if it is too small, then the rounding error becomes important. The central difference method which is more accurate could also be used, but it requires twice as many values of temperature to be calculated as does forward difference.

3.4) Coupling of the Boundary Element Method and Parameter Estimation Method

A computer program has been developed which employs the boundary element method as a subroutine. A first guess of the unknown parameters is made and the boundary element subroutine is called to compute the boundary data corresponding to the guessed parameters. Then, using the parameter estimation technique, the computed data at selected locations are compared with their measured values taken at the same locations, and "corrected" values of the parameters are found. Using equations (3.1.18) for the heat transfer problems or equations (3.2.1) for the elasticity problems the unknown parameters are estimated. The iterations continue until the criteria indicated in equations (3.1.19) are satisfied. **Figure (3.1)** shows the schematic representation of the estimation method. Complete listings of the computer programs are given in Appendix A and Appendix B.

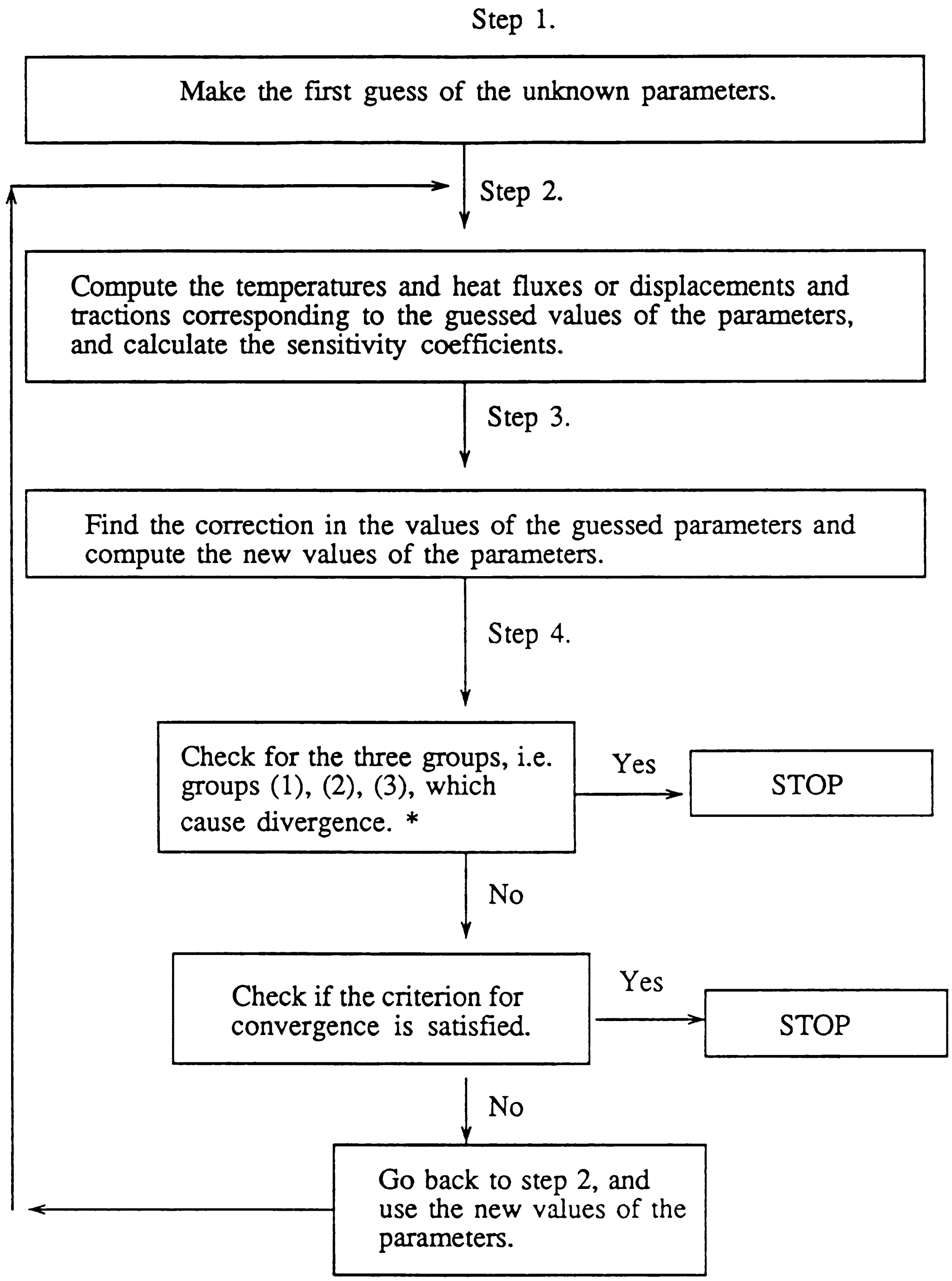

* These three groups will be discussed in the next chapter.

Figure (3.1) Schematic Representation of The Estimation Process.

Chapter 4

Results and Discussion

4.1) Heat transfer

The first problem investigated is the estimation of only one parameter, i.e. the thermal conductivity of the inclusion shown in **Figure (2.3)**, by using one temperature measured at a location on the portion of the outer boundary where heat flux has been specified or one heat flux measured at a location on the portion of the outer boundary where temperature has been specified. The exact value of the inclusion's thermal conductivity is equal to 73.

Table (4.1) shows the results when one temperature measured at different locations on Γ_b is used and **Table (4.2)** shows the results when one heat flux measured at different locations on Γ_a is used to estimate k_2 .

It is observed that it is possible to estimate the thermal conductivity of the inclusion using only one measurement of temperature or heat flux. It is also observed that the first guess of the parameter could be very far from the exact value and still convergence is possible. Initial guesses of 1 and 100 are considered. With the initial guess of $k_2 = 100$, all cases converged. However for the initial guess of $k_2 = 1$, the cases involving nodal locations 2, 3, 4, 5, 6, 8, 11, 21 and 24 diverged due to the fact that the estimated thermal conductivity became negative during the estimation process. Since the inclusion is assumed to be located at the center of the body, the heat fluxes are symmetric about the x_1 axis, and thus the heat fluxes measured at the nodal locations 8, 9, 10, 11, and 12 give the same results as the nodal locations 20, 21, 22, 23, and 24. **Figure (4.1)** shows the sensitivity of the temperatures with respect to k_2 and **Figure (4.2)** shows the sensitivity of heat fluxes with respect to k_2. Note that sensitivity coefficients are nonlinear functions of the unknown parameters and the plot

Table (4.1) Estimating k_2 Using One Temperature Measurement

Case #	Nodal Location Numbers	Converged Iteration #	Diverged Due to
	First Guess of $k_2 = 1.0$		
1	2		Unrealistic Value of k_2
2	3		Unrealistic Value of k_2
3	4		Unrealistic Value of k_2
4	5		Unrealistic Value of k_2
5	6		Unrealistic Value of k_2
6	14	3	
7	15	3	
8	16	3	
9	17	3	
10	18	3	
	First Guess of $k_2 = 100.0$		
11	2	4	
12	3	4	
13	4	4	
14	5	4	
15	6	4	
16	14	3	
17	15	3	
18	16	3	
19	17	3	
20	18	3	

Table (4.2) Estimating k_2 Using One Heat Flux Measurement.

Case #	Nodal Location Numbers	Converged Iteration #	Diverged Due to
	First Guess of $k_2 = 1.0$		
1	8		Unrealistic Value of k_2
2	9	4	
3	10	6	
4	11		Unrealistic Value of k_2
5	12	2	
6	20	2	
7	21		Unrealistic Value of k_2
8	22	6	
9	23	4	
10	24		Unrealistic Value of k_2
	First Guess of $k_2 = 100.0$		
11	8	4	
12	9	3	
13	10	4	
14	11	4	
15	12	3	
16	20	3	
17	21	4	
18	22	4	
19	23	3	
20	24	4	

of sensitivity coefficients presented here, **Figure (4.1)** through **Figure (4.8)**, correspond to the exact values of the parameters.

Again consider the problem shown in **Figure (2.3)**. This time the location, the radius, and the thermal conductivity of the circular inclusion are not known *a priori* and the estimation of these four parameters simultaneously is desired by measuring (a) at least four temperatures on the portion of the boundary where heat fluxes are specified, (b) at least four heat fluxes on the portion of the boundary where temperatures are specified, or (c) some combination of measured temperatures and heat fluxes.

The "experiment" is simulated as follows. The body is analyzed by the boundary element method using the exact values of the four parameters and the unknown boundary temperatures and heat fluxes are computed. These computed values are then used as the "experimental" results.

The first question addressed is the influence of the initial guesses on convergence. A total of 32 sets of initial guesses were examined and "experimental values" were used for all boundary nodal points. Convergence was defined in accordance with equations (3.1.19). Results for the 32 cases are given in **Table (4.3)**. Note that 82.0% of the cases converged to the correct values of the parameters whereas 18.0% of the cases diverged. The reason for divergence becomes apparent after one or two iterations and can be classified into one of three groups: (1) the determinant of [P] for an iteration is zero; (2) the estimated values of (x_c , y_c) and R_c for an iteration are unrealistic, i.e. the estimated inclusion does not lie entirely within the matrix domain; (3) the estimated value of the inclusion thermal conductivity for an iteration is greater than (less than) the thermal conductivity of the matrix material but the actual thermal conductivity of the inclusion is less than (greater than) that of the matrix. All the above three groups can be identified after one or two iterations and the program will stop if any of the above situations occurs. **Table (4.3)** shows that 3.0% of the cases diverged due to (1), 9.0% of the cases diverged due to (2), and 6.0% of the cases diverged due to (3). **Figure (4.1)** through **Figure (4.8)** show the sensitivities of temperatures and heat fluxes with respect to the four parameters. **Figure (4.1)** and **Figure (4.7)** show that the sensitivities of temperatures with respect to k_2 and R_c are very similar in shape which indicates linear dependence of the columns corresponding to the above parameters in the [P] matrix. Similarly **Figure (4.2)** and **Figure (4.7)** reveal the same observation about the sensitivities of the heat fluxes with respect to k_2 and R_c. This is the reason that most of the cases in **Table (4.3)** which diverged were because k_2 or R_c did not converge and went in the wrong direction until the condition indicated by groups (2) or (3) were observed and the program stopped. **Figures (4.3), (4.4), (4.5), (4.6)** show that the sensitivities of temperatures and heat fluxes with respect to the location of the inclusion (x_c , y_c) are not similar in shape but at some boundary nodal locations are very small or zero, and thus the measurement of temperature or heat flux at those locations is not good. Since the initial guess given by case #24 resulted in the most rapid convergence, this guess is used in addressing all of the following questions.

The second question addressed is the number and combination of surface measurements required to simultaneously estimate the unknown parameters. The minimum number of measurements needed is four. We considered 20 different combinations of four temperature locations and 20 different combinations of four heat flux locations on the boundary. The results are presented in **Table (4.4)**. These results show that convergence can be achieved using four measurements. When four temperature measurements were used, 20% of the cases considered converged, 5.0% of the cases diverged due to (1), 25.0% of the cases diverged due to (2), 10.0% of the cases diverged due to (3), and 40.0% of the cases diverged due to (2) and (3). The number of iterations ranged from 4 to 7. When four heat flux measurements were used, 10.0% of the cases considered converged, 20.0% of the cases diverged due to

Table (4.3) Influence of the Initial Guesses on Convergence (Heat Trasfer).

Case #	k_2	Initial guesses (x_c, y_c)	R_c	Converged Iteration #	Diverged Group #
1	50.0	(2.5,2.5)	1.6	7	
2	60.0	(2.5,2.5)	1.6	7	
3	85.0	(2.5,2.5)	1.6	6	
4	100.0	(2.5,2.5)	1.6	7	
5	50.0	(2.5,2.5)	1.8	5	
6	60.0	(2.5,2.5)	1.8	5	
7	85.0	(2.5,2.5)	1.8	6	
8	100.0	(2.5,2.5)	1.8	6	
9	50.0	(2.5,2.5)	2.2	6	
10	60.0	(2.5,2.5)	2.2	6	
11	85.0	(2.5,2.5)	2.2	8	
12	100.0	(2.5,2.5)	2.2		(2)
13	50.0	(2.5,2.5)	2.4	7	
14	60.0	(2.5,2.5)	2.4	8	
15	85.0	(2.5,2.5)	2.4		(2)
16	100.0	(2.5,2.5)	2.4	9	
17	50.0	(3.5,3.5)	1.6		(1)
18	60.0	(3.5,3.5)	1.6		(3)
19	85.0	(3.5,3.5)	1.6		(3)
20	100.0	(3.5,3.5)	1.6	6	
21	50.0	(3.5,3.5)	1.8	9	
22	60.0	(3.5,3.5)	1.8	7	
23	85.0	(3.5,3.5)	1.8	5	
24	100.0	(3.5,3.5)	1.8	4	
25	50.0	(3.5,3.5)	2.2	6	
26	60.0	(3.5,3.5)	2.2	6	
27	85.0	(3.5,3.5)	2.2	6	
28	100.0	(3.5,3.5)	2.2	7	
29	50.0	(3.5,3.5)	2.4	7	
30	60.0	(3.5,3.5)	2.4	7	
31	85.0	(3.5,3.5)	2.4		(2)
32	100.0	(3.5,3.5)	2.4	9	

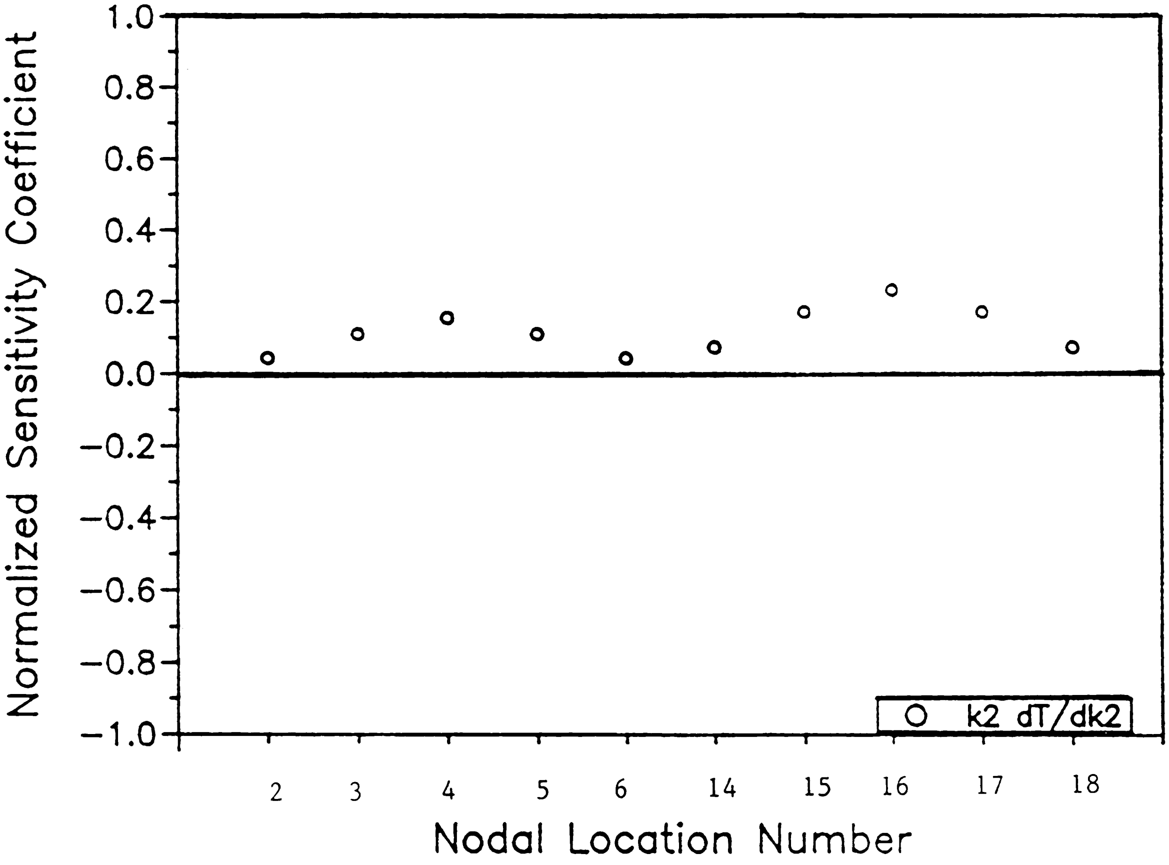

Figure (4.1) - Sensitivity of boundary temperatures with respect to k_2 .

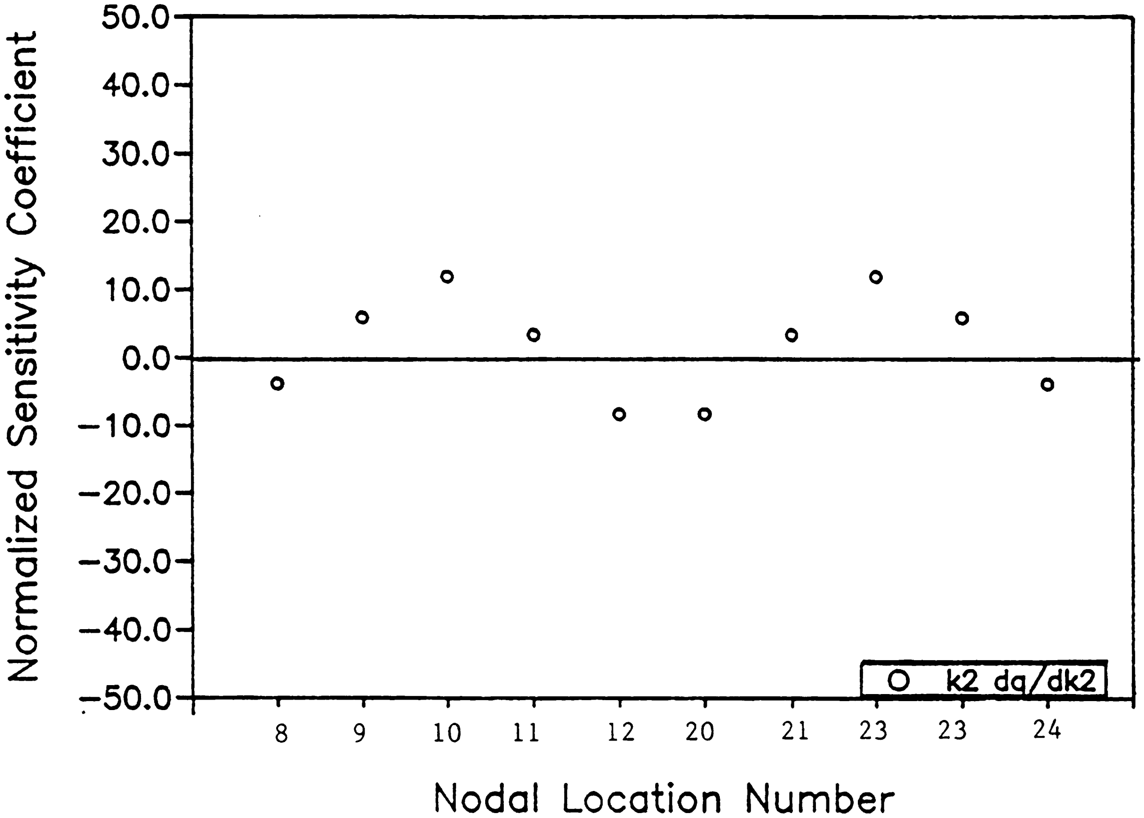

Figure (4.2) - Sensitivity of boundary heat fluxes with respect to k_2 .

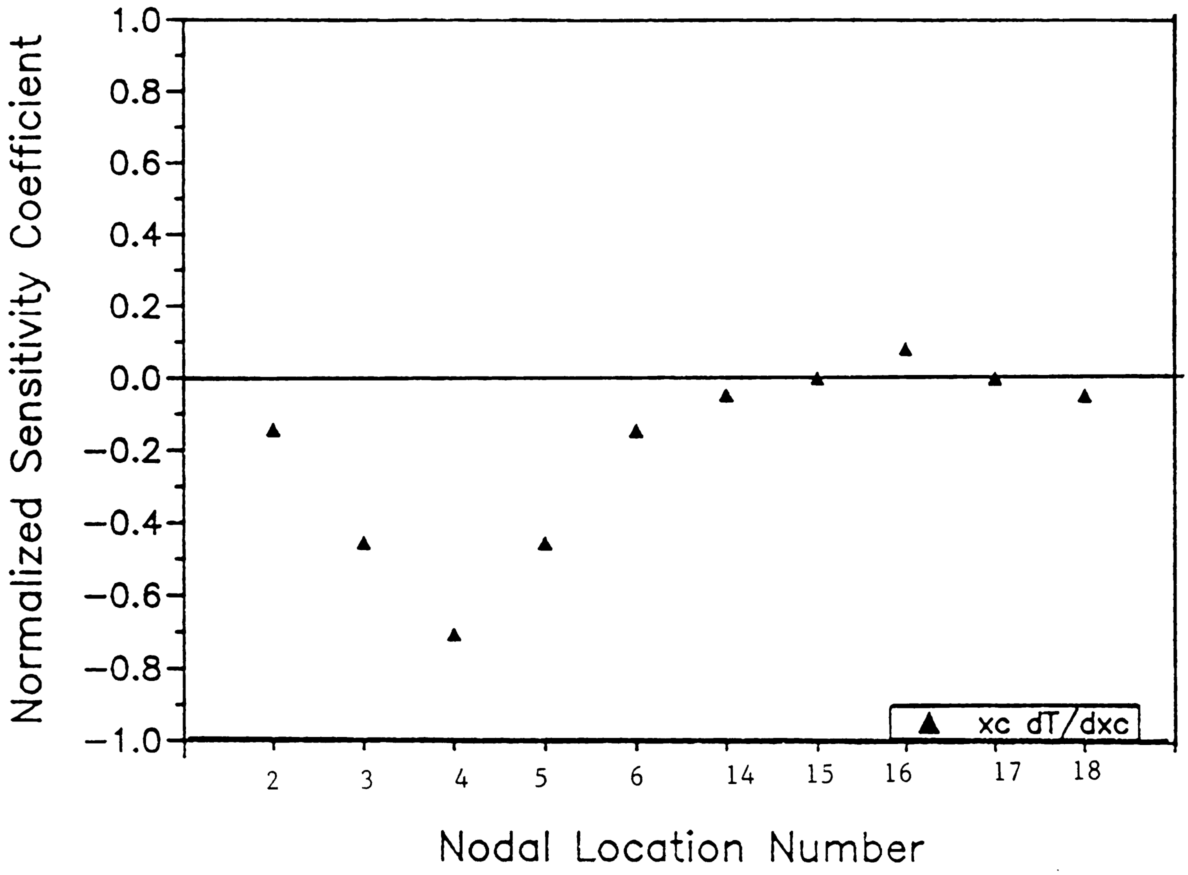

Figure (4.3) - Sensitivity of boundary temperatures with respect to x_c .

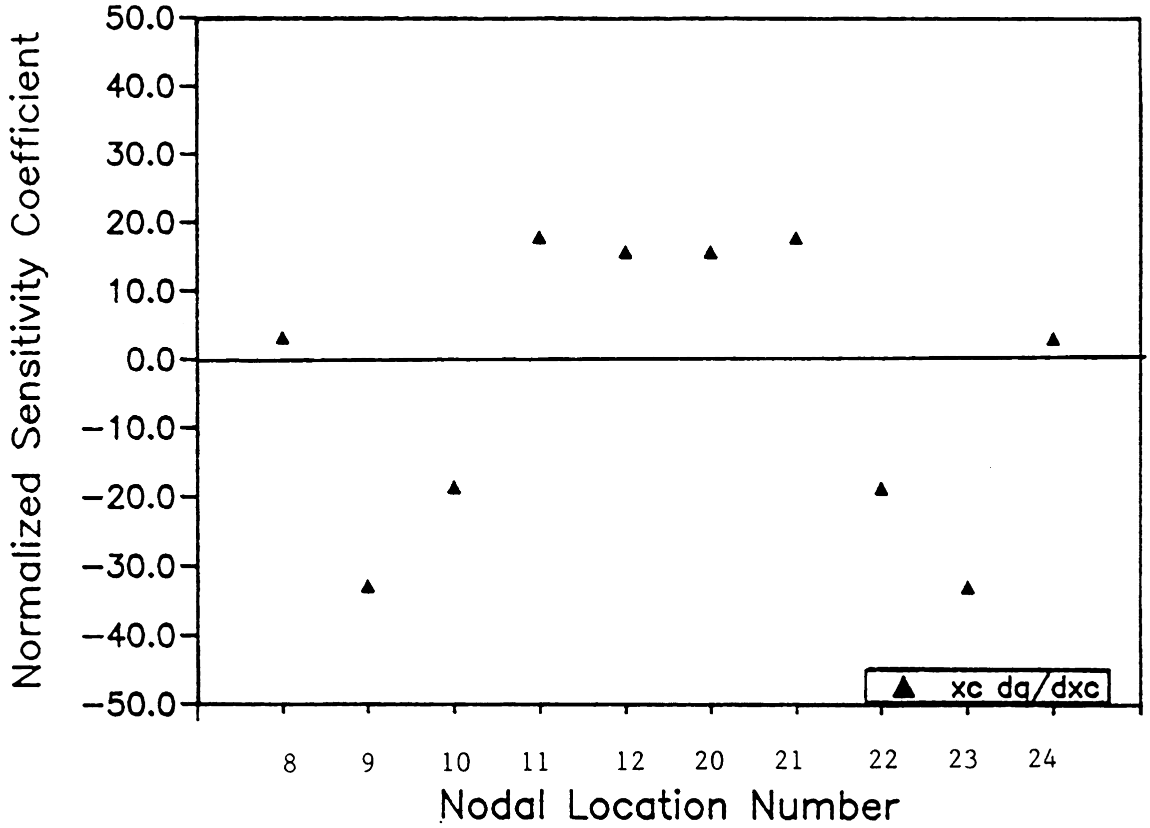

Figure (4.4) - Sensitivity of boundary heat fluxes with respect to x_c .

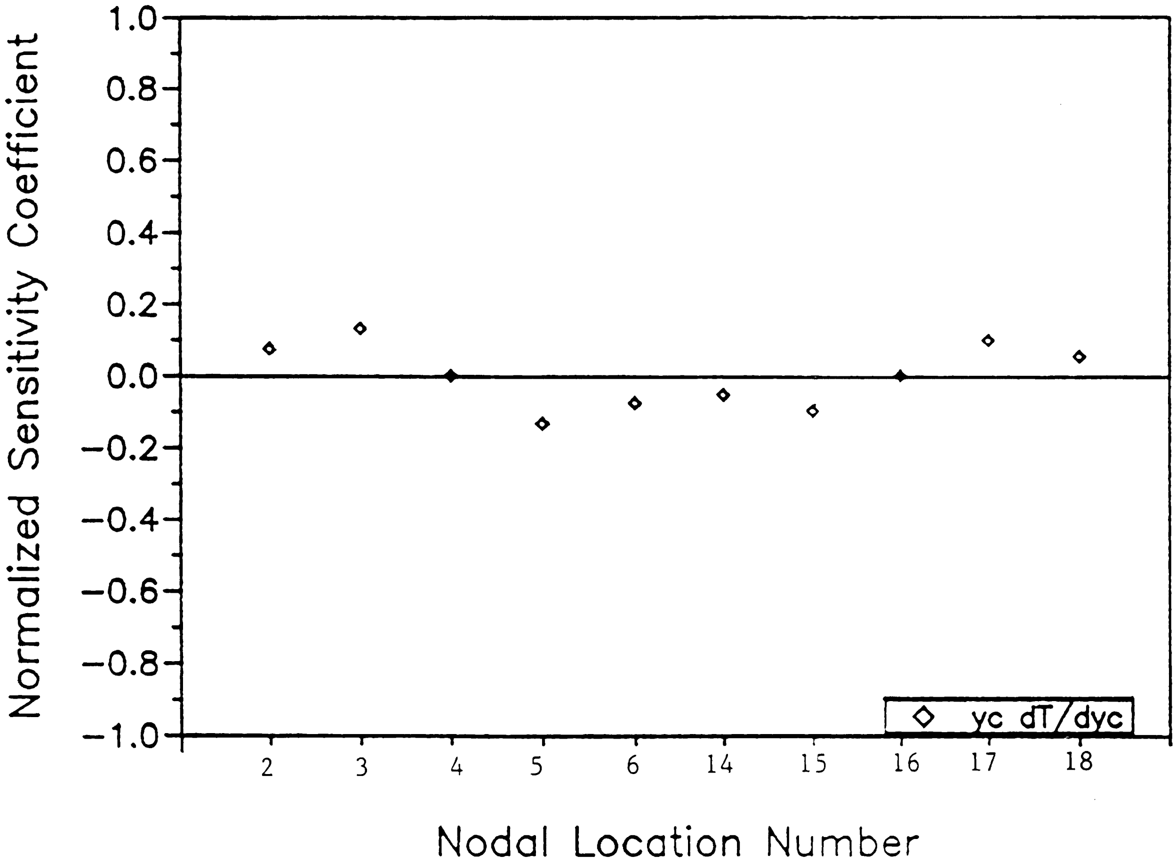

Figure (4.5) - Sensitivity of boundary temperatures with respect to y_c .

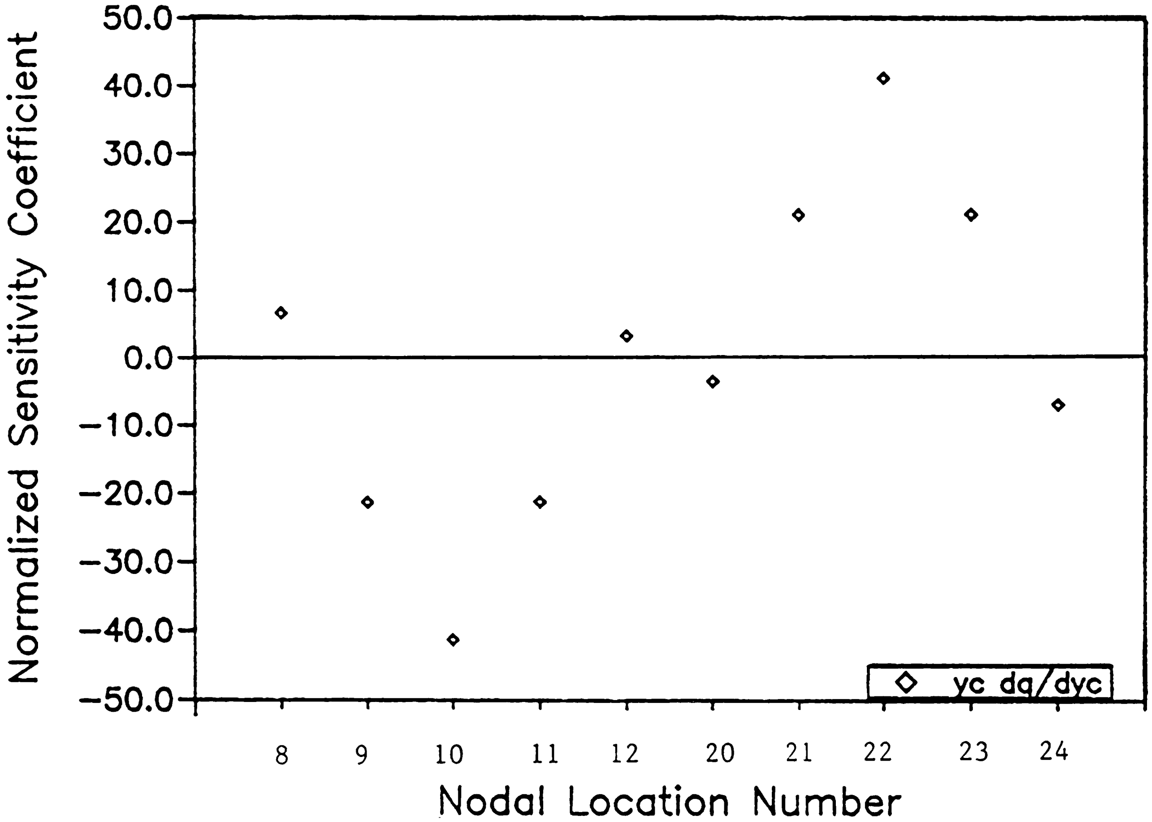

Figure (4.6) - Sensitivity of boundary heat fluxes with respect to y_c .

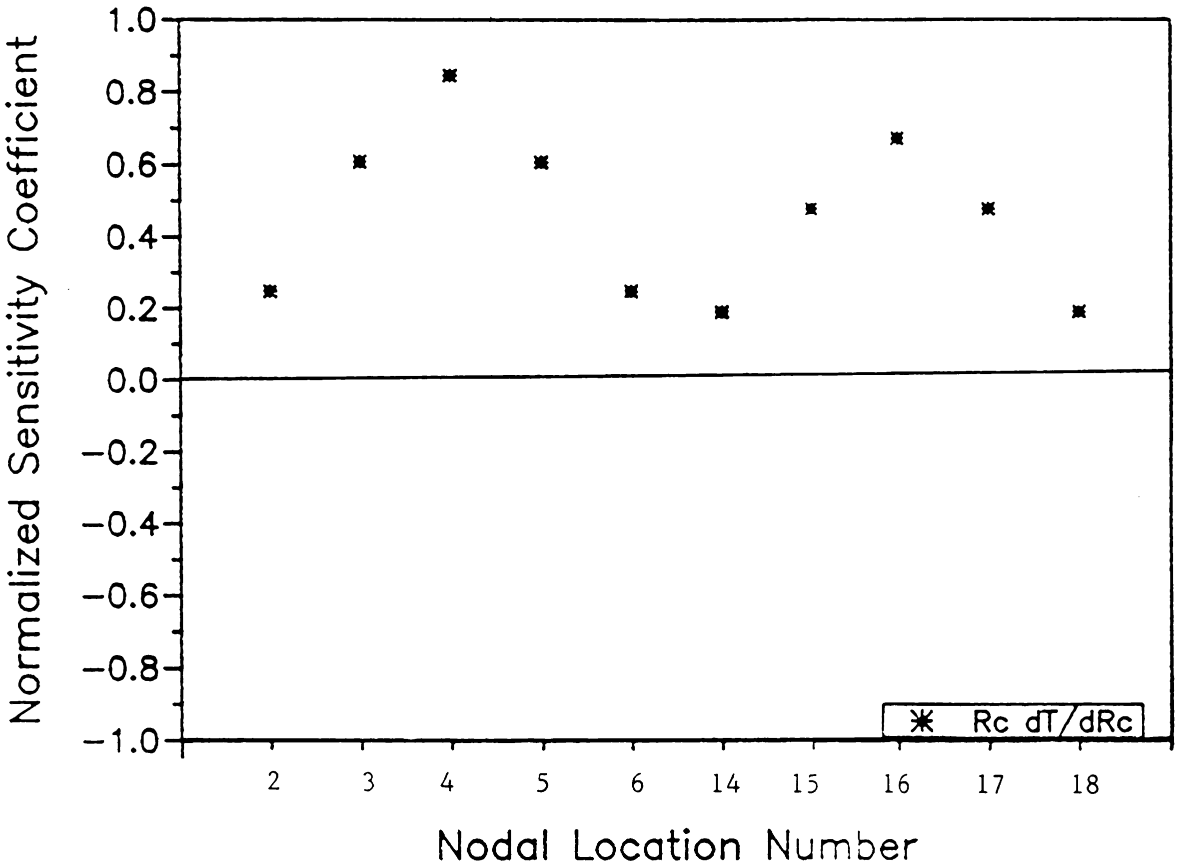

Figure (4.7) - Sensitivity of boundary temperatures with respect to R_c .

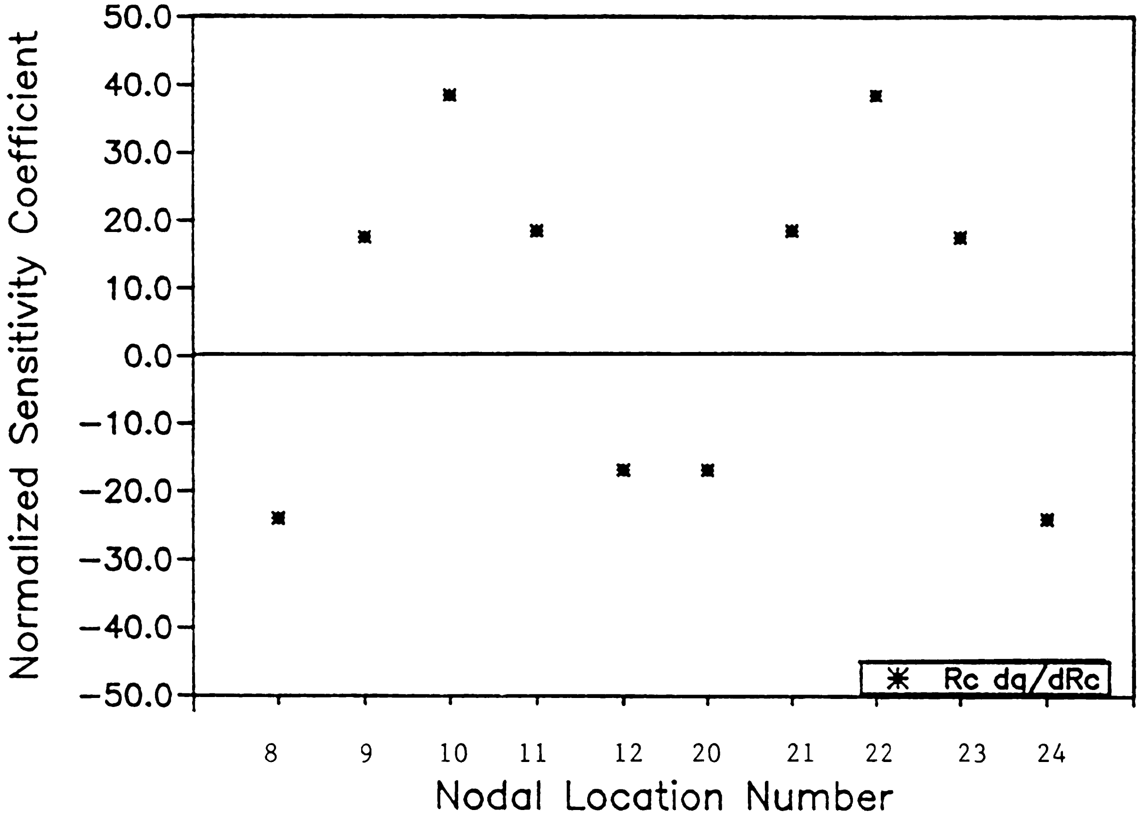

Figure (4.8) - Sensitivity of boundary heat fluxes with respect to R_c .

Table (4.4) Estimating the Unknown Parameters Using Four Temperature or Four Heat Flux Measurements.

Case #	Nodal Location Numbers	Converged Iteration #	Diverged Group #
	Four Temperature Measurements		
1	2 , 3 , 14 , 15	6	
2	2 , 3 , 15 , 16		(2)
3	2 , 3 , 16 , 17		(2), (3)
4	2 , 3 , 17 , 18		(2)
5	3 , 4 , 14 , 15		(1)
6	3 , 4 , 15 , 16		(2), (3)
7	3 , 4 , 16 , 17	4	
8	3 , 4 , 17 , 18		(2)
9	4 , 5 , 14 , 15		(2), (3)
10	4 , 5 , 15 , 16		(3)
11	4 , 5 , 16 , 17		(2), (3)
12	4 , 5 , 17 , 18	5	
13	5 , 6 , 14 , 15		(2), (3)
14	5 , 6 , 15 , 16		(2)
15	5 , 6 , 16 , 17	7	
16	5 , 6 , 17 , 18		(2)
17	2 , 3 , 4 , 5		(2), (3)
18	3 , 4 , 5 , 6		(2), (3)
19	14 ,15 , 16 , 17		(3)
20	15 ,16 , 17 , 18		(2), (3)
	Four Heat Flux Measurements		
21	8 , 9 , 20 , 21		(1)
22	8 , 9 , 21 , 22		(3)
23	8 , 9 , 22 , 23		(2)
24	8 , 9 , 23 , 24		(2), (3)
25	9 ,10 , 20 , 21		(1)
26	9 ,10 , 21 , 22		(2), (3)
27	9 ,10 , 22 , 23		(3)
28	9 ,10 , 23 , 24		(2), (3)
29	10 ,11 , 20 , 21		(2)
30	10 ,11 , 21 , 22		(3)
31	10 ,11 , 22 , 23		(2), (3)
32	10 ,11 , 23 , 24		(2), (3)
33	11 ,12 , 20 , 21		(2)
34	11 ,12 , 21 , 22		(3)
35	11 ,12 , 22 , 23		(1)
36	11 ,12 , 23 , 24	6	
37	8 , 9 , 10 , 11		(1)
38	9 ,10 , 11 , 12		(2)
39	20 ,21 , 22 , 23		(2)
40	21 ,22 , 23 , 24	6	

(1), 25.0% of the cases diverged due to (2), 20.0% diverged due to (3), and 25.0% diverged due to (2) and (3). **Table (4.5)** shows the results when five temperature measurements or five heat flux measurements were used. When five temperature measurements were used, 65.0% of the cases considered converged, 5.0% of the cases diverged due to (1), 20.0% diverged due to (3), and 10.0% diverged due to (2) and (3). The number of iterations ranged from 5 to 8. When five heat flux measurements were used, 41.0% of the cases considered converged, 4.5% of the cases diverged due to (2), 41.0% of the cases diverged due to (3), and 13.5% of the cases diverged due to (2) and (3). The number of iterations ranged from 5 to 6. For the case of five temperature measurements, it is observed that the locations on the top are better than those on the bottom, and for the case of five heat flux measurements, it is observed that the locations on the right side are better than those on the left side. This is because the first guess of the inclusion location is close to the top-right corner and the sensitivity coefficients of the top and right side nodal locations are thus higher than those of the bottom and left side as shown in **Figure (4.9)** and **Figure (4.10)**. **Table (4.6)** shows the results when six temperature measurements were used. It is observed that 70.0% of the cases considered converged, 20.0% of the cases diverged due to (3), and 10.0% of the cases diverged due to (2) and (3). The number of iterations ranged from 5 to 7.

Table (4.7) shows the results when two temperatures and two heat fluxes were used. It is observed that when this combination of temperatures and heat fluxes was used, 40.0% of the cases converged, 26.0% of the cases diverged due to (2), 22.0% of the cases diverged due to (3), and 12.0% of the cases diverged due to (2) and (3). The number of iterations ranged from 5 to 10.

The next question addressed is the effect that the inevitable errors in experimental measurements will have on the ability to estimate the sought parameters. For this case, the "experiment" is simulated as follows. The body is first analyzed by the boundary

Table (4.5) Estimating the Unknown Parameters Using Five Temperature or Five Heat Flux Measurements.

Case #	Nodal Location Numbers	Converged Iteration #	Diverged Group #
	Five Temperature Measurements		
1	2 , 3 , 4 , 5 , 14	7	
2	2 , 3 , 4 , 5 , 15		(2)
3	2 , 3 , 4 , 5 , 16	7	
4	2 , 3 , 4 , 5 , 17		(3)
5	2 , 3 , 4 , 5 , 18		(2), (3)
6	3 , 4 , 5 , 6 , 14	7	
7	3 , 4 , 5 , 6 , 15	8	
8	3 , 4 , 5 , 6 , 16		(3)
9	3 , 4 , 5 , 6 , 17		(3)
10	3 , 4 , 5 , 6 , 18		(3)
11	14 , 15 , 16 , 17 , 2	5	
12	14 , 15 , 16 , 17 , 3	5	
13	14 , 15 , 16 , 17 , 4	6	
14	14 , 15 , 16 , 17 , 5	6	
15	14 , 15 , 16 , 17 , 6	6	
16	15 , 16 , 17 , 18 , 2	5	
17	15 , 16 , 17 , 18 , 3	5	
18	15 , 16 , 17 , 18 , 4	6	
19	15 , 16 , 17 , 18 , 5	7	
20	15 , 16 , 17 , 18 , 6	7	
21	14 , 15 , 16 , 17 , 18		(2), (3)
	Five Heat Flux Measurements		
22	8 , 9 , 10 , 11 , 20		(2), (3)
23	8 , 9 , 10 , 11 , 21		(3)
24	8 , 9 , 10 , 11 , 22		(3)
25	8 , 9 , 10 , 11 , 23		(3)
26	8 , 9 , 10 , 11 , 24		(3)
27	9 , 10 , 11 , 12 , 20		(3)
28	9 , 10 , 11 , 12 , 21		(2)
29	9 , 10 , 11 , 12 , 22		(3)
30	9 , 10 , 11 , 12 , 23		(3)
31	9 , 10 , 11 , 12 , 24		(2), (3)
32	20 , 21 , 22 , 23 , 24	5	
33	20 , 21 , 22 , 23 , 8	5	
34	20 , 21 , 22 , 23 , 9		(3)
35	20 , 21 , 22 , 23 , 10	6	
36	20 , 21 , 22 , 23 , 11	5	
37	20 , 21 , 22 , 23 , 12		(3)
38	21 , 22 , 23 , 24 , 8	5	
39	21 , 22 , 23 , 24 , 9	6	
40	21 , 22 , 23 , 24 , 10	5	
41	21 , 22 , 23 , 24 , 11	6	
42	21 , 22 , 23 , 24 , 12	5	
43	8 , 9 , 10 , 11 , 12		(2), (3)

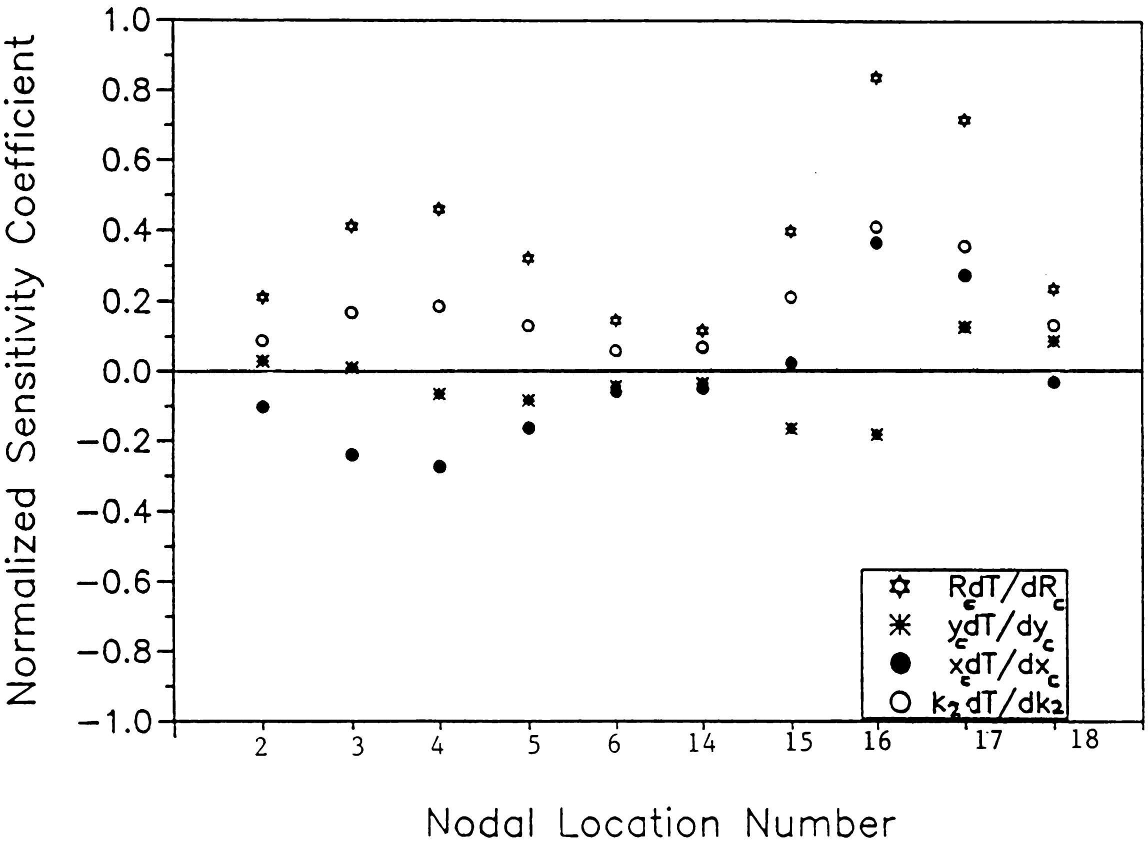

Figure (4.9) - Temperature sensitivity coefficients associated with initial guess of $k_2 = 100$, $(x_c , y_c) = (3.5,3.5)$ and $R_c = 1.8$.

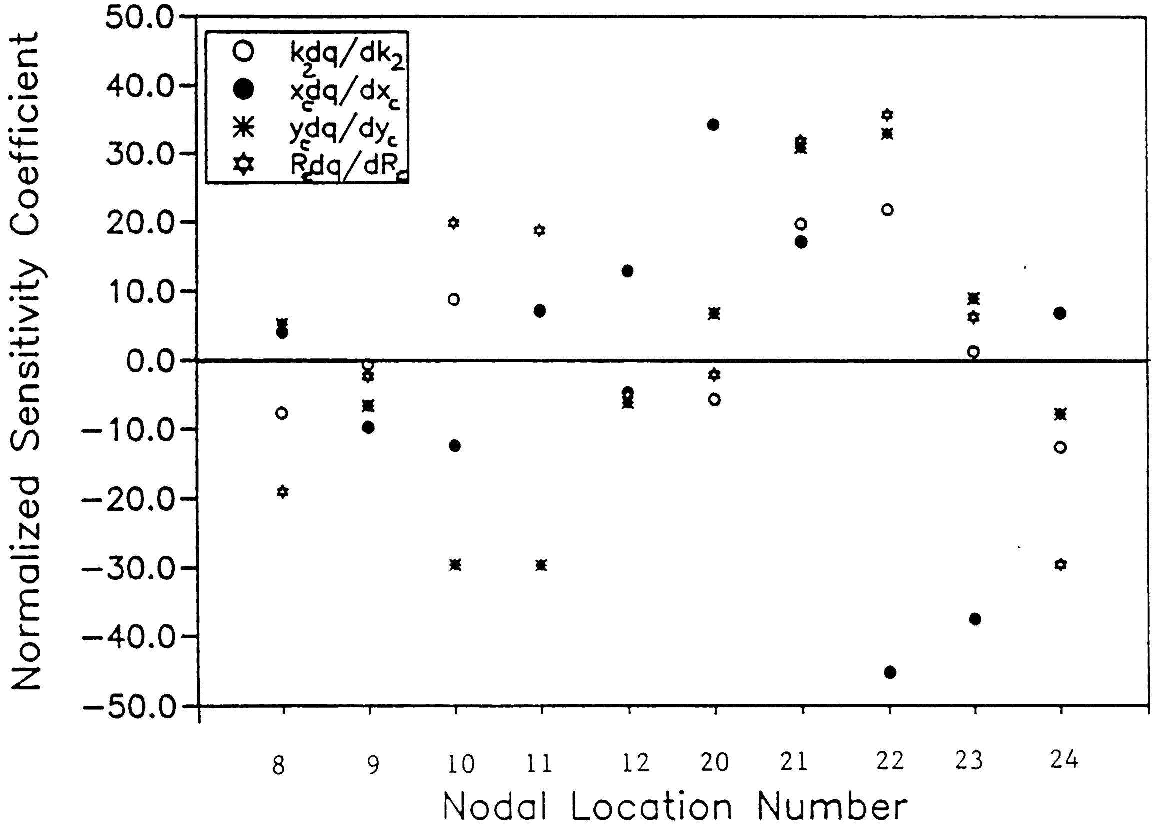

Figure (4.10) - Heat flux sensitivity coefficients associated with initial guess of k_2 = 100, (x_c , y_c) = (3.5,3.5) and R_c = 1.8 .

Table (4.6) Estimating the Unknown Parameters Using Six Temperature Measurements.

Case #	Nodal Location Numbers	Converged Iteration #	Diverged Group #
	Six Temperature Measurements		
1	2 , 3 , 4 , 5 , 6 , 14	7	
2	2 , 3 , 4 , 5 , 6 , 15	7	
3	2 , 3 , 4 , 5 , 6 , 16		(3)
4	2 , 3 , 4 , 5 , 6 , 17		(3)
5	2 , 3 , 4 , 5 , 6 , 18		(2), (3)
6	14, 15 , 16 , 17 , 18 , 2	5	
7	14, 15 , 16 , 17 , 18 , 3	5	
8	14, 15 , 16 , 17 , 18 , 4	6	
9	14, 15 , 16 , 17 , 18 , 5	7	
10	14, 15 , 16 , 17 , 18 , 6	6	

Table (4.7) Estimating the Unknown Parameters Using Two Temperature and Two Heat Flux Measurements.

Case #	Nodal Location Numbers	Converged Iteration #	Diverged Group #
	Two Temperatures,and Two Heat fluxes		
1	2 , 3 , 8 , 9		(3)
2	2 , 3 , 9 , 10		(3)
3	2 , 3 , 10 , 11		(2)
4	2 , 3 , 11 , 12	7	
5	3 , 4 , 8 , 9		(3)
6	3 , 4 , 11 , 10		(2)
7	3 , 4 , 11 , 12	9	
8	3 , 4 , 12 , 13	7	
9	4 , 5 , 8 , 9	10	
10	4 , 5 , 9 , 10		(2)
11	4 , 5 , 10 , 11	8	
12	4 , 5 , 11 , 12	7	
13	5 , 6 , 8 , 9		(3)
14	5 , 6 , 9 , 10		(2)
15	5 , 6 , 10 , 11		(3)
16	5 , 6 , 11 , 12		(2)
17	14 ,15 , 20 , 21		(2), (3)
18	14 ,15 , 21 , 22	9	
19	14 ,15 , 22 , 23	6	
20	14 ,15 , 23 , 24		(3)
21	15 ,16 , 20 , 21		(2), (3)
22	15 ,16 , 21 , 22	6	
23	15 ,16 , 22 , 23	5	
24	15 ,16 , 23 , 24		(2), (3)
25	16 ,17 , 20 , 21		(2), (3)
26	16 ,17 , 21 , 22		(2)
27	16 ,17 , 22 , 23		(2)
28	16 ,17 , 23 , 24	5	
29	17 ,18 , 20 , 21		(2)
30	17 ,18 , 21 , 22	6	
31	17 ,18 , 22 , 23		(3)
32	17 ,18 , 23 , 24	6	

element method using the exact values of the four parameters. Then random errors are added to the computed boundary temperatures and/or heat fluxes, and these are taken to be the "measured" data. The statistical assumptions regarding the introduced errors are that they are additive, non-correlated, normally distributed and have zero mean and constant variance. These errors are generated following a procedure discussed in [2]. **Table (4.8)** shows the results when ten temperature measurements with 0.0%, 0.5%, 1.0%, and 2.0% random errors or ten heat flux measurements with 0.0%, 0.5%, 1.0%, and 2.0% random errors are used. Comparing the results of **Table (4.8)** shows that when heat fluxes are used, convergence is much faster and leads to more accurate values of the unknown parameters. The case of six temperature measurements with 0.0%, 0.5%, 1.0%, and 2.0% random errors to estimate the four unknown parameters is also considered. It is very interesting to note that better results are obtained here using six temperature locations than when ten locations were used. When five heat flux measurements with 0.0%, 0.5%, 1.0%, and 2.0% random errors are used to estimate the four unknown parameters, the results are not as good as when ten locations were used. It should be noted that all the results in **Table (4.8)** are rounded off to one significant figure. Thus, the results for cases 6, 7 and 8 are not exact but are correct when rounded to one decimal place.

The final question addressed is the effect of the inclusion size on the convergence. **Table (4.9)** shows the results when the size of the actual inclusion decreases. The sensitivities of temperatures and heat fluxes decrease as the the size of the inclusion decreases. **Figure (4.11)** and **Figure (4.12)** show that the sensitivity of temperature and heat flux become very small as R_c decreases to the value of 0.5, but it is interesting to note that it is possible to estimate the unknown parameters corresponding to a very small circular inclusion with $R_c = 0.1$. The number of iterations increases as the inclusion size decreases.

Table (4.8) Influence of Experimental Errors on the Estimations (Heat Transfer).

Case #	% Error	Nodal Location Numbers	Iteration #, and Converged Parameter
		Ten Temperature Measurements	
1	0.0	2,3,4,5,6,14,15,16,17,18	4, k_2=73.0, (x_c , y_c)=(3.0,3.0), R_c=2.0
2	0.5	2,3,4,5,6,14,15,16,17,18	7, k_2=79.9, (x_c , y_c)=(2.9,3.0), R_c=2.0
3	1.0	2,3,4,5,6,14,15,16,17,18	9, k_2=84.7, (x_c , y_c)=(2.9,2.9), R_c=1.9
4	2.0	2,3,4,5,6,14,15,16,17,18	10, k_2=89.7, (x_c , y_c)=(2.8,2.8), R_c=1.9
		Ten Heat Flux Measurements	
5	0.0	8,9,10,11,12,20,21,22,23,24	4 , k_2=73.0, (x_c , y_c)=(3.0,3.0), R_c=2.0
6	0.5	8,9,10,11,12,20,21,22,23,24	4 , k_2=73.0, (x_c , y_c)=(3.0,3.0), R_c=2.0
7	1.0	8,9,10,11,12,20,21,22,23,24	4 , k_2=73.0, (x_c , y_c)=(3.0,3.0), R_c=2.0
8	2.0	8,9,10,11,12,20,21,22,23,24	4 , k_2=73.0, (x_c , y_c)=(3.0,3.0), R_c=2.0
		Six Temperature Measurements	
9	0.0	14,15,16,17,18,2	5 , k_2=73.0, (x_c , y_c)=(3.0,3.0), R_c=2.0
10	0.5	14,15,16,17,18,2	5 , k_2=75.1, (x_c , y_c)=(3.0,3.1), R_c=2.0
11	1.0	14,15,16,17,18,2	5 , k_2=77.3, (x_c , y_c)=(3.0,3.1), R_c=2.0
12	2.0	14,15,16,17,18,2	5 , k_2=82.1, (x_c , y_c)=(2.9,3.2), R_c=2.0
		Five Heat Flux Measurements	
13	0.0	20,21,22,23,24	5 , k_2=73.0, (x_c , y_c)=(3.0,3.0), R_c=2.0
14	0.5	20,21,22,23,24	5 , k_2=74.2, (x_c , y_c)=(3.0,3.1), R_c=2.0
15	1.0	20,21,22,23,24	5 , k_2=75.4, (x_c , y_c)=(3.0,3.1), R_c=2.0
16	2.0	20,21,22,23,24	5 , k_2=77.8, (x_c , y_c)=(3.0,3.2), R_c=1.9

Table (4.9) Influence of the Inclusion Size on the Estimation.

	Initial guesses				
Case #	k_2	(x_c , y_c)	R_c	Actual Inclusion size	Converged Iteration #
1	73.0	(3.0,3.0)	1.8	2.0	4
2	73.0	(3.0,3.0)	1.3	1.5	4
3	73.0	(3.0,3.0)	0.8	1.0	5
4	73.0	(3.0,3.0)	0.7	0.5	5
5	73.0	(3.0,3.0)	0.5	0.3	6
6	73.0	(3.0,3.0)	0.3	0.1	8

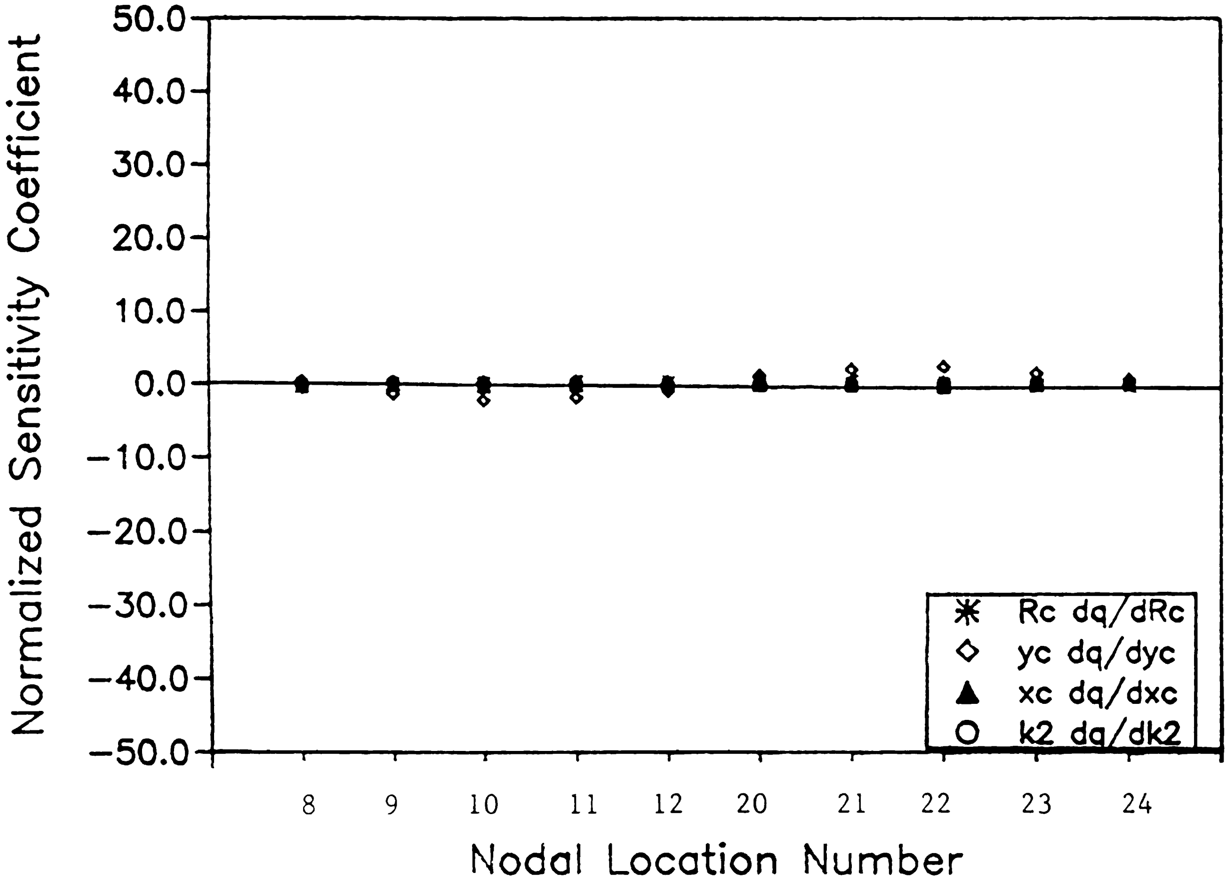

Figure (4.11) - Temperature sensitivity coefficients corresponding to $R_c = 0.5$.

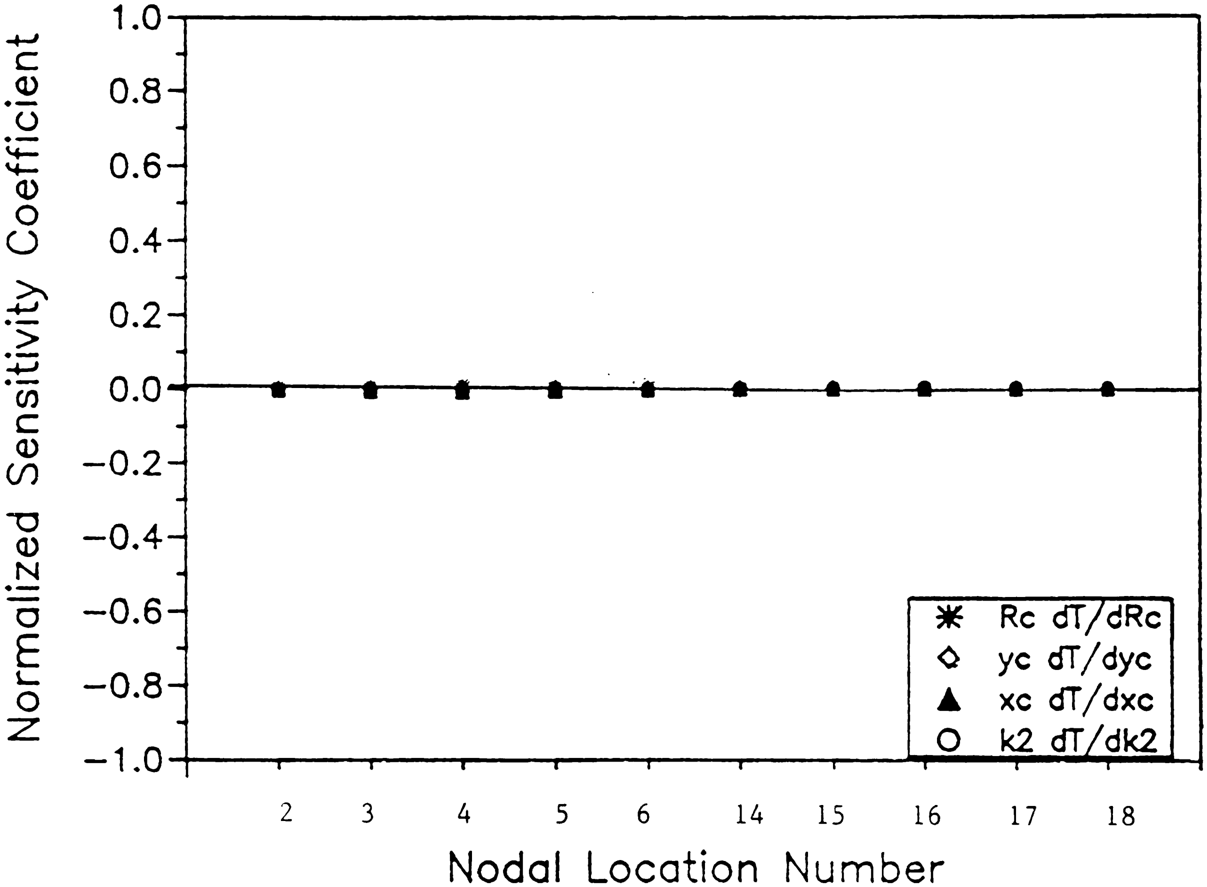

Figure (4.12) - Heat flux sensitivity coefficients corresponding to $R_c = 0.5$.

4.2) Elasticity

Consider the problem shown in **Figure (2.5)**. The location, the radius, the shear modulus and the Poisson's ratio of the circular inclusion are to be estimated simultaneously using the displacements measured on the portion of the boundary where traction is specified and/or the tractions measured on the portion of the boundary where displacement is specified. The "experiment" is simulated as described in the previous section.

The first question addressed is the influence of the initial guesses on convergence. The first attempt was to estimate all five parameters, but it failed despite many different choices of the first guess of the unknown parameters and induced boundary conditions. Next the estimation of four parameters was attempted and it was observed that estimation of any combination of four of the five parameters is possible. A total of 40 sets of initial guesses were examined and "experimental values" at all the boundary nodal locations were used. Convergence was defined in accordance with equations (3.1.19). The first problem investigated is shown in **Figure (2.5)**. Estimation of the location, shear modulus and Poisson's ratio of the circular inclusion with known size, using all measured displacements in the x_1 and x_2 directions and tractions in the x_1 and x_2 directions is attempted and as is shown in **Table (4.10)**. Note that 15.0% of the cases considered converged whereas 85.0% of the cases diverged. The reason for divergence becomes apparent after 3 or 4 iterations and can be classified into one of three groups: (1) the determinant of [P] for an iteration is zero; (2) the estimated values of (x_c , y_c) and R_c for an iteration are unrealistic, i.e. the estimated inclusion does not lie entirely within the matrix domain; (3) the estimated value of the inclusion Poisson's ratio for an iteration is less than zero or greater than 0.5. All the above three groups are identified during the estimation process and the program will stop if any of the above situations occurs. For the above problem 40.0% of the cases diverged

Table (4.10) Influence of the Initial Guesses on Convergence Using Displacement and Traction Measurements (Elasticity Example Problem #1).

Case #	Initial guesses G_2	ν_2	(x_c , y_c)	Converged Iteration #	Diverged Group #
1	2.0E+06	0.30	(2.5,2.5)		(1)
2	1.5E+06	0.30	(2.5,2.5)	15	
3	1.2E+06	0.30	(2.5,2.5)		(2)
4	0.8E+06	0.30	(2.5,2.5)		(2)
5	0.5E+06	0.30	(2.5,2.5)		(1)
6	2.0E+06	0.25	(2.5,2.5)		(2)
7	1.5E+06	0.25	(2.5,2.5)		(3)
8	1.2E+06	0.25	(2.5,2.5)		(3)
9	0.8E+06	0.25	(2.5,2.5)	8	
10	0.5E+06	0.25	(2.5,2.5)		(1)
11	2.0E+06	0.15	(2.5,2.5)		(2)
12	1.5E+06	0.15	(2.5,2.5)	14	
13	1.2E+06	0.15	(2.5,2.5)		(1)
14	0.8E+06	0.15	(2.5,2.5)		(1)
15	0.5E+06	0.15	(2.5,2.5)		(1)
16	2.0E+06	0.10	(2.5,2.5)		(2)
17	1.5E+06	0.10	(2.5,2.5)		(3)
18	1.2E+06	0.10	(2.5,2.5)	9	
19	0.8E+06	0.10	(2.5,2.5)		(1)
20	0.5E+06	0.10	(2.5,2.5)		(1)
21	2.0E+06	0.30	(3.5,3.5)		(2)
22	1.5E+06	0.30	(3.5,3.5)	12	
23	1.2E+06	0.30	(3.5,3.5)		(2)
24	0.8E+06	0.30	(3.5,3.5)		(1)
25	0.5E+06	0.30	(3.5,3.5)		(3)
26	2.0E+06	0.25	(3.5,3.5)		(1)
27	1.5E+06	0.25	(3.5,3.5)	10	
28	1.2E+06	0.25	(3.5,3.5)		(3)
29	0.8E+06	0.25	(3.5,3.5)		(3)
30	0.5E+06	0.25	(3.5,3.5)		(3)
31	2.0E+06	0.15	(3.5,3.5)		(1)
32	1.5E+06	0.15	(3.5,3.5)		(1)
33	1.2E+06	0.15	(3.5,3.5)		(2)
34	0.8E+06	0.15	(3.5,3.5)		(1)
35	0.5E+06	0.15	(3.5,3.5)		(1)
36	2.0E+06	0.10	(3.5,3.5)		(2)
37	1.5E+06	0.10	(3.5,3.5)		(2)
38	1.2E+06	0.10	(3.5,3.5)		(2)
39	0.8E+06	0.10	(3.5,3.5)		(1)
40	0.5E+06	0.10	(3.5,3.5)		(1)

due to (1), 27.5% of the cases diverged due to (2), and 17.5% of the cases diverged due to (3). The number of iterations ranged from 8 to 15. The same problem was investigated using only the displacement measurements at all nodal locations where traction was specified and, as is shown in **Table (4.11)**, 67.5% of the cases converged, 27.5% of the cases diverged due to (1), and 5.0% of the cases diverged due to (2). The number of iterations ranged from 5 to 20. As the result of this observation, another problem with fewer displacement boundary conditions, shown in **Figure (2.6)**, was examined. 18 displacements in the x_1 direction and 18 displacements in the x_2 direction were used and, as is shown in **Table (4.12)**, 90.0% of the cases converged. 2.5% of the cases diverged due to (1), and 7.5% of the cases diverged due to (3). A third problem, shown in **Figure (2.7)**, with an equal number of displacement boundary conditions and traction boundary conditions, was investigated. All the cases involving different first guesses of the unknown parameters diverged. It is concluded that if the body under investigation has more traction boundary conditions, the estimation of the unknown parameters is more successful. The sensitivity of traction in the x_2 direction with respect to parameters G_2 and ν_2 is shown in **Figure (4.13)**. It is observed that the sensitivity coefficients of t_2 with respect to Poisson's ratio and shear modulus are identical in shape and are linearly dependent. This would lead to difficulty when simultanious estimation of these two parameters is attempted by using the measurements of t_2 as extra information. **Figure (4.14)** shows the sensitivity of t_2 with respect to the location of the circular inclusion and it is observed that the sensitivity coefficients corresponding to x_c and y_c are not linearly dependent.

Since the second problem, shown in **Figure (2.6)**, resulted in the best convergence, it is used to investigate the remaining issues. **Figure (4.15)** through **Figure (4.24)** show the sensitivity of displacements in x_1 and x_2 directions with respect to the four parameters being estimated. They correspond to the exact values of the parameters. **Figure (4.15)** and **Figure (4.17)** show that the sensitivities of u_1 with

Table (4.11) Influence of the Initial Guesses on Convergence Using Displacement Measurements (Elasticity Example Problem #1).

Case #	Initial guesses G_2	ν_2	(x_c , y_c)	Converged Iteration #	Diverged Group #
1	2.0E+06	0.30	(2.5,2.5)	9	
2	1.5E+06	0.30	(2.5,2.5)	20	
3	1.2E+06	0.30	(2.5,2.5)	6	
4	0.8E+06	0.30	(2.5,2.5)	6	
5	0.5E+06	0.30	(2.5,2.5)		(1)
6	2.0E+06	0.25	(2.5,2.5)	9	
7	1.5E+06	0.25	(2.5,2.5)	11	
8	1.2E+06	0.25	(2.5,2.5)	6	
9	0.8E+06	0.25	(2.5,2.5)	6	
10	0.5E+06	0.25	(2.5,2.5)		(1)
11	2.0E+06	0.15	(2.5,2.5)		(1)
12	1.5E+06	0.15	(2.5,2.5)	8	
13	1.2E+06	0.15	(2.5,2.5)	6	
14	0.8E+06	0.15	(2.5,2.5)		(1)
15	0.5E+06	0.15	(2.5,2.5)		(1)
16	2.0E+06	0.10	(2.5,2.5)	7	
17	1.5E+06	0.10	(2.5,2.5)	9	
18	1.2E+06	0.10	(2.5,2.5)	5	
19	0.8E+06	0.10	(2.5,2.5)	7	
20	0.5E+06	0.10	(2.5,2.5)		(1)
21	2.0E+06	0.30	(3.5,3.5)		(2)
22	1.5E+06	0.30	(3.5,3.5)	15	
23	1.2E+06	0.30	(3.5,3.5)	11	
24	0.8E+06	0.30	(3.5,3.5)	6	
25	0.5E+06	0.30	(3.5,3.5)		(1)
26	2.0E+06	0.25	(3.5,3.5)		(2)
27	1.5E+06	0.25	(3.5,3.5)	7	
28	1.2E+06	0.25	(3.5,3.5)	11	
29	0.8E+06	0.25	(3.5,3.5)	6	
30	0.5E+06	0.25	(3.5,3.5)		(1)
31	2.0E+06	0.15	(3.5,3.5)	15	
32	1.5E+06	0.15	(3.5,3.5)	6	
33	1.2E+06	0.15	(3.5,3.5)	6	
34	0.8E+06	0.15	(3.5,3.5)	9	
35	0.5E+06	0.15	(3.5,3.5)		(1)
36	2.0E+06	0.10	(3.5,3.5)		(1)
37	1.5E+06	0.10	(3.5,3.5)	6	
38	1.2E+06	0.10	(3.5,3.5)	5	
39	0.8E+06	0.10	(3.5,3.5)	6	
40	0.5E+06	0.10	(3.5,3.5)		(1)

Table (4.12) Influence of the Initial Guesses on Convergence (Elasticity Example Problem #2).

Case #	Initial guesses G_2	ν_2	(x_c , y_c)	Converged Iteration #	Diverged Group #
1	2.0E+06	0.30	(2.5,2.5)	12	
2	1.5E+06	0.30	(2.5,2.5)	7	
3	1.2E+06	0.30	(2.5,2.5)	5	
4	0.8E+06	0.30	(2.5,2.5)	5	
5	0.5E+06	0.30	(2.5,2.5)	6	
6	2.0E+06	0.25	(2.5,2.5)	7	
7	1.5E+06	0.25	(2.5,2.5)	7	
8	1.2E+06	0.25	(2.5,2.5)	5	
9	0.8E+06	0.25	(2.5,2.5)	5	
10	0.5E+06	0.25	(2.5,2.5)	7	
11	2.0E+06	0.15	(2.5,2.5)		(1)
12	1.5E+06	0.15	(2.5,2.5)	9	
13	1.2E+06	0.15	(2.5,2.5)	6	
14	0.8E+06	0.15	(2.5,2.5)	6	
15	0.5E+06	0.15	(2.5,2.5)	8	
16	2.0E+06	0.10	(2.5,2.5)		(3)
17	1.5E+06	0.10	(2.5,2.5)	7	
18	1.2E+06	0.10	(2.5,2.5)	6	
19	0.8E+06	0.10	(2.5,2.5)	6	
20	0.5E+06	0.10	(2.5,2.5)	9	
21	2.0E+06	0.30	(3.5,3.5)	18	
22	1.5E+06	0.30	(3.5,3.5)	8	
23	1.2E+06	0.30	(3.5,3.5)	5	
24	0.8E+06	0.30	(3.5,3.5)	6	
25	0.5E+06	0.30	(3.5,3.5)	8	
26	2.0E+06	0.25	(3.5,3.5)		(3)
27	1.5E+06	0.25	(3.5,3.5)	7	
28	1.2E+06	0.25	(3.5,3.5)	5	
29	0.8E+06	0.25	(3.5,3.5)	6	
30	0.5E+06	0.25	(3.5,3.5)	8	
31	2.0E+06	0.15	(3.5,3.5)	11	
32	1.5E+06	0.15	(3.5,3.5)	11	
33	1.2E+06	0.15	(3.5,3.5)	5	
34	0.8E+06	0.15	(3.5,3.5)	6	
35	0.5E+06	0.15	(3.5,3.5)	9	
36	2.0E+06	0.10	(3.5,3.5)		(3)
37	1.5E+06	0.10	(3.5,3.5)	9	
38	1.2E+06	0.10	(3.5,3.5)	6	
39	0.8E+06	0.10	(3.5,3.5)	6	
40	0.5E+06	0.10	(3.5,3.5)	9	

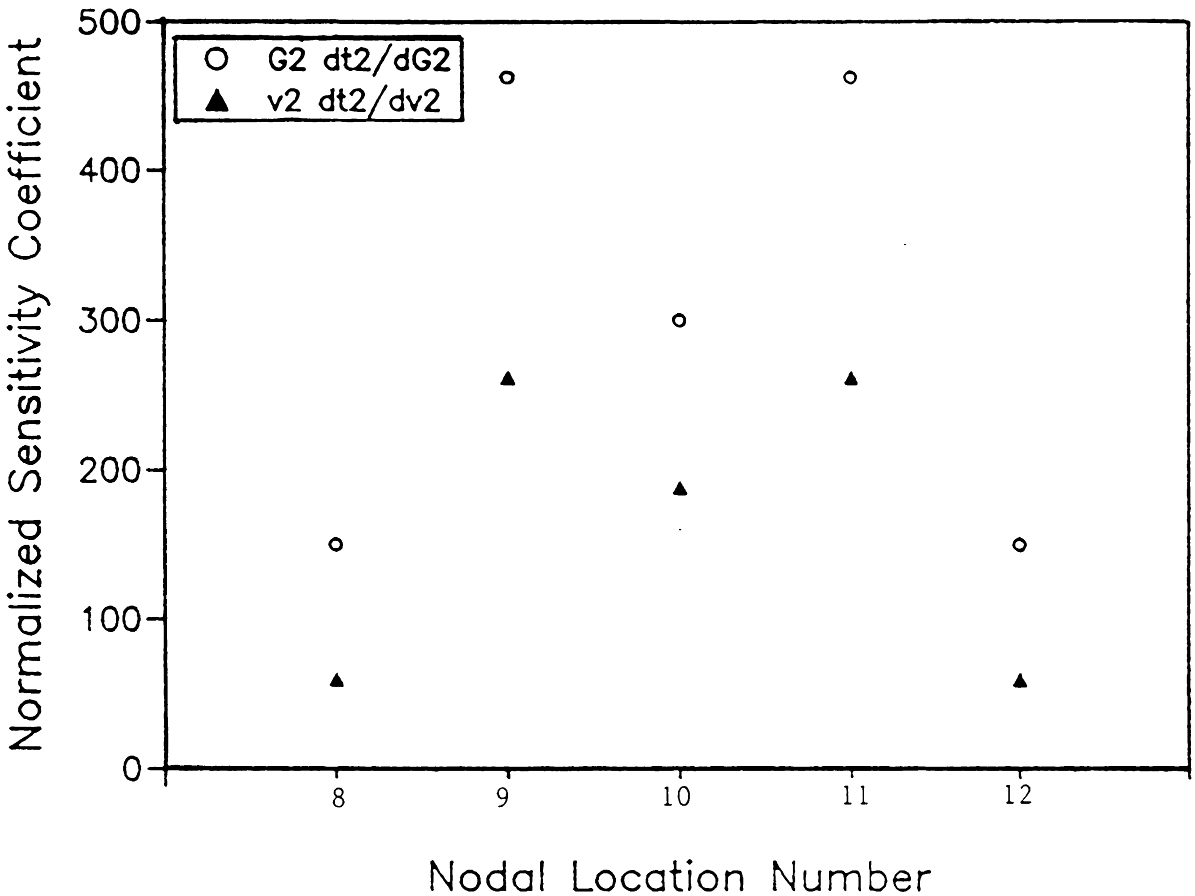

Figure (4.13) - Sensitivity of boundary t_2 values with respect to G_2 and ν_2 (elasticity example problem #1).

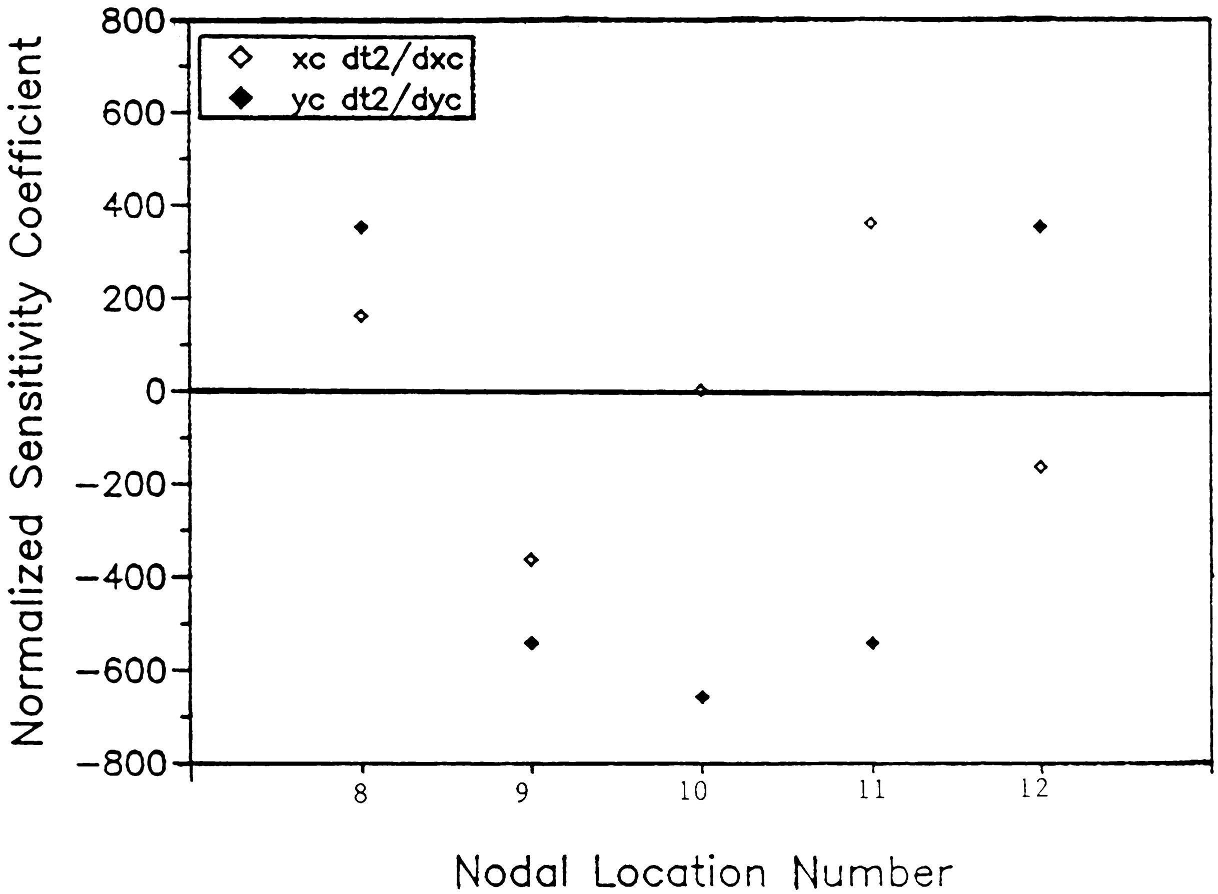

Figure (4.14) - Sensitivity of boundary t_2 values with respect to x_c and y_c (elasticity example problem #1).

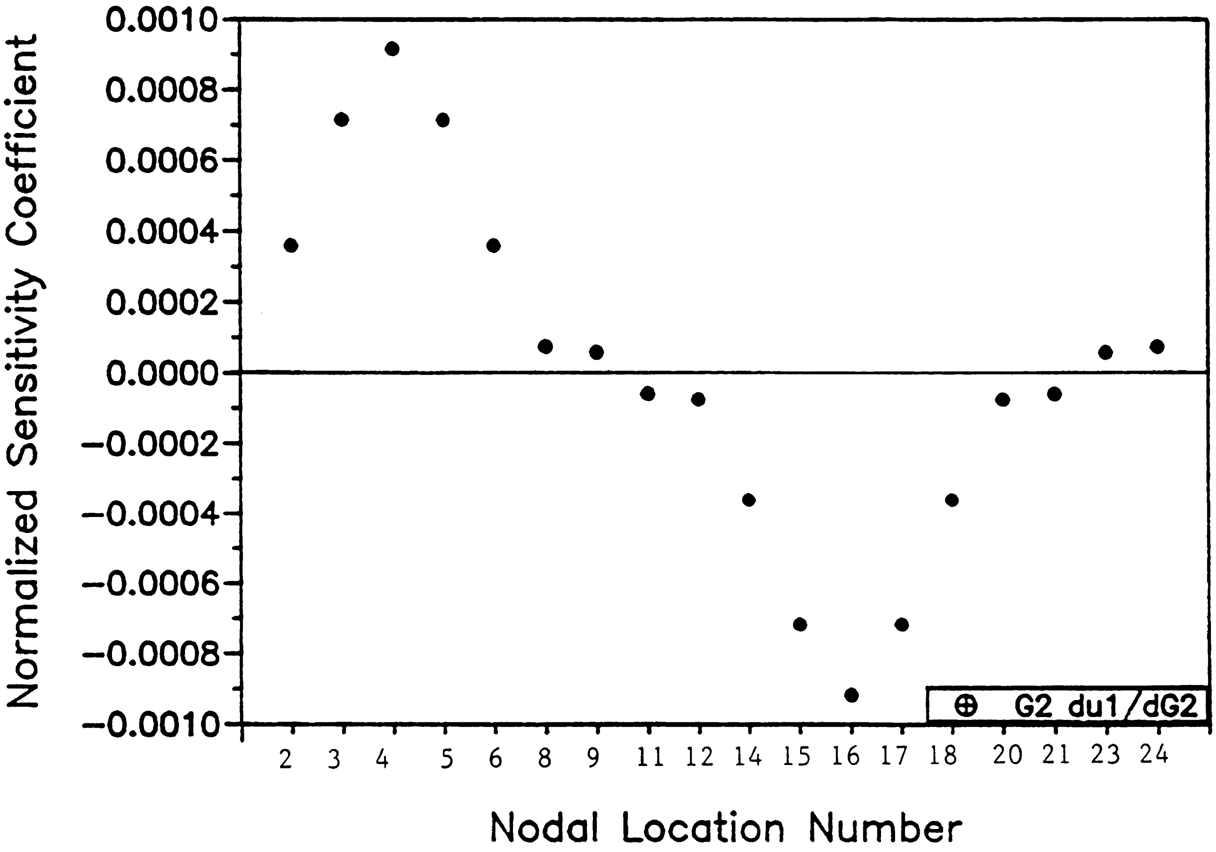

Figure (4.15) - Sensitivity of boundary u_1 values with respect to G_2 .

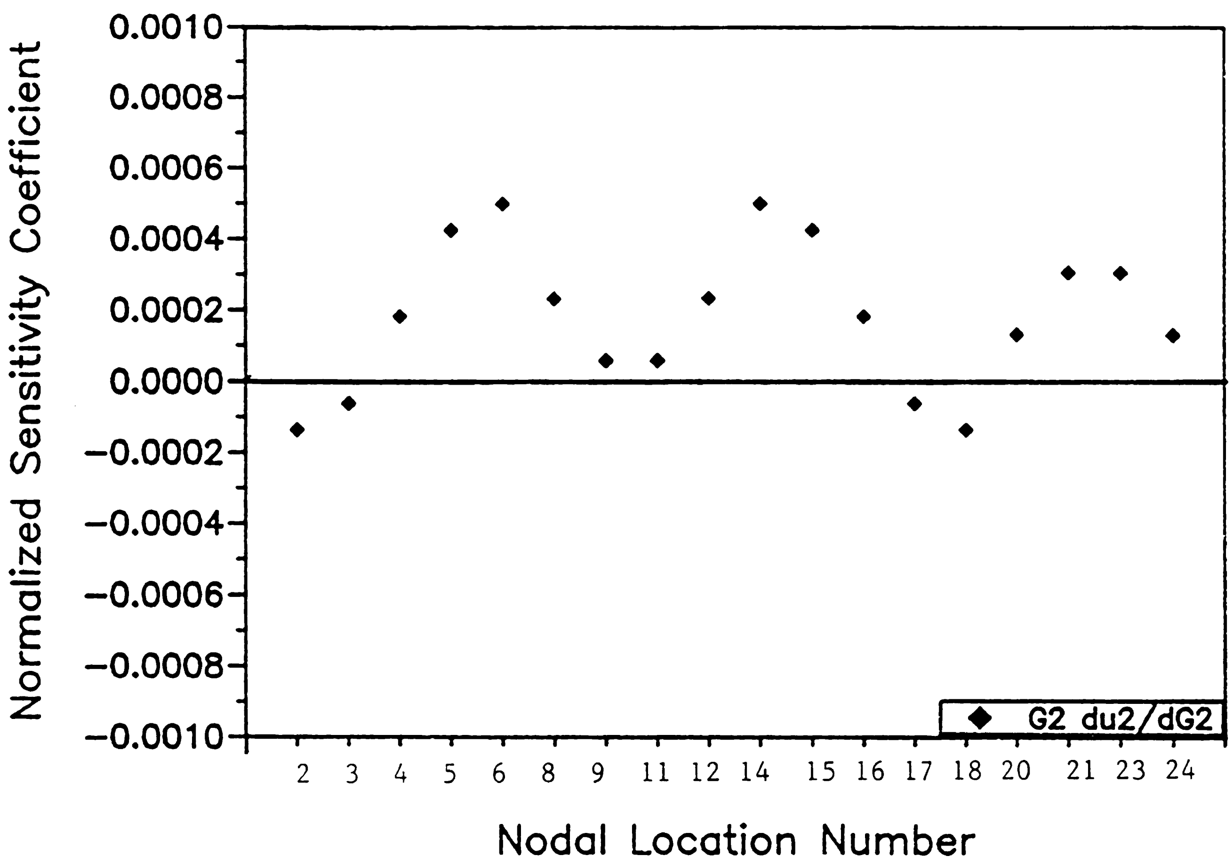

Figure (4.16) - Sensitivity of boundary u_2 values with respect to G_2 .

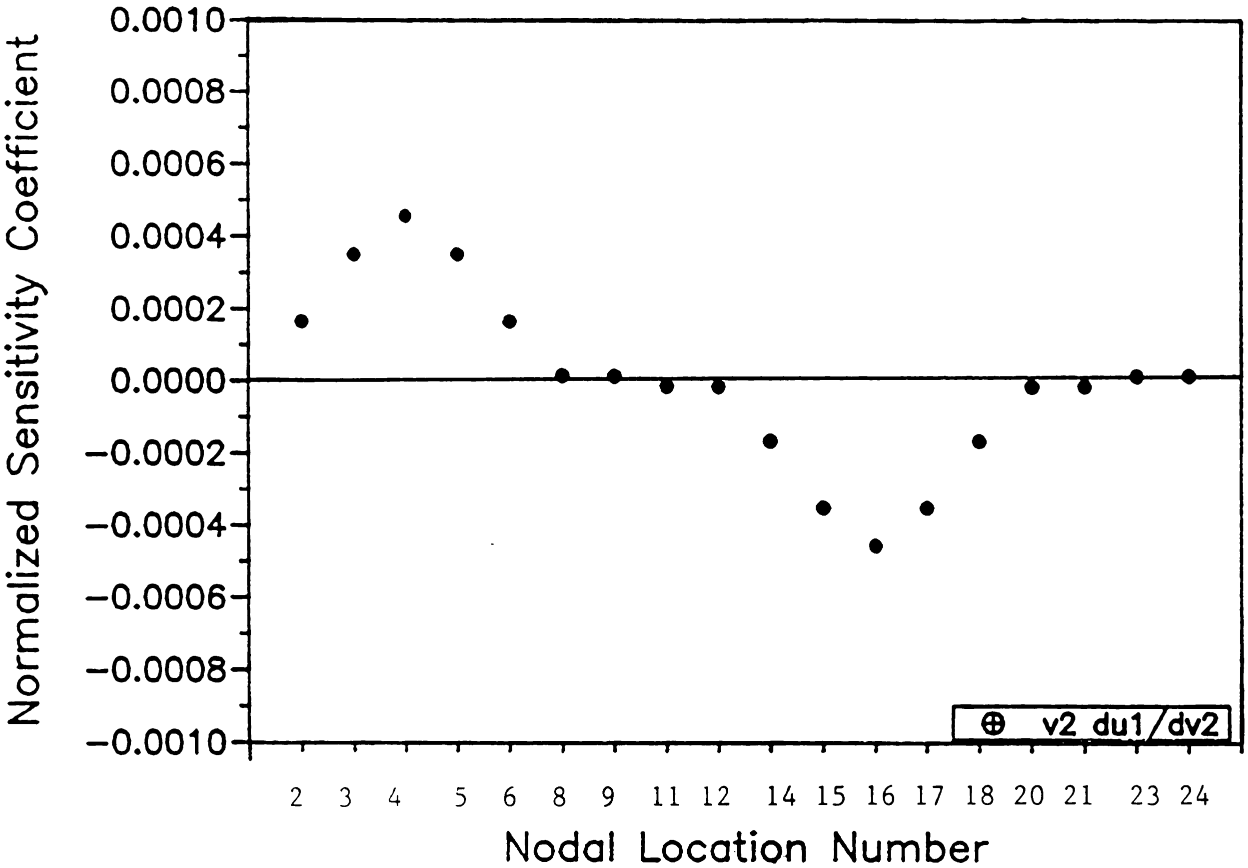

Figure (4.17) - Sensitivity of boundary u_1 values with respect to v_2 .

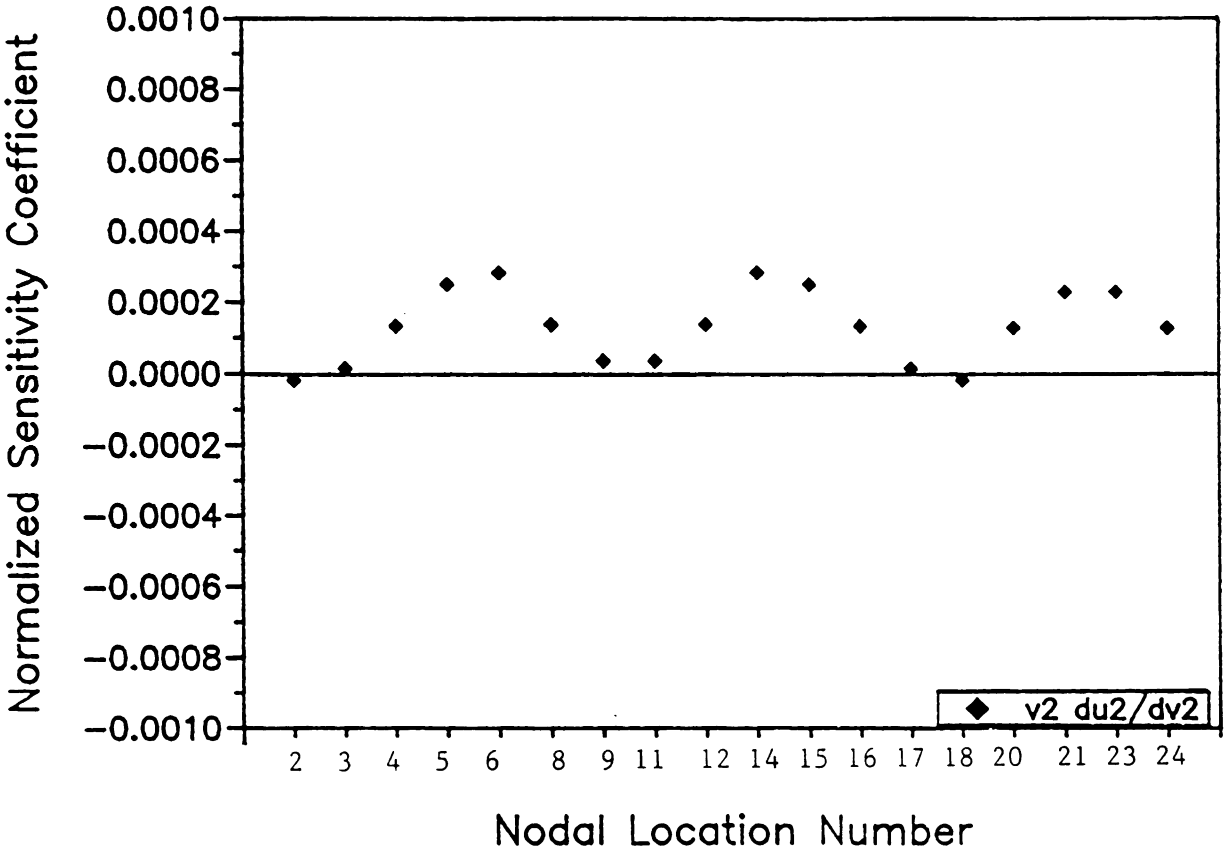

Figure (4.18) - Sensitivity of boundary u_2 values with respect to v_2 .

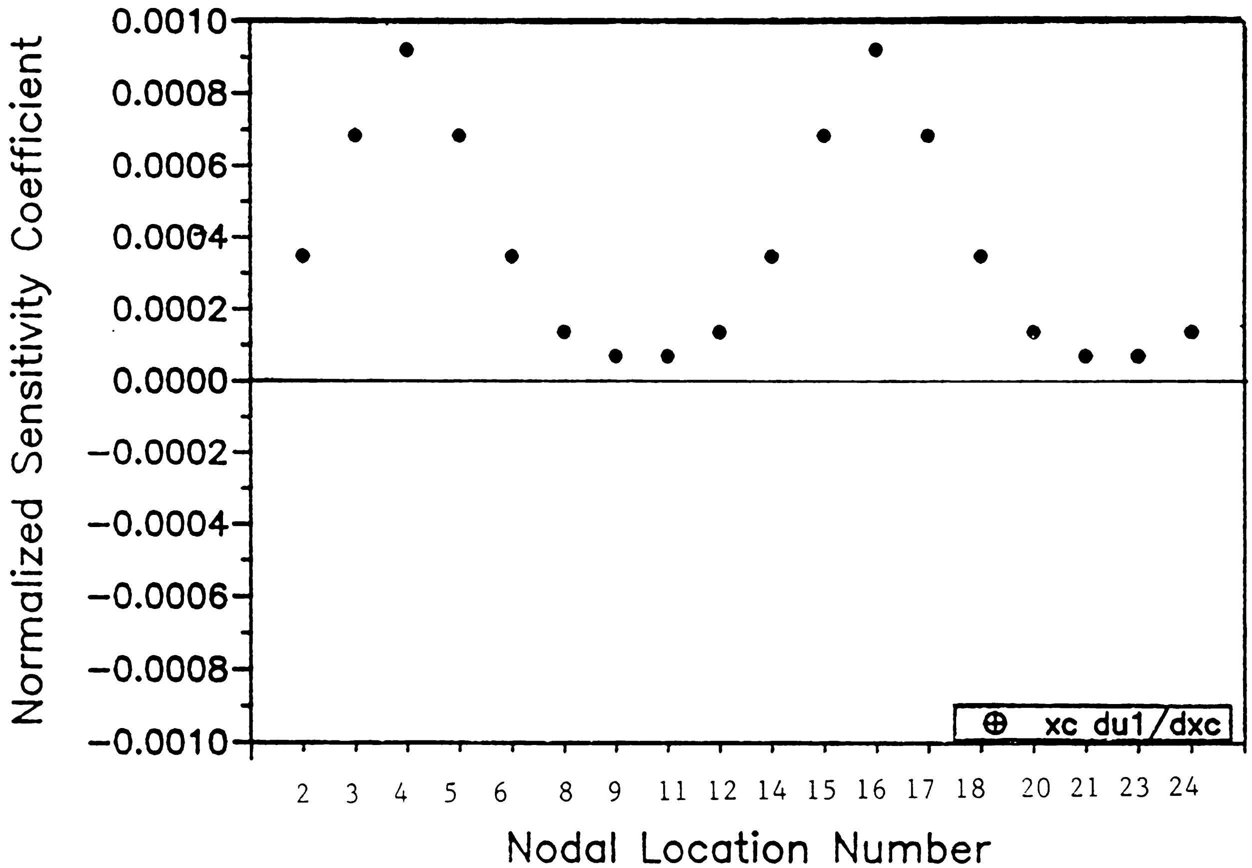

Figure (4.19) - Sensitivity of boundary u_1 values with respect to x_c .

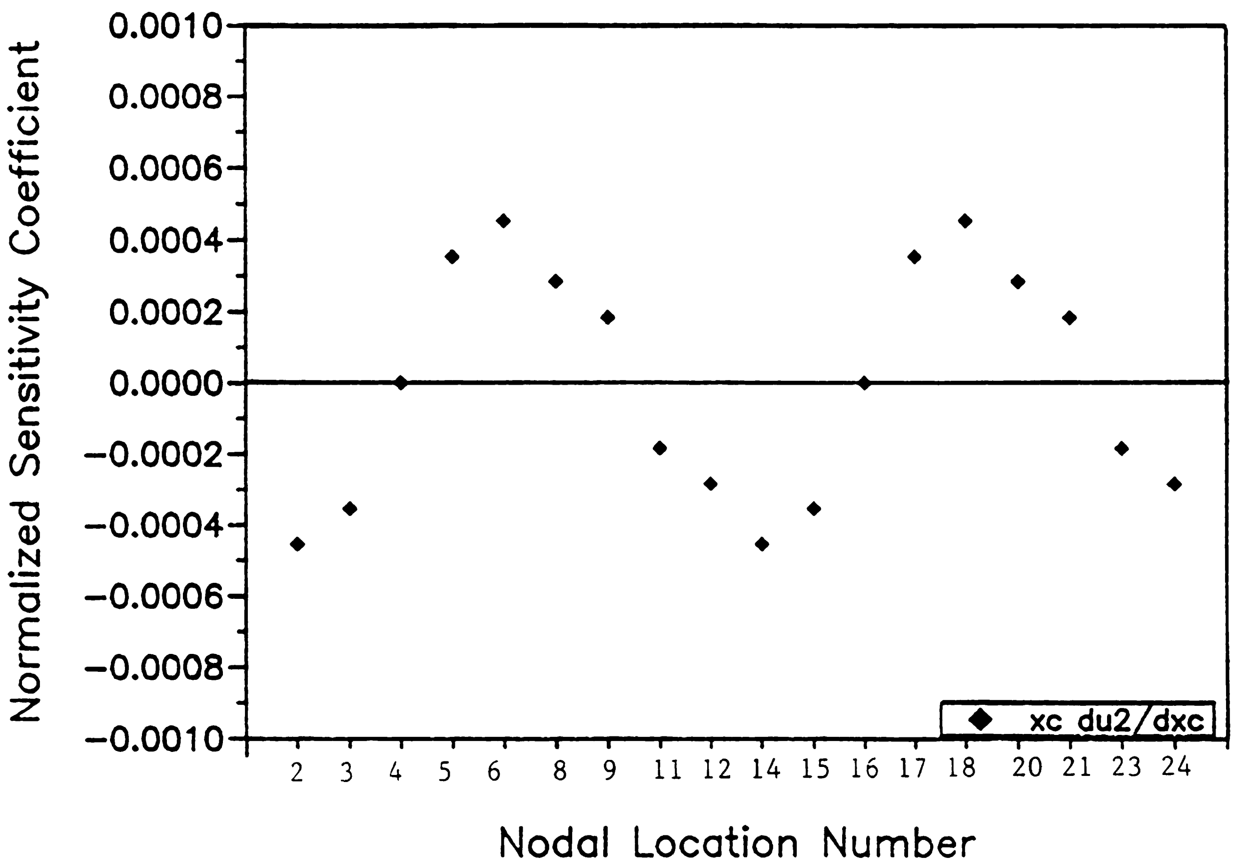

Figure (4.20) - Sensitivity of boundary u_2 values with respect to x_c .

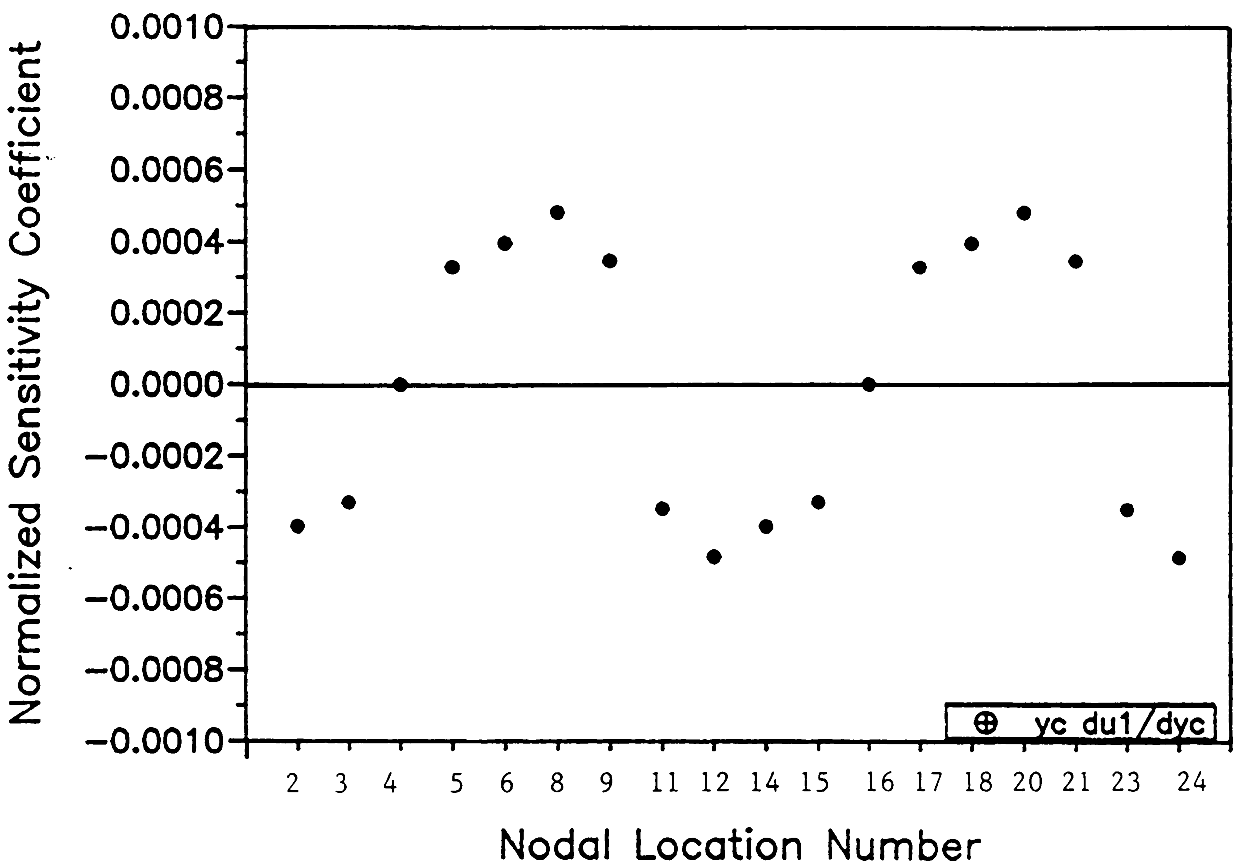

Figure (4.21) - Sensitivity of boundary u_1 values with respect to y_c .

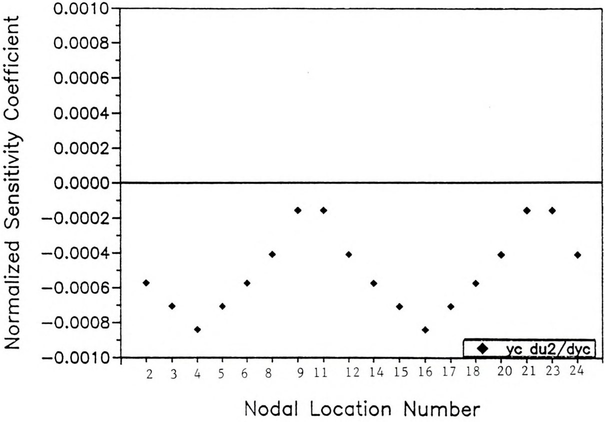

Figure (4.22) - Sensitivity of boundary u_2 values with respect to y_c .

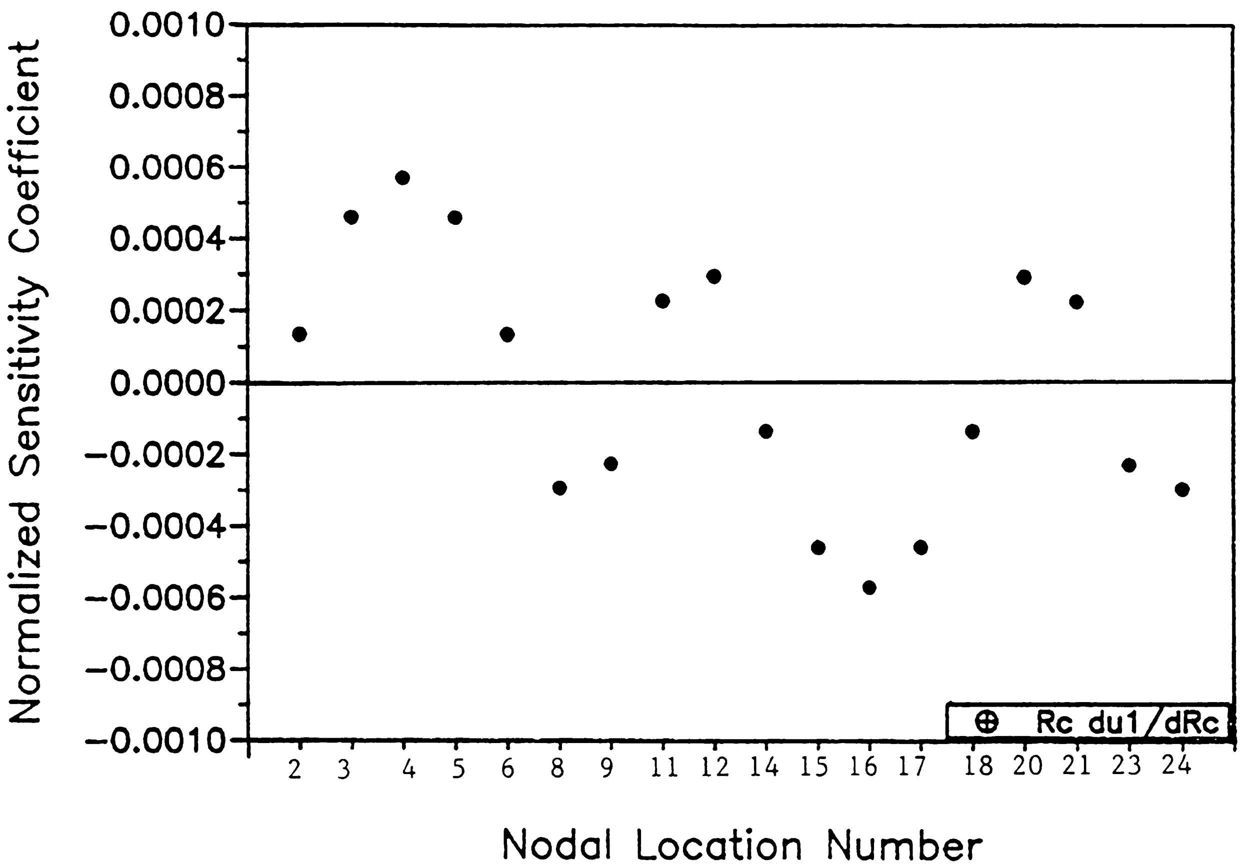

Figure (4.23) - Sensitivity of boundary u_1 values with respect to R_c .

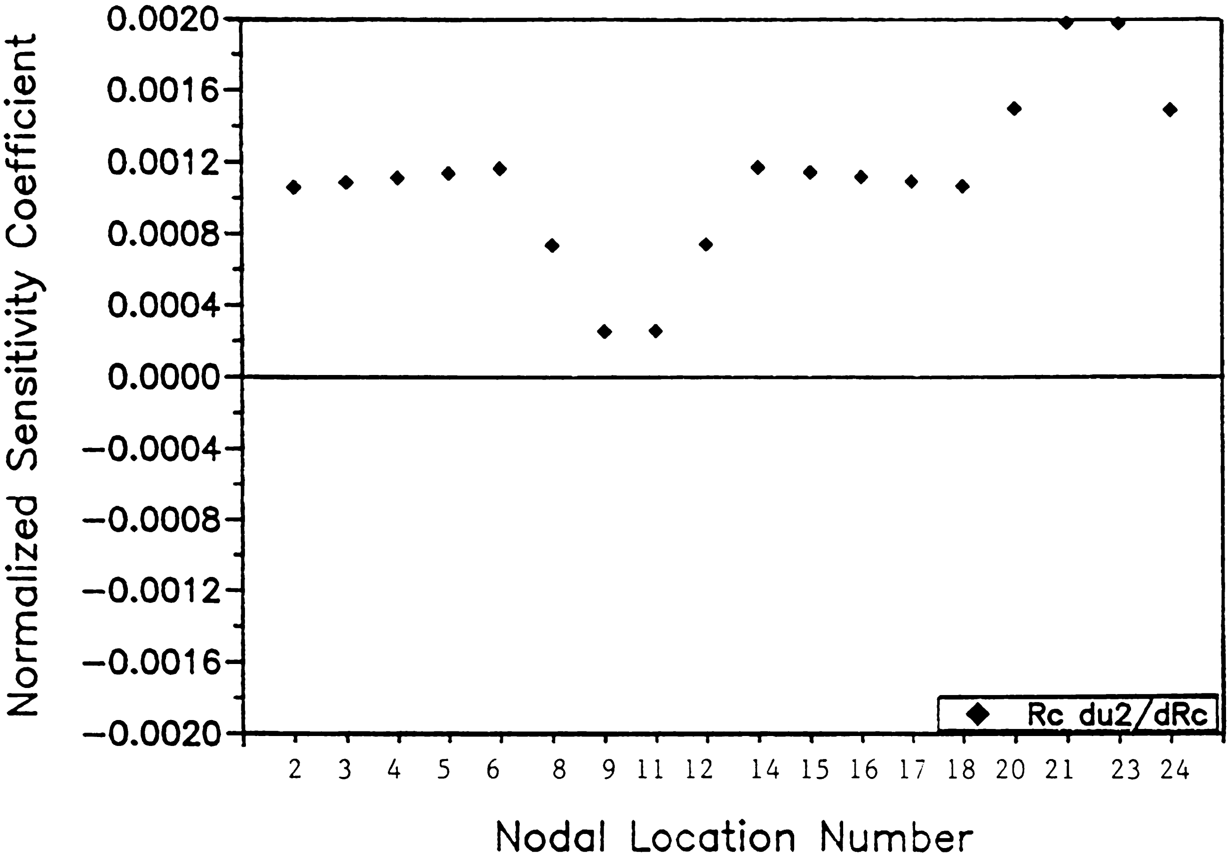

Figure (4.24) - Sensitivity of boundary u_2 values with respect to R_c .

respect to G_2 and ν_2 are very similar in shape. Similarly **Figure (4.16)** and **Figure (4.18)** reveal the same observation about the sensitivities of u_2 with respect to G_2 and ν_2 . Also **Figure (4.20)** and **Figure (4.21)** show that the sensitivty of u_2 with respect to x_c is similar in shape to the sensitivity of u_1 with respect to y_c . All of these combinations lead to the problem of linear dependence of the columns corresponding to the above parameters in the [P] matrix. Comparing the sensitivities of temperature with respect to the sought parameters in the heat transfer problem and the sensitivities of displacement with respect to the sought parameters in the elasticity problem shows that the temperature sensitivities are much larger in magnitude than the displacement sensitivities. The implication of this is apparent when the number of cases which diverged because the determinant of [P] becomes zero, group #(1), in the heat transfer and elasticity problems are compared. It is found that in the elasticity problem, the determinant of [P] becomes zero more frequently. Since the initial guesses given by case #3 of **Table (4.12)** resulted in the most rapid convergence, they are used in addressing all of the following issues.

The second question addressed is the number and combination of surface displacements required to simultaneously estimate the four unknown parameters, i.e. shear modulus, Poisson's ratio, and location of the inclusion. The minimum number of measurements needed to estimate the above four parameters is 20. We considered five different combinations of ten displacements in the x_1 direction and ten displacements in the x_2 direction and, as is shown in **Table (4.13)**, only one case converged.

Estimation of only two parameters, i.e. shear modulus and Poisson's ratio of the circular inclusion with known location and size is investigated next. **Table (4.14)** shows that by selecting the right locations on the surface of the boundary, it is possible to estimate the above two parameters by measuring only eight displacements. This requires analyzing the plots of the sensitivity coefficients, **Figure (4.15)** through **Figure (4.18)**, and selecting the nodal locations with the highest value of u_1 and u_2

Table (4.13) Estimating the Unknown Parameters Using 10 Measured Displacements in the x_1 Direction and 10 Measured Displacements in the x_2 Direction (Elasticity Example Problem #2).

Case #	Nodal Location Numbers	Converged Iteration #	Diverged Group #
1	u_1 at 2,3,4,5,6,14,15,16,17,18 u_2 at 2,3,4,5,6,14,15,16,17,18	5	
2	u_1 at 2,3,4,5,6,8,9,11,12,16 u_2 at 2,3,4,5,6,8,9,11,12,16		(2)
3	u_1 at 2,3,4,5,6,20,21,23,24,16 u_2 at 2,3,4,5,6,20,21,23,24,16		(2)
4	u_1 at 14,15,16,17,18,20,21,23,24,4 u_2 at 14,15,16,17,18,20,21,23,24,4		(2)
5	u_1 at 14,15,16,17,18,8,9,11,12,4 u_2 at 14,15,16,17,18,8,9,11,12,4		(2)

Table (4.14) Estimating G_2 and ν_2 Using Displacement Measurements (Elasticity Example Problem #2).

Case #	Nodal Location Numbers	Converged Iteration #	Diverged Group #
1	u_1 at 2,3,4,5,6,20,21,23,24 u_2 at 2,3,4,5,6,20,21,23,24	6	
2	u_1 at 2,3,4,5,6,8,9,11,12 u_2 at 2,3,4,5,6,8,9,11,12		(1)
3	u_1 at 14,15,16,17,18,20,21,23,24 u_2 at 14,15,16,17,18,20,21,23,24	6	
4	u_1 at 14,15,16,17,18,8,9,11,12 u_2 at 14,15,16,17,18,8,9,11,12		(1)
5	u_1 at 8,9,11,12,20,21,23,24 u_2 at 8,9,11,12,20,21,23,24		(1)
6	u_1 at 3,4,16,17 u_2 at 14,15,22,23	6	
7	u_1 at 3,4,5,15,16,17 u_2 at 22		(1)
8	u_1 at 3,4,16 u_2 at 14,15,22		(1)

sensitivities with respect to the two parameters. **Table (4.14)** shows that even with 18 displacement measurements, if the locations are not selected carefully, the estimation will diverge (cases #2 and #4). Estimation of G_2 and ν_2 using less than eight measurements was not successful.

The final question addressed is the effect that the inevitable errors in experimental measurements will have on the ability to estimate the sought parameters. For this case, the "experiment" is simulated as follows. The body is first analyzed by the boundary element method using the exact values of the four parameters. Then random errors are added to the computed boundary displacements, and these are taken to be the "measured" data. The statistical assumptions regarding the introduced errors are the same as described in the previous section. **Table (4.15)** shows the results when 18 displacements in the x_1 direction and 18 displacements in the x_2 direction, with different percent errors were used to estimate the four unknown parameters. It is observed that as the %error increases, the number of iterations also increases, but it is possible to estimate the unknown parameters with experimental errors as high as 4.0%. All the results in **Table (4.15)** are rounded off to three significant figures.

Table (4.15) Influence of Experimental Errors on the Estimation (Elasticity Example Problem #2).

		Nodal Locations where u_1 and u_2 Are Measured 2,3,4,5,6,8,9,11,12,14,15,16,17,18,20,21,23,24
Case #	% Error	Iteration #, And Converged Values of Parameters
1	0.0	5 , G_2=1.000E+06, ν_2=0.200, (x_c , y_c)=(3.00,3.00)
2	0.5	8 , G_2=1.015E+06, ν_2=0.195, (x_c , y_c)=(3.00,3.00)
3	1.0	10 , G_2=1.029E+06, ν_2=0.190, (x_c , y_c)=(3.01,2.99)
4	2.0	13 , G_2=1.049E+06, ν_2=0.183, (x_c , y_c)=(3.03,2.97)
5	3.0	22 , G_2=0.966E+06, ν_2=0.217, (x_c , y_c)=(3.03,3.01)
6	4.0	32 , G_2=0.967E+06, ν_2=0.217, (x_c , y_c)=(3.03,2.99)

Chapter 5

Conclusions and Recommendations

A technique has been proposed which couples the boundary element and parameter estimation methods for the purpose of characterizing the interior of an inhomogeneous body utilizing surface measurements only. The parameter study presented here addressed several questions which arise regarding implementation of this technique in the heat transfer and elasticity problems. Although the technique does not always converge, the cases which do converge give excellent results. Also, the method never converges to an incorrect solution. Based on the results of this investigation, the following conclusions are drawn.

1. It is possible to estimate the four unknown parameters simultaneously using only four measurements in the heat transfer problem.
2. It is better to use two temperature and two heat flux measurements than four temperature or four heat flux measurements.
3. As the number of measurements increases, the percentage of cases which converge increases.
4. Heat flux measurements with experimental errors give better results than temperature measurements with experimental errors.
5. It is possible to estimate parameters corresponding to a very small inclusion.
6. Better results are obtained for elasticity problems using more displacement measurements.
7. Estimating the unknown parameters in the heat transfer problem appears to be easier than in the elasticity problem.

8. More success was achieved in estimating only the shear modulus and Poisson's ratio of the inclusion in the elasticity problem.

9. It would appear that the best procedure would be to estimate the thermal conductivity, size, and location of the circular inclusion using the boundary temperature and/or heat flux measurements and then, taking the location and size of the inclusion as known, to estimate the mechanical properties of the inclusion using the boundary-measured displacements.

It should be emphasized that for this nonlinear inverse problem, the sensitivity coefficients depend on the current guess of the parameters. Thus if one wants to use the sensitivity coefficients as a predictor of "best" measurement locations, one must recognize that these best locations will change from one iteration to the next. One possible approach would be to test various initial guesses and corresponding sensitivity coefficients *a priori* and to select the initial guesses based on optimal initial sensitivities.

Several additional questions need to be addressed. In particular, the effectiveness of this technique for characterizing more complex situations such as several inclusions or inclusions of unknown shape needs to be examined. Also extension to anisotropy and/or three-dimensional problems would be of practical interest. However, based on the results obtained so far, the method shows considerable promise.

REFERENCES

[1] Brebbia, C.A., and Dominguez J., 1988, *Boundary Elements: An Introductory Course,* Computational Mechanics Publications.

[2] Beck, J.V., and Arnold, K.J., 1977, *Parameter Estimation In Engineering And Science,* John Wiley and Sons.

[3] Murai, T., and Kagawa, Y., 1986, "Boundary element iterative techniques for determining the interface boundary between two Laplace domains: a basic study of impedance plethysmography as an inverse problem", *Intl. J. Num. Meth. Engrg.,* Vol. **23**, pp. 35-47.

[4] Ohnaka, K., and Uosaki, K., 1987, "Simultaneous identification of the external input and parameters of diffusion type distributed parameter systems", *Intl. J. Control,* Vol. **46**, pp. 889-895.

[5] Dulikravich, G.S., 1988, "Inverse design and active control concepts in strong unsteady heat conduction", *Appl. Mech. Rev., Vol.* **41**, pp. 270-277.

[6] Tanaka, M., and Yamagiwa, K., 1989, "A boundary element method for some inverse problems in elastodynamics", *Appl. Math. Modelling,* Vol. **13**, pp. 307- 312.

[7] Kishimoto, K., Miyasaka, H., and Aoki, S., 1989, "Boundary element analysis of an inverse problem in galvanic corrosion", *JSME Intl. J. Series I, Vol.* **32**, pp. 256-262.

[8] Gao, Z., and Mura, T., 1989, "On the inversion of residual stresses from surface displacements", *J. Appl. Mech., Vol.* **56**, pp. 508-513.

[9] Das, S., and Mitra, A. K., 1989, "An algorithm for the solution of inverse Laplace problems using BEM (abstract)", *Developments in Mechanics,* Vol. **15**, pp. 525-526.

Appendix A

Computer Program : Heat Transfer

```
      PROGRAM PROPTQ.FOR
C
C CCCCCCCCCCCCCCCCCCCCCCCCCCCCCCCCCCCCCCCCCCCCCCCCCCCCCCCCCCCC
C
C THIS PROGRAM EMPLOYS THE PARAMETER ESTIMATION METHOD TO
C ESTIMATE THE THERMAL CONDUCTIVITY, LOCATION, AND SIZE OF
C A CIRCULAR INCLUSION. THE BOUNDARY ELEMENT METHOD IS
C IMPLEMENTED AS A SUBROUTINE CALLED INCLUS.
C
C THESE ARE REQUIRED INPUTS.
C
C P1                        THERMAL CONDUCTIVITY OF THE MATRIX
C                           MATERIAL
C
C P(1,1)                    THE FIRST GUESS OF THE THERMAL
C                           CONDUCTIVITY OF THE INCLUSION
C
C P(2,1), P(3,1), P(4,1)    THE FIRST GUESSES OF xc, yc, AND Rc
C
C M                         MAXIMUM NUMBER OF ITERATIONS
C
C NUM1                      NUMBER OF TEMPERATURE MEASUREMENTS
C
C NUM2                      NUMBER OF HEAT FLUX MEASUREMENTS
C
```

```
C IP                          NUMBER OF PARAMETERS TO BE ESTIMATED
C
C PERR                        MEAN % ERROR IN THE MEASUREMENTS
C
C NT(NUM1)                    THE NODE NUMBERS WHERE TEMPERATURE
C                             MEASUREMENTS ARE TAKEN
C
C NQ(NUM2)                    THE NODE NUMBERS WHERE HEAT FLUX
C                             MEASUREMENTS ARE TAKEN
C
C UH1(NUM1)                   MEASURED TEMPERATURES
C
C UH2(NUM2)                   MEASURED HEAT FLUXES
C
C CCCCCCCCCCCCCCCCCCCCCCCCCCCCCCCCCCCCCCCCCCCCCCCCCCCCCCCCCCCCCC
C
      IMPLICIT REAL*8 (A-H,O-Z)
      DIMENSION T(300),P(20,20),X(20,20),XT(20,20),XTX(20,20)
      DIMENSION XTY1(4),Y1(100),UH(100),TS(100),XANS(4)
      DIMENSION SQ(100),XNORM(20,20),XTQY2(4),TOT(20,20)
      DIMENSION XTXQ(20,20),XTXTOT(20,20),XTYTOT(4)
      DIMENSION Q(100),QS(100),XQT(20,20),DIFP(10,10)
      DIMENSION XQ(20,20),Y2(100),Y1SQ(100),Y2SQ(100),DCRIT(10)
      DIMENSION UH1(100),UH2(100),NT(100),NQ(100),XQNORM(20,20)
C
      OPEN(5,FILE='INCLTQT.DAT',STATUS='OLD')
      OPEN(10,FILE='INCLTQQ.DAT',STATUS='OLD')
      OPEN(11,FILE='DTK2TQ.OUT',STATUS='NEW')
      OPEN(2,FILE='DTXCTQ.OUT',STATUS='NEW')
      OPEN(3,FILE='DTYCTQ.OUT',STATUS='NEW')
      OPEN(4,FILE='DTRCTQ.OUT',STATUS='NEW')
```

```
      OPEN(13,FILE='DQK2TQ.OUT',STATUS='NEW')
      OPEN(7,FILE='DQXCTQ.OUT',STATUS='NEW')
      OPEN(8,FILE='DQYCTQ.OUT',STATUS='NEW')
      OPEN(9,FILE='DQRCTQ.OUT',STATUS='NEW')
      OPEN(12,FILE='STOTTQ.OUT',STATUS='NEW')
      OPEN(6,FILE='RESLAPTQ.OUT',STATUS='NEW')
C
C CCCCCCCCCCCCCCCCCCCCCCCCCCCCCCCCCCCCCCCCCCCCCCCCCCCCCCCCCCCC
C          ...READ AND CHECK INPUT DATA ....
C CCCCCCCCCCCCCCCCCCCCCCCCCCCCCCCCCCCCCCCCCCCCCCCCCCCCCCCCCCCC
C
      PRINT *,'WHAT IS THE K1 AND FIRST GUESS FOR K2'
      ACCEPT *,P1,P(1,1)
      PRINT *,'WHAT IS THE FIRST GUESS FOR XC, AND YC,
     +AND RC'
      ACCEPT *,P(2,1),P(3,1),P(4,1)
      WRITE(6,*)'K1 & THE FIRST GUESSES OF K2,XC,YC,
     +AND RC ARE'
      WRITE(6,*)P1,P(1,1),P(2,1),P(3,1),P(4,1)
      PRINT *,'ENTER # OF ITER,# OF T & Q DATA,# PARAMETERS,
     +AND ERROR :'
      ACCEPT *, M,NUM1,NUM2,IP,PERR
      PRINT *,'ENTER THE NODE NUMBERS WHERE T MEASUREMENT
     +ARE TAKEN'
      DO 292 I=1,NUM1
      ACCEPT *, NT(I)
292   WRITE(6,*)'THE NODE NUMBERS WHERE T ARE TAKEN = ',NT(I)
      PRINT *,'.ENTER THE NODE NUMBERS WHERE Q MEASUREMENT ARE
     +TAKEN'
C
      DO 291 I=1,NUM2
```

```
      ACCEPT *, NQ(I)
291   WRITE(6,*)'THE NODE NUMBERS WHERE Q ARE TAKEN = ',NQ(I)
C
      WRITE(6,*)'THE ERROR IN MEASUREMENT IS',PERR
C
      DO 299 I=1,NUM1
      READ(5,*)UH1(I)
299   CONTINUE
C
      DO 2811 I=1,NUM2
      READ(10,*)UH2(I)
2811  CONTINUE
C
C CCCCCCCCCCCCCCCCCCCCCCCCCCCCCCCCCCCCCCCCCCCCCCCCCCCCCCCCCCC
C
C SUBROUTINE INCLUS EMPLOYS THE BOUNDARY ELEMENT METHOD
C (USING LINEAR ISOPARAMETRIC ELEMENTS) TO SOLVE THE TWO-
C DIMENSIONAL STEADY HEAT TRANSFER EQUATION, FOR A BODY
C CONTAINING A CIRCULAR INCLUSION.
C
C VARIABLE DEFINITION :
C
C K                          ITERATION VARIABLE
C
C P1                         THERMAL CONDUCTIVITY OF THE MATRIX
C                            MATERIAL
C
C P(1,K)                     THERMAL CONDUCTIVITY OF THE
C                            INCLUSION MATERIAL
C
C P(2,K), P(3,K)             COORDINATES OF THE CENTER OF THE
```

```
C                                   INCLUSION
C
C P(4,K)                            RADIUS OF THE CIRCULAR INCLUSION
C
C NUM1                              NUMBER OF TEMPERATURE MEASUREMENTS
C
C NUM2                              NUMBER OF HEAT FLUX MEASUREMENTS
C
C NT(NUM1)                          THE NODE NUMBERS WHERE TEMPERATURE
C                                   MEASUREMENTS ARE TAKEN
C
C NQ(NUM2)                          THE NODE NUMBERS WHERE HEAT FLUX
C                                   MEASUREMENTS ARE TAKEN
C
C T(NUM1)                           COMPUTED TEMPERATURES
C
C Q(NUM2)                           COMPUTED HEAT FLUXES
C
C THE FOLLOWING INPUT IS REQUIRED.
C
C N(1), N(2)= NUMBER OF BOUNDARY ELEMENTS EMPLOYED FOR REGION
C             ONE AND TWO, RESPECTIVELY
C
C XN(I), YN(I)= THE COORDINATES OF THE OUTER BOUNDARY NODES
C FOR I=1,N(1)
C
C IBC(I), BC(I) = TYPE OF SPECIFIED BOUNDARY CONDITION AT ELEMENT
C                 NODE (1=T, 2=Q) AND VALUE OF SPECIFIED CONDITION.
C                 ENTER ONE ELEMENT PER LINE, 2 CONDITIONS PER LINE,
C                 N(1) LINES. ENTER ONLY FOR OUTER BOUNDARY NODES.
C
```

```
C CCCCCCCCCCCCCCCCCCCCCCCCCCCCCCCCCCCCCCCCCCCCCCCCCCCCCCCCCCCC
C
      DO 300 K=1,M
C
      CALL INCLUS(P1,P(1,K),P(2,K),P(3,K),P(4,K),NUM1,NUM2,
      +NT,NQ,T,Q)
C
      Y1SQT=0.
      DO 103 J=1,NUM1
      Y1(J)=UH1(J)-T(J)
      Y1SQ(J)=Y1(J)**2
      TS(J)=T(J)
103   Y1SQT=Y1SQT+Y1SQ(J)
      Y2SQT=0.
      DO 1033 J=1,NUM2
      Y2(J)=UH2(J)-Q(J)
      Y2SQ(J)=Y2(J)**2
      QS(J)=Q(J)
1033  Y2SQT=Y2SQT+Y2SQ(J)
      STOT=Y1SQT+Y2SQT
      WRITE(6,*)'AFTER K ITERATION STOT IS = ',K,STOT
C
C CCCCCCCCCCCCCCCCCCCCCCCCCCCCCCCCCCCCCCCCCCCCCCCCCCCCCCCCCCCCC
C
C     SENSITIVITY COEFFICIENTS ARE COMPUTED.
C
C CCCCCCCCCCCCCCCCCCCCCCCCCCCCCCCCCCCCCCCCCCCCCCCCCCCCCCCCCCCCC
C
      DELTA=0.0001
      CON=1.0+DELTA
      DO 104 I=1,IP
```

```
      P(I,K)=P(I,K)*CON
      CALL INCLUS(P1,P(1,K),P(2,K),P(3,K),P(4,K),NUM1,NUM2,
     +NT,NQ,T,Q)
      P(I,K)=P(I,K)/CON
      DO 1044 J=1,NUM1
      X(J,I)=(T(J)-TS(J))/(P(I,K)*DELTA)
      XT(I,J)=X(J,I)
      XNORM(J,I)=X(J,I)*P(I,K)
      IF(I.EQ.1) WRITE(11,*)J,XNORM(J,I)
      IF(I.EQ.2) WRITE(2,*)J,XNORM(J,I)
      IF(I.EQ.3) WRITE(3,*)J,XNORM(J,I)
      IF(I.EQ.4) WRITE(4,*)J,XNORM(J,I)
1044  CONTINUE
C
      DO 1045 J=1,NUM2
      XQ(J,I)=(Q(J)-QS(J))/(P(I,K)*DELTA)
      XQT(I,J)=XQ(J,I)
      XQNORM(J,I)=XQ(J,I)*P(I,K)
      IF(I.EQ.1) WRITE(13,*)J,XQNORM(J,I)
      IF(I.EQ.2) WRITE(7,*)J,XQNORM(J,I)
      IF(I.EQ.3) WRITE(8,*)J,XQNORM(J,I)
      IF(I.EQ.4) WRITE(9,*)J,XQNORM(J,I)
1045  CONTINUE
104   CONTINUE
C
      DO 107 I=1,IP
      DO 107 J=1,IP
      XTXTOT(I,J)=0.
      XTXQ(I,J)=0.
107   XTX(I,J)=0.
C
```

```
      DO 108 I=1,IP
      DO 108 J=1,IP
      DO 108 LIJ=1,NUM1
108   XTX(I,J)=XT(I,LIJ)*X(LIJ,J)+XTX(I,J)
C
      DO 1081 I=1,IP
      DO 1081 J=1,IP
      DO 1081 LIJ=1,NUM2
1081  XTXQ(I,J)=XQT(I,LIJ)*XQ(LIJ,J)+XTXQ(I,J)
C
      DO 1088 I=1,IP
      DO 1088 J=1,IP
1088  XTXTOT(I,J)=XTX(I,J)+XTXQ(I,J)
C
      DO 106 I=1,IP
      XTY1(I)=0.
106   XTQY2(I)=0.
C
      DO 1066 I=1,IP
      DO 1066 J=1,NUM1
1066  XTY1(I)=XT(I,J)*Y1(J)+XTY1(I)
C
      DO 1061 I=1,IP
      DO 1061 J=1,NUM2
1061  XTQY2(I)=XQT(I,J)*Y2(J)+XTQY2(I)
C
      DO 1064 I=1,IP
1064  XTYTOT(I)=XTY1(I)+XTQY2(I)
C
C CCCCCCCCCCCCCCCCCCCCCCCCCCCCCCCCCCCCCCCCCCCCCCCCCCCCCCCCCC
C
```

```
C SUBROUTINE FOR MANIPULATION OF MATRICES AND VECTORS
C TOT(IP,IP) = XTXTOT(IP,IP)
C IP = NUMBER OF PARAMETERS
C
C CCCCCCCCCCCCCCCCCCCCCCCCCCCCCCCCCCCCCCCCCCCCCCCCCCCCCCCCCCC
C
      CALL MATEQ (XTXTOT, TOT, IP, IP)
      WRITE (6,*)'THE TOTAL SENSITIVITY MATRIX IS:'
      DO 15 I=1,IP
15    WRITE (6,207) (TOT(I,J), J=1,IP)
      TOT(1,5)=XTYTOT(1)
      TOT(2,5)=XTYTOT(2)
      TOT(3,5)=XTYTOT(3)
      TOT(4,5)=XTYTOT(4)
C CCCCCCCCCCCCCCCCCCCCCCCCCCCCCCCCCCCCCCCCCCCCCCCCCCCCCCCCCCCC
C
C GAUSS-JORDAN ELIMINATION WITH MAXIMUM PIVOT STRATEGY.
C SIMUL = DETERMINANT
C INDIC < 0 COMPUTES INVERSE OF TOT (IPXIP)
C INDIC = 0 COMPUTES XANS, THE SOLUTION OF THE SYSTEM IN TOT
C           (IPXIP+1)
C           ALSO REPLACES A WITH ITS INVERSE
C INDIC > 0 SOLVES TOT (IPXIP+1) BUT DOES NOT REPLACE IT
C           WITH INVERSE
C DETER = DETERMINANT OF THE MATRIX TOT (IPXIP).
C
C CCCCCCCCCCCCCCCCCCCCCCCCCCCCCCCCCCCCCCCCCCCCCCCCCCCCCCCCCCCCC
C
      INDIC=1
      EPSS=0.1D-19
      DETER = SIMUL ( IP, TOT, XANS, EPSS, INDIC, 20)
```

```
      WRITE(6,*)'DETERMINANT OF XTXTOT (temp + flux) IS',DETER
C
C CCCCCCCCCCCCCCCCCCCCCCCCCCCCCCCCCCCCCCCCCCCCCCCCCCCCCCCCCCCCC
C     UPDATE THE PARAMETERS
C CCCCCCCCCCCCCCCCCCCCCCCCCCCCCCCCCCCCCCCCCCCCCCCCCCCCCCCCCCCCC
C
      DO 166 I=1,IP
      P(I,K+1)=P(I,K)+XANS(I)
      DCRIT(I)=abs(P(I,K+1)-P(I,K))/(P(I,K)+.0000000001)
166   WRITE(6,*)'AFTER K ITERATION PRAMETER IS=',K,P(I,K+1)
C
      DIFP(2,K)=P(2,K)+P(4,K)
      DIFP(3,K)=P(3,K)+P(4,K)
C
C CCCCCCCCCCCCCCCCCCCCCCCCCCCCCCCCCCCCCCCCCCCCCCCCCCCCCCCCCCCC
C     CHECK THE CONDITIONS WHICH CAUSE DIVERGENCE
C CCCCCCCCCCCCCCCCCCCCCCCCCCCCCCCCCCCCCCCCCCCCCCCCCCCCCCCCCCCC
C
      IF(DETER.EQ.0.) GOTO 1008
      IF(DIFP(2,K).GE.6..OR.DIFP(3,K).GE.6..OR.P(1,K).GT.P1.
     +OR.P(1,K).LT.0.0) GOTO 1030
C
C CCCCCCCCCCCCCCCCCCCCCCCCCCCCCCCCCCCCCCCCCCCCCCCCCCCCCCCCCCCC
C     CHECK IF THE CRITERION FOR CONVERGENCE IS SATISFIED.
C CCCCCCCCCCCCCCCCCCCCCCCCCCCCCCCCCCCCCCCCCCCCCCCCCCCCCCCCCCCC
```

```
C
      IF(DCRIT(1).LT.DELTA.AND.DCRIT(2).LT.DELTA.AND.
     +DCRIT(3).LT.DELTA.AND.DCRIT(4).LT.DELTA) GOTO 1060
C
300   CONTINUE
      GO TO 1009
1060  WRITE(6,*)'CRITERION IS SATISFIED, PROGRAM STOPPED'
      GO TO 1009
1030  WRITE(6,*)'UNREALISTIC PARAMETERS, PROGRAM STOPPED'
      GO TO 1009
1008  WRITE(6,*)'DETERMINANT OF XTX=0, PROGRAM STOPPED'
C
1009  WRITE(6,*)'End'
C
C CCCCCCCCCCCCCCCCCCCCCCCCCCCCCCCCCCCCCCCCCCCCCCCCCCCCCCC
C          ...FORMAT FOR INPUT AND OUTPUT STATEMENTS....
C CCCCCCCCCCCCCCCCCCCCCCCCCCCCCCCCCCCCCCCCCCCCCCCCCCCCCCC
C
207   FORMAT (1h, 4f16.5)
C
      STOP
      END
```

Appendix B

Computer Program : Elasticity

```
      PROGRAM PROPU.FOR
C
C CCCCCCCCCCCCCCCCCCCCCCCCCCCCCCCCCCCCCCCCCCCCCCCCCCCCCCCCCCCC
C
C THIS PROGRAM EMPLOYS THE PARAMETER ESTIMATION METHOD TO
C ESTIMATE THE SHEAR MODULUS, POISSON'S RATIO, AND LOCATION
C OF A CIRCULAR INCLUSION. THE BOUNDARY ELEMENT METHOD IS
C IMPLEMENTED AS A SUBROUTINE CALLED ELAS.
C
C THESE ARE REQUIRED INPUTS.
C
C P1,P2                   SHEAR MODULUS AND POISSON'S RATIO
C                         OF THE MATRIX MATERIAL
C
C P(1,1),P(2,1)           THE FIRST GUESS OF THE SHEAR
C                         MODULUS AND POISSON'S RATIO OF THE
C                         INCLUSION MATERIAL
C
C P(3,1), P(4,1)          THE FIRST GUESS OF COORDINATES OF
C                         THE CENTER OF THE CIRCULAR INCLUSION
C
C M                       MAXIMUM NUMBER OF ITERATIONS
C
C NUM1                    NUMBER OF DISPLACEMENT MEASUREMENTS
C                         IN THE X1 DIRECTION
C
C NUM2                    NUMBER OF DISPLACEMENT MEASUREMENTS
C                         IN THE X2 DIRECTION
C
C IP                      NUMBER OF PARAMETERS TO BE ESTIMATED
C
```

```
C PERR                    MEAN % ERROR IN THE MEASUREMENTS
C
C NT(NUM1)                THE NODE NUMBERS WHERE DISPLACEMENTS
C                         IN THE X1 DIRECTION ARE MEASURED
C
C NQ(NUM2)                THE NODE NUMBERS WHERE DISPLACEMENTS
C                         IN THE X2 DIRECTION ARE MEASURED
C
C UH1(NUM1)               MEASURED DISPLACEMENTS IN THE X1
C                         DIRECTION
C
C UH2(NUM2)               MEASURED DISPLACEMENTS IN THE X2
C                         DIRECTION
C
C CCCCCCCCCCCCCCCCCCCCCCCCCCCCCCCCCCCCCCCCCCCCCCCCCCCCCC
C
      IMPLICIT REAL*8 (A-H,O-Z)
      DIMENSION UX(100),P(20,20),Xw(20,20),XT(20,20)
      DIMENSION XTY1(3),Y1(100),UH(100),TS(100),XANS(3)
      DIMENSION PRAM(3),SQ(100),XNORM(20,20),XTQY2(3)
      DIMENSION XTXQ(20,20),XTXTOT(20,20),XTYTOT(3)
      DIMENSION UY(100),QS(100),XQT(20,20),DIFP(10,10)
      DIMENSION XQ(20,20),Y2(100),Y1SQ(100),Y2SQ(100)
      DIMENSION UH1(100),UH2(100),NT(100),NQ(100),XTX(20,20)
      DIMENSION TOT(20,20),XQNORM(20,20),DCRIT(10)
C
      OPEN(5,FILE='INCLUX4p.DAT',STATUS='OLD')
      OPEN(10,FILE='INCLUY4p.DAT',STATUS='OLD')
      OPEN(12,FILE='STOTTQ4p.OUT',STATUS='NEW')
      OPEN(6,FILE='RESELAST4p.OUT',STATUS='NEW')
      OPEN(13,FILE='RES14p.OUT',STATUS='NEW')
```

```
      OPEN(7,FILE='RES24p.OUT',STATUS='NEW')
      OPEN(8,FILE='RES34p.OUT',STATUS='NEW')
      OPEN(9,FILE='RES44p.OUT',STATUS='NEW')
      OPEN(11,FILE='RES64p.OUT',STATUS='NEW')
      OPEN(2,FILE='RES74p.OUT',STATUS='NEW')
      OPEN(3,FILE='RES84p.OUT',STATUS='NEW')
      OPEN(4,FILE='RES94p.OUT',STATUS='NEW')
C
C CCCCCCCCCCCCCCCCCCCCCCCCCCCCCCCCCCCCCCCCCCCCCCCCCCCCCCCCC
C          ...READ AND CHECK INPUT DATA ....
C CCCCCCCCCCCCCCCCCCCCCCCCCCCCCCCCCCCCCCCCCCCCCCCCCCCCCCCCC
C
      PRINT *,'WHAT IS G(1), PR(1) AND FIRST GUESS OF G(2),
     +AND PR(2)'
      ACCEPT *,P1,P2,P(1,1),P(2,1)
      PRINT *,'WHAT IS THE FIRST GUESS FOR XC, AND YC,
     +AND WHAT IS THE VALUE OF RC'
      ACCEPT *,P(3,1),P(4,1),P5
C
      WRITE(6,*)'G(1),PR(1) & FIRST GUESS OF G(2),PR(2),XC,
     +YC AND THE VALUE OF RC ARE'
      WRITE(6,*)P1,P2,P(1,1),P(2,1),P(3,1),P(4,1),P5
C
      PRINT *,'ENTER # OF ITER,# OF UX,UY DATA,# OF BETA,
     +AND ERROR :'
      ACCEPT *, M,NUM1,NUM2,IP,PERR
      NUM=NUM1+NUM2
      PRINT *,'ENTER THE NODE NUMBERS WHERE UX MEASUREMENT
     +ARE TAKEN'
C
      DO 292 I=1,NUM1
```

```
      ACCEPT *, NT(I)
292   WRITE(6,*)'THE NODE NUMBERS WHERE UX ARE TAKEN = ',NT(I)
      PRINT *,'ENTER THE NODE NUMBERS WHERE UY MEASUREMENT
     +ARE TAKEN'
C
      DO 291 I=1,NUM2
      ACCEPT *, NQ(I)
291   WRITE(6,*)'THE NODE NUMBERS WHERE UY ARE TAKEN = ',NQ(I)
      WRITE(6,*)'THE ERROR IN MEASUREMENT IS',PERR
C
      DO 299 I=1,NUM1
      READ(5,*)UH1(I)
299   CONTINUE
C
      DO 2811 I=1,NUM2
      READ(10,*)UH2(I)
2811  CONTINUE
C
      DO 300 K=1,M
C
C CCCCCCCCCCCCCCCCCCCCCCCCCCCCCCCCCCCCCCCCCCCCCCCCCCCCCCCCCCCC
C
C THIS PROGRAM EMPLOYS THE DIRECT BOUNDARY ELEMENT
C METHOD USING LINEAR ISOPARAMETRIC ELEMENTS
C TO SOLVE PLANE PROBLEMS OF LINEAR ELASTICITY, WITH AN
C INCLUSIOIN. UNIT THICKNESS IS ASSUMED.
C
C VARIABLE DEFINITION :
C
C K                   ITERATION VARIABLE.
C
```

```
C P1,P2                SHEAR MODULUS AND POISSON'S RATIO
C                      OF THE MATRIX MATERIAL
C
C P(1,K),P(2,K)        SHEAR MODULUS AND POISSON'S RATIO OF THE
C                      INCLUSION MATERIAL
C
C P(3,K), P(4,K)       COORDINATES OF THE LOCATION
C                      OF THE CIRCULAR INCLUSION
C
C P5                   RADIUS OF THE INCLUSION
C
C NUM1                 NUMBER OF DISPLACEMENT MEASUREMENTS
C                      IN THE X1 DIRECTION
C
C NUM2                 NUMBER OF DISPLACEMENT MEASUREMENTS
C                      IN THE X2 DIRECTION DIRECTION
C
C NT(NUM1)             THE NODE NUMBERS WHERE DISPLACEMENTS
C                      IN THE X1 DIRECTION ARE MEASURED
C
C NQ(NUM2)             THE NODE NUMBERS WHERE DISPLACEMENTS
C                      IN THE X2 DIRECTION ARE MEASURED
C
C UX(NUM1)             COMPUTED DISPLACEMENTS IN X1
C                      DIRECTION
C
C UY(NUM2)             COMPUTED DISPLACEMENTS IN X2
C                      DIRECTION
C
C THE FOLLOWING INPUT IS REQUIRED:
C
```

```
C
C IPLANE   = DESIGNATION OF PLANE STRESS OR PLANE STRAIN.
C            LET IPLANE EQUAL 1 FOR PLANE STRESS, 2 FOR
C            PLANE STRAIN.
C
C N(1), N(2) = THE NUMBER OF NODES ON THE BOUNDARY OF REGION
C              1, AND REGION 2, RESPECTIVELY. ENTER IN
C              FREE FORMAT.
C
C XN(I),YN(I) = THE COORDINATES OF THE OUTER BOUNDARY
C FOR I=1,N(1)  NODES. ENTER IN FREE FORMAT.
C
C IBC(I), BC(I) = TYPE OF SPECIFIED BOUNDARY CONDITION AT
C                 ELEMENT NODE (1=u, 2=t) AND VALUE OF
C                 SPECIFIED CONDITION. ENTER ONE ELEMENT
C                 PER LINE, N(1) LINES. ENTER ONLY FOR OUTER
C                 BOUNDARY NODES.
C
C CCCCCCCCCCCCCCCCCCCCCCCCCCCCCCCCCCCCCCCCCCCCCCCCCCCCCCCCCC
C
      CALL ELAS(P1,P2,P(1,K),P(2,K),P(3,K),P(4,K),P5,NUM1,
     +NUM2,NT,NQ,UX,UY)
C
      Y1SQT=0.
C
      DO 1803 J=1,NUM1
      Y1(J)=UH1(J)-UX(J)
      Y1SQ(J)=Y1(J)**2
      TS(J)=UX(J)
1803  Y1SQT=Y1SQT+Y1SQ(J)
C
```

```
      Y2SQT=0.
      DO 1033 J=1,NUM2
      Y2(J)=UH2(J)-UY(J)
      Y2SQ(J)=Y2(J)**2
      QS(J)=UY(J)
1033  Y2SQT=Y2SQT+Y2SQ(J)
C
      STOT=Y1SQT+Y2SQT
      WRITE(6,*)'AFTER K ITERATION STOT IS = ',K,STOT
C
C CCCCCCCCCCCCCCCCCCCCCCCCCCCCCCCCCCCCCCCCCCCCCCCCCCCCCCCC
C
C     SENSITIVITY COEFFICIENTS ARE COMPUTED
C
C CCCCCCCCCCCCCCCCCCCCCCCCCCCCCCCCCCCCCCCCCCCCCCCCCCCCCCCC
C
      DELTA=0.0001
      CON=1.0+DELTA
C
      DO 104 I=1,IP
      P(I,K)=P(I,K)*CON
      CALL ELAS(P1,P2,P(1,K),P(2,K),P(3,K),P(4,K),P5,NUM1,
     +NUM2,NT,NQ,UX,UY)
      P(I,K)=P(I,K)/CON
C
      DO 1044 J=1,NUM1
      Xw(J,I)=(UX(J)-TS(J))/(P(I,K)*DELTA)
      XT(I,J)=Xw(J,I)
      XNORM(J,I)=Xw(J,I)*P(I,K)
      IF(I.EQ.1) WRITE(11,*)J,XNORM(J,I)
      IF(I.EQ.2) WRITE(2,*)J,XNORM(J,I)
```

```
      IF(I.EQ.3) WRITE(3,*)J,XNORM(J,I)
      IF(I.EQ.4) WRITE(4,*)J,XNORM(J,I)
1044  CONTINUE
C
      DO 1045 J=1,NUM2
      XQ(J,I)=(UY(J)-QS(J))/(P(I,K)*DELTA)
      XQT(I,J)=XQ(J,I)
      XQNORM(J,I)=XQ(J,I)*P(I,K)
      IF(I.EQ.1) WRITE(13,*)J,XQNORM(J,I)
      IF(I.EQ.2) WRITE(7,*)J,XQNORM(J,I)
      IF(I.EQ.3) WRITE(8,*)J,XQNORM(J,I)
      IF(I.EQ.4) WRITE(9,*)J,XQNORM(J,I)
1045  CONTINUE
104   CONTINUE
C
      DO 107 I=1,IP
      DO 107 J=1,IP
      XTXTOT(I,J)=0.
      XTXQ(I,J)=0.
107   XTX(I,J)=0.
C
      DO 1108 I=1,IP
      DO 1108 J=1,IP
      DO 1108 LIJ=1,NUM1
1108   XTX(I,J)=XT(I,LIJ)*Xw(LIJ,J)+XTX(I,J)
C
      DO 1081 I=1,IP
      DO 1081 J=1,IP
      DO 1081 LIJ=1,NUM2
1081  XTXQ(I,J)=XQT(I,LIJ)*XQ(LIJ,J)+XTXQ(I,J)
C
```

```
      DO 1088 I=1,IP
      DO 1088 J=1,IP
1088  XTXTOT(I,J)=XTX(I,J)+XTXQ(I,J)
C
      DO 106 I=1,IP
      XTY1(I)=0.
106   XTQY2(I)=0.
C
      DO 1066 I=1,IP
      DO 1066 J=1,NUM1
1066  XTY1(I)=XT(I,J)*Y1(J)+XTY1(I)
C
      DO 1061 I=1,IP
      DO 1061 J=1,NUM2
1061  XTQY2(I)=XQT(I,J)*Y2(J)+XTQY2(I)
C
      DO 1064 I=1,IP
1064  XTYTOT(I)=XTY1(I)+XTQY2(I)
C
C CCCCCCCCCCCCCCCCCCCCCCCCCCCCCCCCCCCCCCCCCCCCCCCCCCCCCCCCCCC
C
C SUBROUTINE FOR MANIPULATION OF MATRICES AND VECTORS
C TOT(IP,IP) = XTXTOT(IP,IP)
C IP = NUMBER OF PARAMETERS
C
C CCCCCCCCCCCCCCCCCCCCCCCCCCCCCCCCCCCCCCCCCCCCCCCCCCCCCCCCCCC
C
      CALL MATEQ (XTXTOT, TOT, IP, IP)
      WRITE (6,*)'THE TOTAL XTX MATRIX IS:'
C
      DO 1323 I=1,IP
```

```
1323  WRITE (6,*) (TOT(I,J), J=1,IP)
      TOT(1,5)=XTYTOT(1)
      TOT(2,5)=XTYTOT(2)
      TOT(3,5)=XTYTOT(3)
      TOT(4,5)=XTYTOT(4)
C
C CCCCCCCCCCCCCCCCCCCCCCCCCCCCCCCCCCCCCCCCCCCCCCCCCCCCCCCCCCC
C
C GAUSS-JORDAN ELIMINATION WITH MAXIMUM PIVOT STRATEGY.
C SIMUL = DETERMINANT
C INDIC < 0 COMPUTES INVERSE OF TOT (IPXIP)
C INDIC = 0 COMPUTES XANS, THE SOLUTION OF THE SYSTEM IN TOT
C           (IPXIP+1). ALSO REPLACES TOT WITH ITS INVERSE
C
C INDIC > 0 SOLVES TOT (IPXIP+1) BUT DOSE NOT REPLACE IT WITH
C           INVERSE
C DETER = DETERMINANT OF THE MATRIX TOT (IPXIP).
C
C CCCCCCCCCCCCCCCCCCCCCCCCCCCCCCCCCCCCCCCCCCCCCCCCCCCCCCCCCCCCC
C
      INDIC=1
      EPSS=0.1D-19
      DETER = SIMUL ( IP, TOT, XANS, EPSS, INDIC, 20)
      WRITE(6,*)'DETERMINANT OF XTXTOT (Ux + Uy) IS',DETER
C
C CCCCCCCCCCCCCCCCCCCCCCCCCCCCCCCCCCCCCCCCCCCCCCCCCCCCCCCCCCCCC
C     UPDATE THE PARAMETERS
C CCCCCCCCCCCCCCCCCCCCCCCCCCCCCCCCCCCCCCCCCCCCCCCCCCCCCCCCCCCCC

      DO 166 I=1,IP
      P(I,K+1)=P(I,K)+XANS(I)
```

```
      DCRIT(I)=abs(P(I,K+1)-P(I,K))/(P(I,K)+.0000000001)
166   WRITE(6,207)'AFTER K ITERATION PRAMETER IS=',K,P(I,K+1)
C
      DIFP(2,K)=P3+P(3,K)
      DIFP(3,K)=P4+P(3,K)
C
C CCCCCCCCCCCCCCCCCCCCCCCCCCCCCCCCCCCCCCCCCCCCCCCCCCCCCCCCCCC
C     CHECK FOR THE CONDITIONS WHICH CAUSE DIVERGENCE
C CCCCCCCCCCCCCCCCCCCCCCCCCCCCCCCCCCCCCCCCCCCCCCCCCCCCCCCCCCC
C
      IF(DETER.EQ.0.) GOTO 1008
      IF(DIFP(2,K).GE.6..OR.DIFP(3,K).GE.6.) GOTO 1030
      IF(P(2,K).GT.0.5.OR.P(2,K).LT.O.) GOTO 1031
C
C CCCCCCCCCCCCCCCCCCCCCCCCCCCCCCCCCCCCCCCCCCCCCCCCCCCCCCCCCCC
C     CHECK IF THE CRITERION FOR CONVERGENCE IS SATISFIED.
C CCCCCCCCCCCCCCCCCCCCCCCCCCCCCCCCCCCCCCCCCCCCCCCCCCCCCCCCCCC
C
      IF(DCRIT(1).LT.DELTA.AND.DCRIT(2).LT.DELTA.AND.DCRIT(3)
     +.LT.DELTA) GOTO 1060
C
300   CONTINUE
C
      GO TO 1009
1060  WRITE(6,*)'CRITERION IS SATISFIED, PROGRAM STOPPED'
      GO TO 1009
1030  WRITE(6,*)'UNREALISTIC PARAMETERS, OUT, PROGRAM STOPPED'
      GO TO 1009
1031  WRITE(6,*)'UNREALISTIC PARAMETERS, G2,PR2 PROGRAM STOPPED'
      GO TO 1009
1008  WRITE(6,*)'DETERMINANT OF XTX=0, PROGRAM STOPPED'
```

```
C
1009  WRITE(6,*)'End'
C
C CCCCCCCCCCCCCCCCCCCCCCCCCCCCCCCCCCCCCCCCCCCCCCCCCCCCCCCCC
C         ...FORMAT FOR INPUT AND OUTPUT STATEMENTS....
C CCCCCCCCCCCCCCCCCCCCCCCCCCCCCCCCCCCCCCCCCCCCCCCCCCCCCCCCC
C
207   FORMAT (1h, 5f14.5)
C
      STOP
      END
```